2011

ELUCIDATION OF KEY MEDIATORS OF TUMOUR CELL MIGRATION USING AN IN VIVO INHIBITORY RNA SCREEN

Amy Elizabeth Robertson

ELUCIDATION OF KEY MEDIATORS OF TUMOUR CELL MIGRATION USING AN IN VIVO INHIBITORY RNA SCREEN

(Spine title: Tumour Cell Migration In Vivo)

(Thesis format: Monograph)

by

Amy E. Robertson

Graduate Program in Medical Biophysics: Molecular Imaging

A thesis submitted in partial fulfillment
of the requirements for the degree of
Master of Science

The School of Graduate and Postdoctoral Studies
The University of Western Ontario
London, Ontario, Canada

THE UNIVERSITY OF WESTERN ONTARIO
School of Graduate and Postdoctoral Studies

CERTIFICATE OF EXAMINATION

Supervisor

Dr. John D. Lewis

Supervisory Committee

Dr. Ann Chambers

Dr. Lynne-Marie Postovit

Examiners

Dr. Alison Allan

Dr. Christopher Ellis

Dr. Lisa Hoffman

The thesis by

Amy Elizabeth Robertson

entitled:

ELUCIDATION OF KEY MEDIATORS OF TUMOUR CELL MIGRATION USING AN IN VIVO INHIBITORY RNA SCREEN

is accepted in partial fulfillment of the
requirements for the degree of
Master of Science

Date

Chair of the Thesis Examination Board

Abstract

Metastatic disease, or the migration of cancer cells from the primary tumor to distant locations in the body, contributes to over 90% of cancer mortalities. Migration is a requirement of metastasis and involves the detachment of cancer cells from the primary tumour *in vivo*, followed by invasion of the cell into the surrounding stromal tissue. Tumour cells that are migration-deficient are incapable of detaching from the primary tumour and exhibit compact phenotypes in the chicken embryo model. Based on these findings, it was hypothesized that mediators of migration could be identified using an RNAi genomic library and screening for compact tumour phenotypes in the chicken embryo model. It was also postulated that knockdown of two proteins known to be involved in migration, rhoA and cortactin, would prevent migration of human epidermoid carcinoma (HEp3) cells *in vivo*, serving as a positive control and proof-of-principle for the RNAi screen. Results of this study identify rhoA and cortactin as positive regulators of migration, both *in vitro* and *in vivo*, and demonstrate the feasibility of the RNAi screen. Furthermore, execution of an RNAi screen, covering 5000 human genes, identified three novel mediators of tumour cell migration: MESCD1, KIF3B and ARHGAP12.

Keywords

Cell Migration, Cell Invasion, Cancer, Tumour, Metastasis, RNAi, Screen, *In Vivo*, Ex-Ovo Chicken Embryo Model, Viral Transduction, MOI.

Abbreviations

Bp- Basepair

CT- Cycle Threshold

DIC- Differential Interference Contrast

DMEM- Dulbecco's Modified Eagle's Medium

dsRNA- Double stranded RNA

ECM- Extracellular Matrix

EDTA- Ethylenediaminetetraacetic acid

FITC- Fluorescein isothiocyanate

FOV- Field of view

iFBS- Inactivated Fetal Bovine Serum

FA- Focal Adhesion

FAK- Focal Adhesion Kinase

GFP- Green fluorescent protein

i.v- intravenous

IVVM- Intravital video microscopy

KDa- KiloDalton

LB- Luria Bertani broth

MOI- Multiplicity of Infection

Nt- Nucleotides

PAX- Paxillin

PBS- Phosphate Buffered Saline

ROCK- RhoA Kinase

RT-PCR- Quantitative Real-Time Polymerase Chain Reaction

TU- Transducing Units

Dedication

To my best friend, words cannot express how much your love and support has helped me through the last two years. Without always fully understanding what exactly was keeping me so late at the lab, even when I said I would be ready to go in 10 minutes… and really wasn't for another 40, you were always waiting, with a smile and encouragement, and words of wisdom that this day would finally come, even when I never believed you. You were right. We did it, together as a team! You have taught me what it means to be supportive, helping out in all aspects of daily life, just so I didn't have to worry about doing laundry and experiments, keeping appointments and going to class, moving across the country and writing a thesis. Without your help, I just couldn't have done it. Plain and simple. My only hope is that when the tables are turned, I can handle everything you took on with as much patience, graciousness, compassion and willingness as you have done for me. What you have given to me in this last two years is one of the biggest gifts anyone has ever given me and will last forever. Thank-you for giving me the gift of knowledge, allowing me to develop and find my talents, and for providing me with confidence, all of which will surely come in handy for starting the next chapter of our lives. To my loving husband, Jeff, this is for you.

Acknowledgments

I would like to acknowledge the following people for their contributions to my project:

First and foremost, I would like to acknowledge my supervisor; Dr. John D. Lewis, for his creativity that was lent to the design of the project and for key recommendations that helped to develop some key experiments performed in the study. Also, I would like to address the fact that his inspiration of these necessary experiments, led to answering important scientific questions that facilitated in the progress of this project. Dr. Lewis was also very accommodating to my suggestions and creativity throughout the project allowing me to become fully engaged in the process. He provided unique opportunities for learning such as weekly lab meetings, retreats and scientific conferences that deeply enriched my understanding of the project at hand. Thank-you!

Next I would like to recognize my teammate, Dr. Hon Sing Leong, for his contributions to the project including assistance with experimental design and technical issues. Dr. Leong was involved with many of the components of this project, some of which were quite laborious: he aided in organizing flow cytometry experiments, assisted with the injection of 150 chicken embryos, and screened for the compact phenotype in each of these animals with enthusiasm! He also came through at a critical point in the project and helped with the PCR and sequencing analysis of the hits identified in this screen. His assistance to the project and friendship has not gone unnoticed and will be forever appreciated.

I would also like to thank Amber Ablack for her significant assistance as the technician of our lab. Without the assistance of this helpful and hard-working woman, I would not have had the confidence to carry out most of the experiments performed in the study. Her generous nature allowed me to ask questions, sometimes relentlessly, regarding pertinent experimental techniques and regents involved in most procedures performed in the study. She was also very sharing of personal experiences she has had in the lab with respect to most techniques I performed and provided insight into interpretation of my results. I wish all the best to her in her future endeavors in California; they are lucky to have her.

I would like to acknowledge Dr. Ann Chambers for her generosity exemplified by lending out lab space and equipment for the purpose of tissue culture procedures. I would also like to thank her lab technician David Dales and the members of the Chambers lab for their friendly assistance.

Finally, I would like to thank all of the members of the Lewis Lab for their support, friendship and advice over the last two years. You guys have made the experience one to remember and enjoy!

Table of Contents

List of Tables

List of Figures

List of Appendices

Chapter 1

1 Introduction

1.1 Cell Migration in the Human Body

Cell migration is necessary for a diverse range of biological processes in the human body. The body's defense system relies on the ability of immune cells to migrate throughout the tissues in the body, in the event an immune response is warranted. Part of the body's front line response to pathogens, such as viruses and bacteria, are natural killer cells, an especially motile immune cell that circulates the body in search of pathogens to 'kill' using specialized enzymes (Walzer and Vivier 2011). Natural killer cells can also participate in extravasation, or movement out of blood vessels, into the site of infection (Walzer and Vivier 2011). Hematopoietic stem cell migration into recipient bone marrow space is required for a successful bone marrow transplantation, and the mechanisms of stem cell migration have implied roles for a number of migratory mediators such as the Rho-GTPase, RhoA and its effector ROCK (Fonseca and Corbeil 2011). Endothelial cell migration is well documented and the ability of endothelial cell movement is highly influenced by endothelial growth factor (VEGF) and mitrochondrial reactive oxygen species (Wang 2011). Endothelial cell migration, mediated by these factors, can assist in the repair of damaged tissues such as blood vessels that become injured from high blood pressure in atherosclerosis (Wang 2011). In reproduction, the movement of germ cells and spermatocytes across the seminiferous epithelium is important to the process of spermatogenesis and germ cells employ mediators such as matrix metalloproteases to assist in their migration through dense tissue (Chen 2011). The process of cell migration is clearly an important underlying feature of many biological processes, even processes that are completely unrelated, such as reproduction and wound healing. In cancer, many of the cell migration strategies used in normal physiological processes such as extravasation, RhoA/ROCK signaling pathways, migration in response to growth factor stimulation, and release of matrix metalloproteases, are executed to assist in migration and metastasis (Hanahan and Weinberg 2000; Wyckoff 2006; Lai 200; Mader 2011 and Boire 2005).

1.2 Cell Migration and Metastasis in Cancer

Metastasis, or the capacity of tumour cells to colonize secondary organs distant from the primary tumour, contributes to 90% of cancer related mortalities (Hanahan and Weinberg 2000). Cancer cell metastasis is regarded as the sixth hallmark of cancer because it relies on previous events to establish the primary tumour, yet the cellular modifications that promote metastasis are required for further cancer progression (Hanahan and Weinberg 2000). The process of metastasis is often defined as the 'invasion-metastasis cascade' because it consists of consecutive, rate-limiting steps and the entire process can be prevented by blocking a requirement of any one step (Talmadge and Fidler 2010). Briefly, the steps in the invasion-metastasis cascade involve: the migration and invasion of cancer cells from the primary tumour into surrounding tissue, intravasation into the blood or lymph, survival in the circulation, and extravasation out of vessels at the secondary site using invasion and migration programs, followed by 'colonization' or growth at the secondary site (Figure 1.2.1) (Talmadge and Fidler 2010). One of the early steps in metastasis requires cells to migrate away from the primary tumor and blocking this step has been demonstrated to prevent the remainder of the metastatic cascade (Zijlstra 2008). This observation made by Zijlstra *et al* supports the body of evidence that implicate tumour cell migration as a prerequisite for metastasis (Palmer 2011; Yansong 2001 and Shieh 1999).

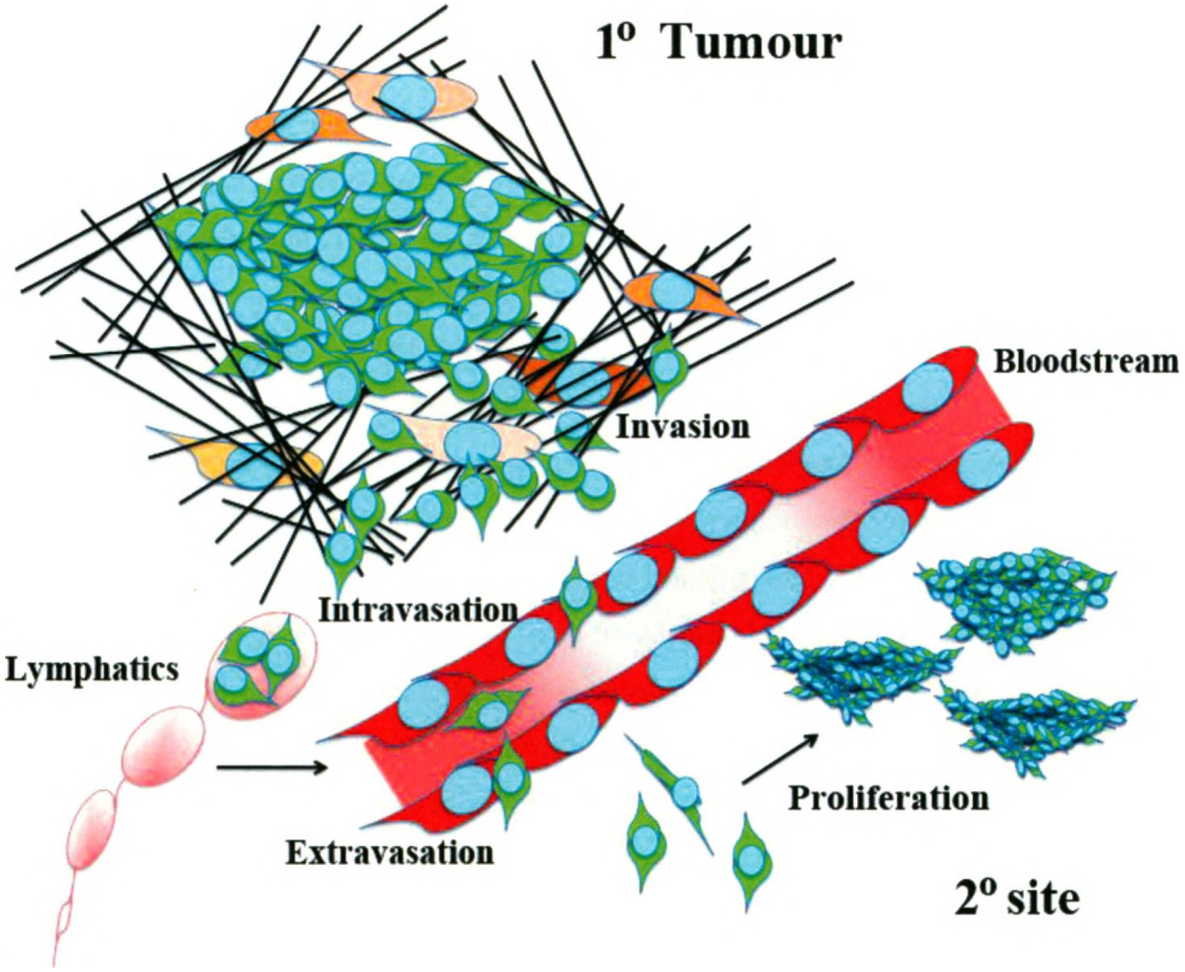

Adapted from: Steeg, P.S., *Nature Reviews Cancer* **3**, 3 (2003)

Figure 1.2.1: Steps in metastasis

The steps in the 'invasion-metastasis-cascade' are initiated following the migration and invasion of cancer cells (green) from the primary tumour into surrounding extracellular matrix, composed of stromal cells (orange), and matrix proteins such as collagen and fibronectin (black). Intravasation into the bloodstream through endothelial cells (red) or at their junctions and/or into the lymphatics, provides a route for cancer cell dissemination throughout the body. Cells that survive in the circulation can extravasate, or move out of the vasculature at secondary sites. The invasion and migration programs used to move into the vasculature are also required to move out of these vessels and into the surrounding stroma at the secondary site. Proliferative cells at the secondary sites progress to form micrometastases that can progress into clinically relevant metastases.

1.2.1 Requirements of Cancer Cell Migration

There are a plethora of molecules involved in enabling cancer cell migration, from cell surface receptors that receive external cues to structural components that physically generate cell movement (Jones and Ehrlich 2001 and Olsen and Sahai 2009). Although components of the migratory machinery seem all encompassing, many of these molecules work in concert to drive select functions of cancer cell migration (Tomar and Schlaepfer 2009). On the basis of certain characteristic molecules used in cancer cell migration strategies, cancer cell migration has even been loosely described as belonging to one of two main arms: protease-dependent, mesenchymal migration and protease-independent, amoeboid migration (Rowe and Weiss 2008 and Hanahan and Weinberg 2011). Together, these two forms of migration cover the three fundamental requirements of cancer cell migration in a 3D environment: cytoskeletal reorganization, protease matrix degradation and recognition of the matrix by cellular adhesion molecules (CAMs). This section focuses on the three requirements of cell migration, highlighting many of the key players and regulators involved in each requirement, and emphasizes the role of these migratory mediators in potentiating metastasis.

1.2.1.1 Cytoskeletal Reorganization

Cell motility is propagated through cytoskeletal reorganization events such as the polymerization of actin monomers (G-actin) into filaments (F-actin). There is tight control over actin polymerization rates by proteins that directly bind actin and signaling molecules that orchestrate these binding events. To coordinate with cell migration, the 'barbed' or 'plus' ends of actin filaments are facing the plasma membrane and it is at these ends that new actin monomers are added to advance the cell toward the stimulus (Olsen and Sahai 2009). There are many important regulators of actin polymerization to keep cell migration in check, and often the aberrant behavior of these regulators can promote cancer progression. Proteins involved in the polymerization of actin include: formin homology (FH), members of the Ena/VASP family, Cofilin, Arp2/3 complex, WASP, WAVE, cortactin, and Rho family of GTPases (Olsen and Sahai 2009; Loureiro 2002; Miki, Suetsugu and Takenawa 1998; Artym 2006 and Tomar and Schlaepfer 2009).

Proteins Involved in Actin Polymerization

Formin Homology (FH) Proteins

The FH proteins contain three important domains, FH1, FH2 and CRIB, important in both nucleating actin filaments and regulating polymerization (Olsen and Sahai 2009). The FH1 and FH2 domains work together to build actin, with profilin binding to the FH1 domain, and bringing a G-actin monomer with it, and the FH2 domain binding to F-actin to bring the FH1-profilin-G-actin-monomer in association with the F-actin filament (Olsen and Sahai 2009). The CRIB domain is bound by many GTPases, which will be discussed in more detail in the next section, including Cdc42, RhoA, RhoB and Rif (Olsen and Sahai 2009). Binding of these regulatory GTPases to CRIB allows FH to be in an active 'open' conformation so that actin polymerization can proceed (Olsen and Sahai 2009).

The Enabled/Vasodilator-Stimulated Phosphoprotein (Ena/VASP)

The Ena/VASP family of proteins have the same function as FH proteins, and interact with the barbed end to recruit monomeric actin, but in addition, these proteins influence the branching density of F-actin within lamellipodia (Breitsprecher 2011). Lamellipodia are a fan-like cell protrusions that are often seen at the front of migrating cells in 2D cultures and are related to the metastatic potential of cancer cells (Olsen and Sahai 2009 and Kim 2011). Ena/VASP proteins have three functionally conserved domains: c-terminal Ena/VASP homology 1, (EVH1), a proline-rich domain, and a N-terminal EVH2. EVH1 is required for cellular targeting, the proline rich domain, like the FH1 domain in FH proteins, binds profilin-monomeric-actin complexes, and the EVH2 domain, similar to the FH2 domain of FH, binds filamentous actin (Breitsprecher 2011). The difference between FH and Ena/VASP proteins is that FH proteins remain associated with the actin filament, simultaneously protecting it from capping proteins that hinder actin elongation, and rely on the recruitment of profilin to bring in monomeric actin (Breitsprecher 2011). Conversely, profilin is dispensable to Ena/VASP for actin chain elongation, and is not needed to protect the growing chain from capping proteins *in vitro,* however, profilin does appear to *enhance* Ena/WASP protection of the actin chain from capping proteins in a dose dependent manner (Breitsprecher 2011; Pula and Krause 2008). Phosphorylation negatively regulates

Ena/VASP-mediated actin elongation by decreasing its ability to protect the growing actin chain from capping proteins (Pula and Krause 2008). More importantly, the phosphorylation state of Ena/VASP appears to play a role in the regulation of cell motility as seen by the decrease in fibroblast migration upon phosphorylation of mammalian Ena (Mena) (Loureiro 2002).

Cofilin

Cofilin, unlike FH and Ena/VASP proteins, severs filamentous actin, rather than elongating it, but can still contribute to the overall actin polymerization by creating more available barbed ends for actin propagation (Olsen and Sahai 2009). Cofilin can be modulated by capping proteins, which sterically hinder the interaction of cofilin with the filamentous chain, and by LIM kinase, which decreases the activity of cofilin (Olsen and Sahai 2009).

Actin Related Proteins 2 and 3 (Arp2/3 complex)

Arp2/3 are two components of an actin-nucleating complex that aid in the polymerization of branched actin filaments by associating with the side of a pre-existing actin filament (Olsen and Sahai 2009). Apr2/3 is regulated by the WASP (Wiskott– Aldrich syndrome protein) and WAVE (WASP family Verprolin-homologous protein) proteins that, like FH or Ena/VASP actin nucleating proteins, can bind to actin monomers but in this case allow G-actin to come into close contact with the Arp2/3 complex and increase the rate of actin polymerization (Olsen and Sahai 2009). WAVE and WASP are folded into an auto-inhibited conformation and upon the binding of a GTPase (Cdc42 or rac1) the conformation changes to an open active form (Miki, Suetsugu and Takenawa 1998 and Olsen and Sahai 2009). Thus, Arp2/3 complex is under at least three layers of regulation: 1) the binding of GTPases to WASP and WAVE conferring an active status to these proteins, 2) the binding of monomeric actin to WAVE/WASP and 3) the binding of active WASP and WAVE to the Arp2/3 complex. Arp2/3 complexes are also associated with invasive cell structures called invadopodia that often accumulate in regions of matrix degradation and are implicated in invasion, migration and metastasis *in vivo* (Artym 2006 and Yansong 2001). Cortactin, a protein required for the maturation of invadopodia, binds

Arp2/3 complex, locating it to regions of cell invasion to form these invasive cell protrusions by actin polymerization (Artym 2006 and Olsen and Sahai 2009).

RhoGTPases

Rho-family of GTPases (Ras-homology-family of guanine triphosphates) are regulatory proteins that act as switches to activate many proteins involved in cell migration. The prototypical Rho-GTPases involved in actin polymerization are: Rho, Rac1 and Cdc42. These molecular switches are 'turned on' by the Rho-GEFs (guanine exchange factors) that exchange a GDP for a GTP, rendering the Rho-GTPase in the active form and are 'turned off' by Rho-GAPs (GTPase activating proteins) that, counterintuitive to their name, inactivate Rho-GTPases (Tomar and Schlaepfer 2009). Activation of Rho-GTPases by GEFs can be initiated upon adhesion of cells to the extracellular matrix (ECM) to initiate cell migration (Tomar and Schlaepfer 2009). In response to such extracellular signals, cdc42 binds to the CRIB domain on FH and activates barbed end (180°) actin polymerization, which produces actin-rich spikes called filopodia (Olsen and Sahai 2009). Filopodia structures are used by the cell for directional cell migration on a 2D substratum, and the occurrence of filopodia are associated with cell invasion (Olsen and Sahai 2009 and Pan 2011). Cdc42 can also bind WASP, however this initiates Arp2/3 mediated branched actin (70°) and would form lamellipodia in 2D matrices (Olsen and Sahai 2009). Lamellipodia may correspond to invadopodia seen in 3D matrices since both lamellipodia and invadopodia rely on Arp2/3 mediated actin polymerization (Olsen and Sahai 2009). Rac-1 is also activated upon cell adhesion and like cdc42, can bind to WAVE to induce Arp2/3 mediated formation lamellipodia-at the leading edge of migrating cells in 2D, often referred to as a pseudopod in 3D matrices (Olsen and Sahai 2009). RhoA has at least two different functions in cell migration upon activation: 1) form stress fibers to aid in cell adhesion during the initial events of cell migration 2) induce cell contractility during the late phase of cell migration (Tomar and Schlaepfer 2009). Although cell contractility itself is unrelated to actin polymerization, the inhibition of cofilin severing through downstream effectors of RhoA (ROCK and LIM-Kinase) during contraction decreases the availability of barbed ends for actin nucleation. This second function, therefore, may act to halt

polymerization in the event of actomyosin-contraction mediated by RhoA-ROCK (Tomar and Schlaepfer 2009 and Maekawa 1999).

Proteins Involved in Actin Polymerization and their Connection to Cancer

Mediators of actin polymerization can facilitate cell migration through the formation of cell protrusions and invasive structures and have been associated with increased tumour invasion and metastasis, predicting poor patient outcome. These findings emphasize the importance of actin cytoskeletal reorganization in human cancer progression and identify a strong association between the mediators of cancer cell migration and metastasis. Recently, the actin polymerizing proteins, FH and Ena/VASP, have been shown to increase invasion and motility in human cancer cells and more importantly an increased expression of an Ena/VASP family protein, hMena, confers poor prognosis in a variety of cancers (Kitzing 2010; Di Modugno 2006 and Toyoda 2009).

Increases in cofilin activity have been found in rat mammary carcinoma cells and, in concert with Arp2/3, caused enhanced lamellipodia formation, which is a critical step in the initiation of migration and indicative of the potential for metastasis (DesMarais 2004 and Kim 2011). In human gastric carcinoma Arp2 and 3 are overexpressed compared to adjacent gastritis tissue and positively correlate with tumor size, depth of invasion and venous invasion, however, a survival disadvantage in Arp2/3 overexpressing cancer was not found (Zheng 2008). This study suggests that Arp 2/3 complex is important in the progression of gastric cancer to a metastatic phenotype. As for cofilin, expression of wild-type, or non phosphorylatable (constitutively active) mutant cofilin increases the migration and invasion of melanoma cells (Dang, Bamburg and Ramos 2006). Furthermore, increasing positive regulators of cofilin, such as Aur-A, induces mammary cell migration and breast cancer metastasis, and vice versa, an increase in negative regulators of cofilin, such as LIM kinase, abolishes lamellipodia formation and polarized cell migration (Wang 2010 and Zebda 2000).

RhoGTPases are important regulators of cytoskeletal reorganization, both promoting and inhibiting actin polymerization to suit the migratory needs of the cell. Recently, RhoA was identified as one of the most significantly upregulated plasma membrane-associated

proteins in hepatocellular carcinoma (HCC) as determined by highly purified plasma membrane proteins from clinical tissue samples followed by proteomics identification. In the same study, immunohistochemistry on clinical samples for HCC confirmed RhoA expression and suggested that RhoA may contribute to poor differentiation and increased cancer stage (Gou 2011). L. Gou *et al.* also demonstrated that RhoA was required for cell migration of hepatocellular carcinoma cell lines since RNA interference of RhoA led to a significant decrease in cell migration of these cells through a transwell membrane, emphasizing the migratory role of RhoA and making a connection between the migratory capacity RhoA confers and the poor patient outcome (Gou 2011). Rac1 expression is also increased in human gastric cancer and not only does expression increase in higher grade tumors, but Rac1-positive, high grade tumors also correlated with decreased survival (Walch 2008). Rac1-GTP (active Rac1) expression is also associated with increased grade of upper urinary tract cancers and contributes to lymph node invasion and metastasis (Kamai 2010).

Taken together, these findings indicate a clear association between the mechanistic role of actin-polymerizing proteins in cell migration and their enhanced metastatic potential upon expression of these proteins. In this respect, cytoskeletal reorganization is not only a requirement of cell migration, but is necessary for the progression of human cancers. Identification of novel actin nucleating proteins that assist in the formation of invasive structures such as filopodia, lamellipodia and invadopodia could potentially provide new targets for metastasis.

1.2.1.2 Protease Degradation

Proteases are one of the largest groups of enzymes in the human genome as there are 570 known proteases that are also tightly regulated, in part, by a smaller group of protease inhibitors (Mason and Joyce 2011). There are five human protease classes grouped by catalytic mechanism (matrix, cysteine, metallo, serine, and threonine) however, the matrix metalloproteases (MMPs) are the most heavily involved in cancer progression (Kessenbrock, Plaks and Werb 2010). MMPs are initially expressed in an enzymatically inactive state and must be modified, sometimes by enzymatic cleavage by another protease, to become proteolytically active. MMPs can be divided into two general classes:

the secreted MMPs (MMP-1, -2, -3, -7, -8, -9, -10, -11, -12, -13, -19, -20, -21, -22, -27, -28) and the membrane-type MMPs (MT-MMPs), (MMP-14, -15,-16, -17, -23, -24, -25), the latter using a transmembrane domain with a cytoplasmic domain attached, a glycosylphosphatidylinositol anchor, or an amino-terminal signal anchor, in order to remain bound to the cell surface. MMPs, in the context of aggressive cancer, function to disrupt cell-cell adhesion and mediate cell migration away from the tumour, degrade the ECM to permit tumour cell migration and invasion into the stroma, and mediate signaling cascades that ultimately lead to the metastatic capacity of tumour cells. The numerous publications detailing the suppression of MMPs, followed by decreases in tumour invasiveness, led to clinical trials for MMP inhibitors, however, these trials failed to increase survival rates in patients (Kessenbrock, Plaks and Werb 2010). This recent twist in events has led to the accepted conclusion that although MMPs do degrade physical barriers of tumour cells, they also have more complex functions in the human body. The focus of this section will be to explore the three main roles of MMPs that make them a requirement of migration and invasion for most cells, whether by their ECM degradative function, or by their more complex signaling roles recently postulated.

Disruption of Cell Adhesions by Mmps Enhances Cell Migration and Invasion

There are several mechanisms that MMPs can employ to facilitate invasion and tumour cell migration. One way is by disruption of cell-cell adhesion molecules, permitting cells to migrate away from each other. One example of MMP-mediated cell de-adhesion and tumor progression is the cleavage of the cell adhesion molecule epithelial (E)-cadherin by MMP-3,-9,-7, and MT1-MMP (MMP-14) (Van Roy and Berx 2008). E-cadherin is a transmembrane, cell adhesion molecule (CAM) that maintains tissue organization and forms adherent junctions between cells tightly holding them together in a 'sheet' (Aplin 1998). Loss or disruption of this CAM is associated with many malignancies, contributing to a disorganized tissue phenotype and transitioning cells from an 'epithelial' phenotype, to that of a more motile 'mesenchymal' state (Hanahan and Weinberg 2000). In addition to the disruption of cell junctions, cleavage of E-cadherin can result in a soluble fragmented form that can act as a signaling molecule to further increase aggressiveness of cancer cells. The appearance of this soluble fragment of E-cadherin was concurrently observed with

MMP-9 expression, increased cell migration and invasion and transition to a more aggressive mesenchymal phenotype in stimulated head and neck small cell carcinoma cells. In the same study, the direct role of MMP-9 on E-cadherin disruption was confirmed by knockdown of MMP-9 using siRNA, which inhibited the production of soluble E-cadherin during EGF-stimulated cell migration and invasion (Zuo 2011). Although not directly tested in the study, this soluble form of E-cadherin has been shown in other studies to work in a paracrine manner to increase cell invasion further potentiating the effect of E-cadherin disruption of cell migration and invasion (Lynch 2010).

The findings from *in vitro* studies regarding E-cadherin cleavage by MMPs have also correlated to what is found in the clinic. In a study where EGFR, MMP-9 and E-cadherin expression levels in ovarian epithelial cancer tissues were examined, it was observed that both EGFR and MMP-9 were overexpressed in high grade and advanced stages of the disease, however E-cadherin expression was inversely proportional to cancer progression (Alshenawy 2010). Patient tissue samples of esophageal squamous cell carcinoma have also been shown to possess high expression of MMP-2 and a low expression of E-cadherin. Furthermore, silencing a common upstream mediator of MMP-2 and E-cadherin, in an esophageal cell line (EC-1), mimicked this expression pattern and decreased the migration of these cells through a transwell membrane (Zhang 2011). Although MMP-2 does not directly cleave E-Cadherin, this study emphasizes the necessary coordination of cell-cell contact loss and MMP function in the invasion and progression of human malignancies.

Degradation of the Extracellular Matrix (ECM) and Basement Membrane (BM) by MMPs Enhances Cell Migration and Invasion

While the loosening of cell contacts allows cancer cells to detach, protease degradation of the ECM and basement membrane (BM) enables these invasive cells to migrate into the surrounding tissue and vasculature. In this manner, MMPs 'clear the way' for migrating cells by expanding the pore size through the basement membrane to which cells must move through. The BM itself is an extensively complex barrier, made up of more than 50 distinct molecules to form a 100-300nm-thick lamina that is laid down under all epithelia and endothelium and structurally supports these cells (Rowe and Weiss 2008). The BM is composed of both polymerized laminin and type IV collagen that are crosslinked to

provide a dynamic, mesh-like framework and the BM pore size is determined by both the amount of cross-linking as well as the quantity of ECM (Rowe and Weiss 2008). BM pore sizes are in the neighborhood of 50nm and since cells can only efficiently move through pores of more than 2mm, there is a spatial conundrum of how the cell can get through the BM (Rowe and Weiss 2008). Surprisingly, the cell employs invasive machinery that can either be of the proteolytic or non-proteolytic variety, in order to traverse the membrane. While the proteolytic mechanisms used to remodel the BM and ECM are discussed in detail in this section, non-proteolytic methods of cell invasion are discussed in 'Types of Migration Machinery'.

Upon adhesion of a cell to the ECM, proteases are recruited to the location of the cell that makes contact with the ECM (called a focal contact or focal adhesion site). At the focal contact site, the membrane bound proteases, such as MT1-MMP, are in the perfect position to cleave ECM components such as collagen, fibronectin and laminins, as well as pro-MMPs, to create active soluble MMPs such MMP-2,-9 and -7 (Friedl and Wolf 2003). MMP-2 (aka gelatinase A) and MMP-9 (gelatinase B) are also type IV collagenases and, in addition, can degrade the BM. For example, overexpression of MT1-MMP-tagged with green fluorescent protein (GFP) in HT1080 fibrosarcoma cells, embedded in a collagen 3D matrix, resulted in a simultaneous increase of MT1-MMP-GFP at the surface of the cell and accumulation of cleaved collagen product (Wolf 2007). Furthermore, knockdown of MT1-MMP by RNAi, decreased the rate at which collagen was cleaved, as monitored by fluorescein isothiocyanate (FITC) release from cleaved collagen lattices (Wolf 2007). More importantly, the overexpression of MT1-MMP in HT1080 cells caused an increase in cell migration, that was reverted upon treatment with an MMP inhibitor (Wolf 2007). This study by K. Wolf *et al.* demonstrates the functional role of MMPs, in particular MT1-MMP, in the degradation of BM matrices for enhanced cell migration through these matrices.

MMP-Mediated Signal Transduction Enhances Cell Migration and Invasion

A third way to increase invasion through MMPs is by MMP-mediated signal transduction. Recent findings are emerging that suggest a role for MMPs, not only in the degradation of ECM, but in the modulation of signaling cascades that result in increased migration and

invasion. An example of a signal-altering MMP that results in increased metastasis is MMP-1. MMP-1 can be released into the tumour microenvironment by fibroblasts and has been found to activate a G- protein coupled receptor through proteolytic cleavage of its extracellular domain (Boire 2005). G-protein coupled receptors are membrane bound and associate with many cytoplasmic proteins that engage in signal transduction. To prove the hypothesis that MMP-1 cleaves a receptor responsible for signaling to downstream cell migration events, A. Boire *et al* added exogenous MMP-1 to media of breast carcinoma cells that do not express MMP-1. They observed that addition of MMP-1, but not other soluble MMPs (-2,-3 -7,-9), caused the number of cells that migrated through a transwell membrane to double (Boire 2005). Furthermore, this cell migration could be inhibited through knockdown of the receptor or by addition of MMP inhibitors clarifying the importance of both MMP1 and the signaling receptor in transducing cell migration.

1.2.1.3 Cellular Adhesion through Cell Adhesion Molecules

Cell-adhesion molecules (CAMs) have many important functions in the human body including the control of migration, maintenance of tissue integrity and adhesion of cells, such as immune mediators, to endothelial cells prior to transendothelial migration. In addition to their structural functions, CAMs also modulate signal-transduction pathways by interacting with molecules such as receptor tyrosine kinases, components of the Rho-family of GTPases, and molecules that upregulate MMPs. CAMs can also incur posttranslational modifications, adding another layer of cell adhesion regulation. Recent experimental evidence indicates that such processes have a crucial role in tumour progression, in particular during invasion and metastasis.

INTEGRINS

Integrins are single membrane spanning cell surface glycoproteins composed of heterodimers, α and β. They engage with the ECM, as well as counter receptors on neighboring cells, and transduce signals regarding the cell surroundings into the cell via their cytoplasmic tails. Integrins engage with the cytoskeleton of the cell as well as matrix degradation enzymes and these relationships allow integrins to have a hand in cell adhesion, motility and invasion. In particular, integrins can change their subtype to

recognize different tissues the cell may encounter, in order to facilitate invasion in concert with MMPs. One of the most important roles of integrins in cell migration is the assembly of focal adhesions by stimulation of focal adhesion kinase.

Integrin subtype expression and tissue recognition

There are more than 22 integrin subtypes formed by the various permutations between more than 16 α subunits and 8 β subunits (Hanahan and Weinberg 2000). As cells change environments throughout the process of metastasis and invasion, they can change the expression of their integrin subtypes in order to recognize and bind the various ECM they will encounter, from blood vessel endothelial cells to protease degraded ECM to intact stroma.

Under physiological conditions, cells can adapt to their surroundings in order to activate necessary responses through integrin signaling. Normal dermal fibroblasts play a role in tissue remodeling in response to changes in tissue rigidity in wound healing. When fibroblasts are plated on collagen, which is then overlaid onto substrata with varying rigidity, the cells change their expression of integrins as well as α smooth muscle actin (αSMA) to accommodate for the changes in surface structure (Jones and Ehrlich 2011). The fibroblasts, when plated onto a high rigidity surface, had increased expression of αvβ3 integrin and αSMA and enhanced stress fibers whereas on low rigidity surfaces, the cells expressed α2β1 integrin and had finer cytoskeletal microfilaments with less αSMA (Jones and Ehrlich 2011). These findings suggest that cells can change integrin expression patterns in response to their environment, influencing the actin cytoskeleton, and possibly affecting cell motility.

Interestingly, αvβ3 is one of the most versatile integrins, allowing adhesion to many different ECM components, and its expression allows for cells to migrate on almost any matrix protein it encounters (Johnson 1991). Additionally, expression of αvβ3 protein has been shown to coincide with the tumorigenicity of melanoma cells in murine models, which may be attributed to the β3 subunit because cells that have a mutated form of this subunit are unable to metastasize in comparison to cells with an intact β3 subunit (Jones and Ehrlich 2011 and Johnson 1991). The finding that increased expression of β3 integrin

is found in late stage and metastatic melanoma patient samples, in comparison to melanocytes and non-tumorigenic, microinvasive lesions, supports the notion that the β3 subunit imparts aggressive attributes to cancer cells (Van Belle 1999).

Integrin association with MMPs and invasion

Preferential expression of integrins facilitates migration and invasion through the recognition of surrounding matrices and can further potentiate invasion by localizing matrix metalloproteases (MMPs) to these sites. The first study to solidify the interaction between a particular active MMP and an integrin was performed by P. Brooks *et al.* in 1996. In the study, secreted, active MMP2 and the αvβ3 integrin were co-localized on the surface of both melanoma cells and angiogenic blood vessels *in vivo*. In culture, melanoma cells expressing αvβ3 bound directly to soluble MMP-2, but not a C-terminally truncated form, on the surface of invasive tumor cells (Aplin 1998).

More recently, it was demonstrated that the interaction between MMP-2 and αvβ3 is critical for the promotion of endothelial ECM degradation when in association with the membrane type 1 MMP (MT1-MMP) (Leroy-Dudal 2005). In this study, MT1-MMP cleaved pro-MMP-2, and in this active form, interacted with αvβ3 integrins on the cell surface, localizing the proteolytic activity to the invasive front of tumor cells (Leroy-Dudal 2005). More importantly, pharmacological inhibition of the MMP2- αvβ3 interaction decreased the transmigration of ovarian carcinoma cells through human umbilical vein endotheial cells (HUVECs) (Leroy-Dudal 2005). This study highlights a role for integrins, in concert with active MMP-2, in the migration of cancer cells through endothelial ECM that surrounds the vasculature. The evidence reported in these elegant studies combines the knowledge that integrins facilitate cell movement, and provide a mechanism by which integrins aid in invasion.

Integrins can facilitate migration by adjusting their subtype to accommodate their surroundings, and by expressing subtypes that participate in matrix degradation to clear a path for invasion. Integrins also have an important role to play in cell migration by regulating the assembly and disassembly of adhesion complexes to meet the migratory requirements of the cell. Integrin-mediated cell adhesion events rely on many effectors to

deliver external signals into the cell, interact with the cytoskeleton, and regulate adhesion/de-adhesion events to ultimately orchestrate motility.

Integrin mediated cell adhesion

There are a number of intracellular proteins that bind directly to the cytoplasmic domain of integrin receptors and link outside integrin signaling to inside cytoskeletal interactions. In this manner, integrins and their effectors work on the cytoskeleton to assist in the assembly of focal contacts. Focal contacts are specialized structures that allow the cell to connect with the ECM. Within focal contacts are sites of adhesion where clusters of integrins bind not only to the ECM proteins outside the cell but also to distinct cytoplasmic proteins that interface with actin filaments inside the cell. The cytoplasmic proteins that directly bind to integrins at focal contacts include talin and α-actinin (Aplin 1998). Talin and α-actinin connect the actin cytoskeleton to focal adhesions through their actin-binding partner, vinculin, and are necessary to form nascent focal adhesions (Aplin 1998). Vinculin, in addition to binding actin, also binds to paxillin. Paxillin and talin can both bind to focal adhesion kinase (FAK), which serves as a switch to potentiate, as well as shut down, focal adhesion (Figure 1.2.2).

<u>Integrin-mediated assembly of Focal Adhesions (FAs) through Focal Adhesion Kinase (FAK) activation in cell migration</u>

FAK is a cytoplasmic, non-receptor, protein tyrosine kinase and upon integrin clustering at focal adhesions, FAK has been shown to experience enhanced tyrosine phosphorylation, rendering it 2-3 fold active upon adhesion in fibroblasts (Aplin 1998). Overexpression of FAK has been shown to increase the migration of chinese hamster ovary cells across fibronectin and the expression levels of FAK promote the progression of aggressive melanoma phenotype (Cary 1996 and Hess 2005). FAK knockout cells, conversely, have reduced cell migration and decreased tyrosine phosphorylation of FA-associated proteins, but the number of stable FAs is increased (Ilic 1995). These counterintuitive results from work done with FAK -/- cells can be taken together to imply a role for FAK in the *turnover* rather than creation of FAs, to induce cell motility.

But how does FAK mediate FA assembly/disassembly and, consequently, cell migration? In a study performed earlier this year, it was demonstrated that by altering the ability to phosphorylate the Tyr-925 residue of FAK, focal adhesion turnover is altered along with migration rates (Deramaudt 2011). In more detail, this study used FAK-/- embryonic fibroblast cells to introduce one of two constructs, a non-phosorylatable form of FAK and a constitutively phosphorylated type of FAK (Deramaudt 2011). The differences found between these two forms was that unphosphorylated-FAK led to FA stabilization, decreased FA disassembly and reduced cell migration, similar to previous findings with FAK -/- cells, while conversely, phosphorylated-FAK did not experience any reduction in FA disassembly, had increased FAs at cell leading edge, more cell protrusions and higher migration speeds, similar to results seen previously in FAK over-expressing cells (Deramaudt 2011). Taken together, these results show that FAK phosphorylation acts as a switch that coordinates either FA disassembly when phosphorylated, or stabilizes FAs when dephosphorylated. These findings offer an explanation for how FAK works as a regulator to increase FAs at the leading edge for initiation of protrusion formation, yet disassembles these focal adhesions during cell movement and contractility.

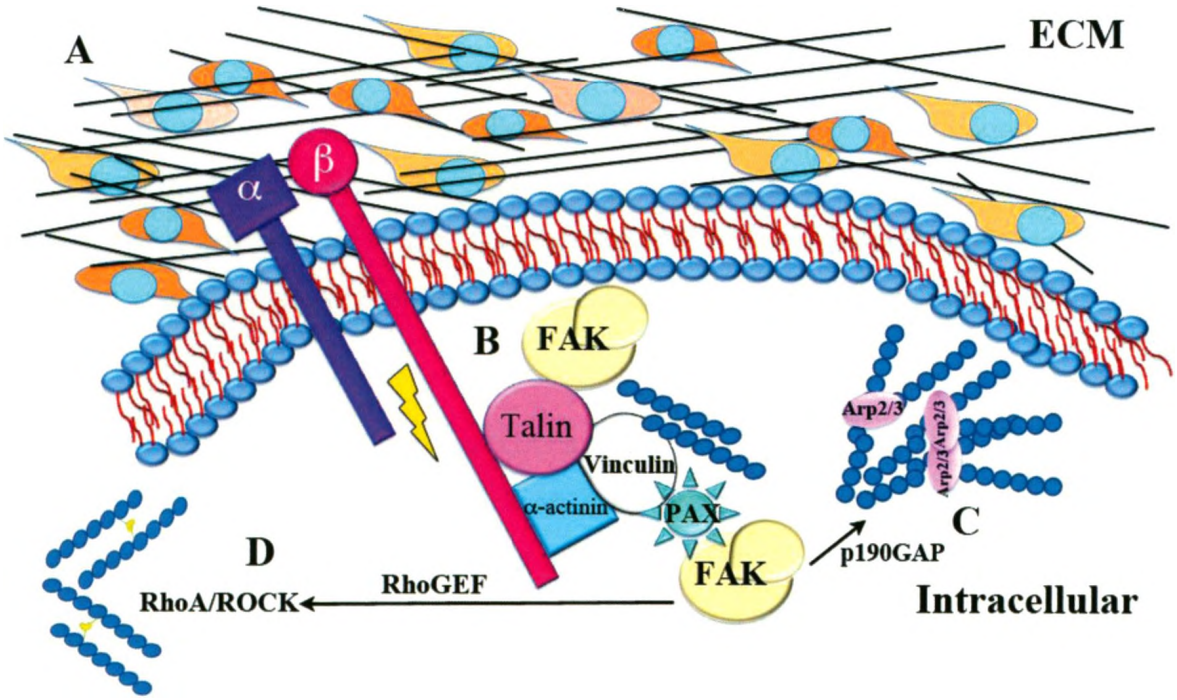

Adapted from Tomar, A. and Schlaepfer, D.D. *Curr. Opin. Cell. Biol.* **5** (2009)

Figure 1.2.2: Integrin-mediated focal adhesion formation

A. Upon binding to the fibronectin-rich ECM, integrins signal as heterodimers (α and β) to transduce the outside-signal-in to intracellular binding partners of the β-subunit for formation of focal adhesion contacts. **B.** Focal adhesions are formed along the outside of the cell where it makes contact with the ECM. The intracellular integrin binding partners, Talin and α-actinin, link the signal to the actin cytoskeleton through their common binding partner Vinculin. Paxillin (PAX) is also recruited to the site of focal adhesion formation and both PAX and Talin bind Focal Adhesion Kinase (FAK). **C.** FAK serves as a switch to potentiate, as well as shut down, focal adhesion. In the inactive form (dephosphorylated), FAK can increase focal adhesion and bind the Arp3 complex to initiate the recruitment of Arp2/3 complex. At the early stages of cell migration, activation of FAK (phosphorylated) leads to disassembly of focal adhesions and phosphorylation of p190RhoGAP, a RhoA inactivating protein. FAK phosphorylation thus allows for the formation of Rac1- mediated, Arp2/3 branched actin nucleation, resulting in lamellipodia. **D.** Phosphorylation of RhoGEF, a RhoA activating protein, by active FAK, allows for RhoA/ROCK mediated actomyosin contraction in the later stages of cell migration.

FAK-mediated regulation of cell migration through GTPases

Another model of FAK-mediated regulation of FAs and migration, suggests that FAK regulates guanine nucleotide exchange factors (GEFs) and GTPases-activating proteins (GAPs) to control the temporal activation of Rho and Rac GTPases (Tomar and Schlaepfer 2009). GEFs work to activate GTPases by increasing the release of GDP and allowing GTP to bind, and GAPs work in the opposite manner by increasing the hydrolysis of GTP and promoting the inactivation of GTPases (Aplin 1998). Evidence to support this model comes from the fact that FAs at the leading edge mature under high contractility, through GEF-mediated activation of RhoA, a contractility molecule, and that FA disassembly occurs upon loss of this contractility through inactivation of RhoA (Gupton and Waterman-Storer 2006).

FAK mediated cell migration through GAPs and GEFs functions at both the beginning and end of the migration cycle (Figure 1.2.3). At the onset of cell migration, RhoA is in the leading edge of the cell and it is here that it will be activated by GEFs to induce actin stress fibers (Olsen and Sahai 2009). Stress fiber formation is a form of actomyosin contraction and thus, favors the assembly of FAs at the front of the cell whereas RhoA inhibition, through GAPs, decreases contractility, leading to FA turnover. In fact, this exact scenario is seen in the early stages of lamellipodia formation (15-45 minutes) whereby FAK inhibits RhoA by regulating p190RhoGAP, a GAP specific for RhoA, and at the same time FAK enhances Rac activation by phosphorylation of p130Cas or PIX (Tomar and Schlaepfer 2009). RhoA is also inhibited by Rac1, but not vice versa, and so RhoA will not be active at the same time as Rac1 (Tomar and Schlaepfer 2009). Focal contacts are initially formed to give the cell some traction, however when FAK and Rac1 inactivate RhoA, FAs are disassembled at the front of the cell and Rac-mediated lamellipodia formation, which would not favor focal contacts of the cell to the ECM, can occur. (Tomar and Schlaepfer 2009). This model also corroborates with what is seen in FAK-null fibroblasts because it makes sense that without FAK to inhibit RhoA, there would be a high incidence of FAs in these cells. In fact, in the literature, FAK-/- or FAK mutant cells have high RhoA activity and FA turnover defects, leading to many FAs (Tomar and Schlaepfer 2009 and Ilic 1995).

If these mechanisms occur at the leading edge of the cell, what happens in the rear? At about +60 minutes post fibronectin induced lamellipodia formation, FAK has been shown to phosphorylate Rgnef, a RhoGEF at the rear, resulting in high Rho activity and increased actomyosin contraction, and, in a completely opposite manner to the front, contraction promotes the trailing edge disassembly of weaker FAs at the back by pulling on stronger FAs at the front (Tomar and Schlaepfer 2009 and Gupton and Waterman-Storer 2006). To achieve contractility, RhoA signals to its effector, ROCK (Rho-Kinase), which can directly bind myosin light chain II (MLCII) (Narumiya, Tanji and Ishizaki 2009). ROCK-mediated phosphorylation of MLCII forces myosin to take on an active conformation, resulting in the binding of MLC II to actin filaments and gliding them against one another to create cell contraction (Olsen and Sahai 2009). Actomyosin contraction allows the cell to pull apart from the ECM and advance in the location of the stimulus (Tomar and Schlaepfer 2009). This conclusion is supported by the reduced motility and tail retraction defects, however no effect on cell spreading, seen in fibroblasts when RhoGEF is knocked down and RhoA activation is reduced (Lim 2008).

In summary, many studies are in support of the temporal model of FA regulation by FAK and GEFs/GAPs where upon fibronectin-Integrin stimulated cell spreading, RhoA is first activated, then inactivated, followed by final RhoA activation. Put simply in a review by A. Tomar and D. Schlaepfer, FAK 'pushes' the cell forward by Rac-mediated lamellipodia formation in early cell spreading by activating p190RhoGAP to inhibit RhoA and by phosphorylation of p130Cas or PIX to activate Rac (Johnson 1991). FAK then follows up the push by 'pulling up the rear' of the cell late in cell spreading by activating RhoGEF and subsequent activation of RhoA (Tomar and Schlaepfer 2009).

In summary, integrins play a role in cancer migration and invasion by altering their subtype to better interact with surrounding extracellular matrices as well as degrade them. In addition to the preferential expression of integrins to promote matrix degradation and migration, cancer cells can also regulate assembly and disassembly of adhesion complexes to adapt to the migratory requirements of the cell through the actions of FAK.

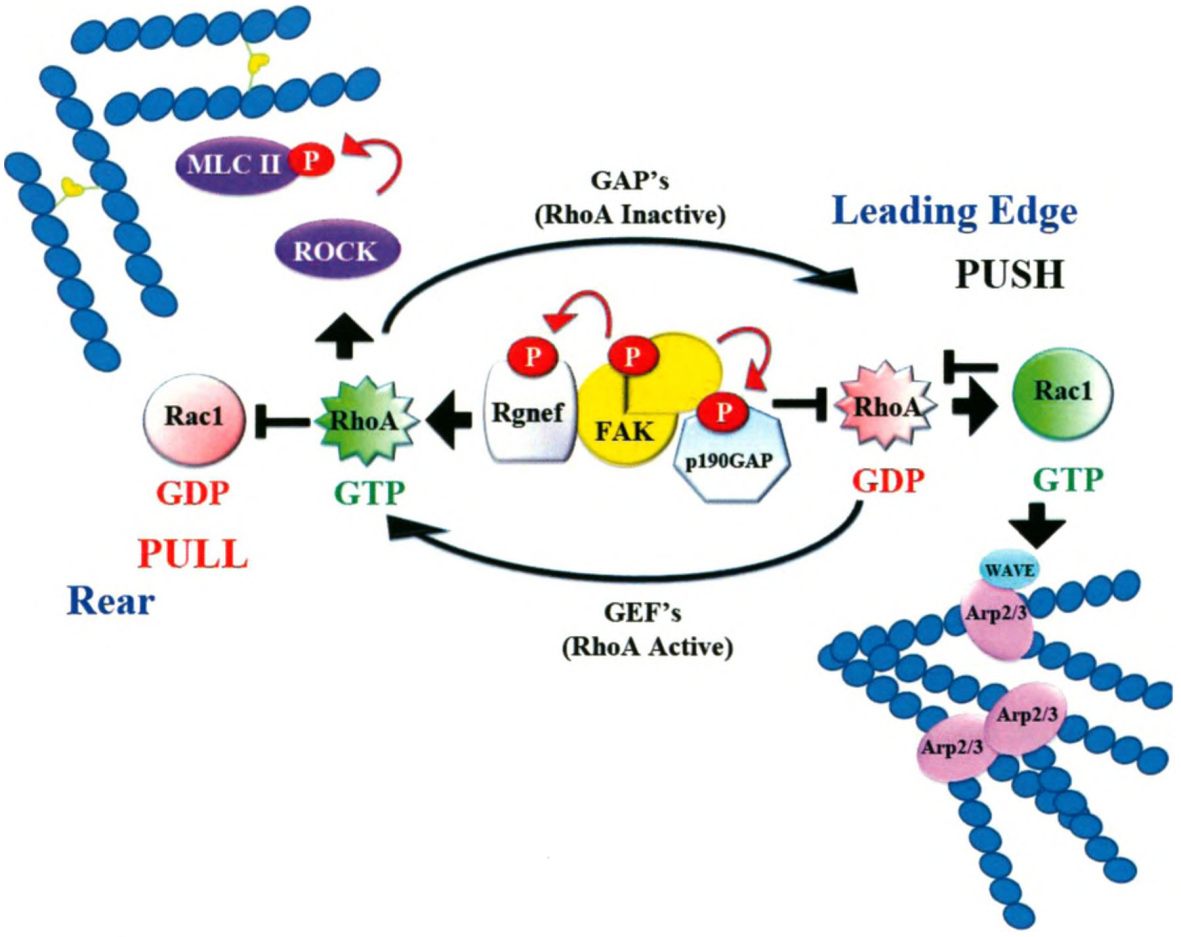

Adapted from Tomar, A. and Schlaepfer, D.D. *Curr. Opin. Cell. Biol.* **5** (2009)

Figure 1.2.3: Focal Adhesion Kinase regulation of cell motility

FAK regulates guanine nucleotide exchange factors (GEFs) and GTPases-activating proteins (GAPs) to control the temporal activation of Rho and Rac GTPases. At the early stages of cell migration (15-45 minutes) active FAK inhibits RhoA by regulating p190RhoGAP, a GAP specific for RhoA, and at the same time, FAK enhances Rac1. Rac1 also inhibits RhoA to further potentiate Rac1-mediated lamellipodia formation (PUSH). In the later stages of migration (+60 minutes) FAK phosphorylates Rgnef, a RhoGEF at the rear, resulting in high RhoA activity and increased actomyosin contraction. Contraction promotes the rear disassembly of weak FAs at the back by pulling on stronger FAs at the front. To achieve contractility, RhoA signals to its effector, ROCK, which can directly bind myosin light chain II (MLCII) for actomyosin contraction (PULL).

CADHERINS

Classical cadherins are single spanning transmembrane proteins and are comprised of more than 5 subtypes, with E- and N- subtypes most often implicated in cancer (Cavallaro and Christofori 2004). One specific subtype of cadherin binds exclusively to the same subtype on the surface of another cell, unlike the integrins, which bind to many different ligands. Cadherins localize to adherence junctions, or sites of cell-cell contact, and it is here that they mediate cell-cell adhesion by transduction of signals to the actin-cytoskeleton. Cadherins mediate cell signaling through the interaction of their cytoplasmic tails with a family of intracellular proteins called catenins. Briefly stated, the cytoplasmic tail of the cadherin molecule binds to β-catenin and this process is essential to the function of cadherins because truncating the cytoplasmic domain also deletes catenin binding sites, abolishing cadherin-mediated adhesion (Aplin 1998). The α-catenin protein serves to bind both β-catenin and the actin cytoskeleton by direct binding to α-actinin (actin bundling protein), which is a similar downstream effector of integrin-mediated adhesion (Figure 1.2.4). Disruption of this cadherin-catenin- complex is detrimental to establishing cell-cell contacts and is a common mechanism used during the progression to tumour malignancy (Cavallaro and Christofori 2004). For example, epithelial (E)-cadherin is altered in most epithelial tumours and its loss supports tumour cell migration, invasion and metastatic dissemination (Cavallaro and Christofori 2004). Likewise, transformation of normal epithelial cells with v-Src, phosphorylates β-catenin, leading to loss of cytoskeletal interactions and adherence junctions (Aplin 1998).

Loss of E-Cadherin and tumor cell migration and invasion

The first group to show a causal link between the loss of Epithelial (E)-cadherin and tumor cell invasion and metastasis *in vivo* was Christofori's group in 1998. Using a Rip1Tag mouse model of pancreatic β-cell carcinoma in comparison to Rip1Tag mice crossed with a dominant negative form of E-cadherin, this group demonstrated that mice with normal E-cadherin arrested their tumour development at the adenoma stage while mice that were dominant negative for E-cadherin developed carcinoma with early invasion and metastasis (Perl 1998). More recently, a model for non-small cell lung carcinoma (C-Raf x conditional knock out of E-cadherin gene) was used to demonstrate effects of E-cadherin

loss *in vivo.* Upon E-cadherin ablation in this model, normally benign lesions gave rise to micrometastasis (Ceteci 2007). The elegant work that has been done *in vivo* to date, demonstrates the importance of E-cadherin in suppressing invasion and metastasis.

E-Cadherin loss promotes the Epithelial-Mesenchymal Transition (EMT) and promotes cell migration and invasion

The loss of E-cadherin has been associated with the onset of a developmental regulatory program, called the 'epithelial-mesenchymal transition' (EMT). EMT defines a characteristic change in phenotype of transformed epithelial cells as they transition from what Hanahan and Weinberg describe as: a 'polarized, polygonal/epithelial morphology to that of a more spindly/fibroblastic morphology'. In addition to morphological changes, cells that undergo EMT are associated with an increase in matrix-degrading enzymes and cell motility increasing their ability to metastasize (Hanahan and Weinberg 2011).

Loss in the expression of epithelial cell markers, such as E-cadherin and cytokeratin, and gain in expression of mesenchymal markers, such as Neural (N)-cadherin, cadherin-11, (expressed by osteoblasts), Vimentin intermediate filament protein, and distinct transcriptional factors, accompany the EMT process (Kallergi 2011). The process of exchanging expression of E-cadherin to N-cadherin and cadherin-11, in particular, is called the 'cadherin switch' and is associated with increases in invasion and migration (Cavallaro and Christofori 2004).

The invasive qualities that N-cadherin and cadherin-11 impart upon the cell post-EMT have been theorized to allow the tumour cell to move into its surroundings. This theory rests upon the fact that epithelial cells express E-cadherins, however the 'mesenchymal'-like cells express N-cadherin and caderin-11, which are cadherins often found in stromal cells (Cavallaro and Christofori 2004). It is thought that the loss of E-cadherin not only prevents adherence between adjacent tumour cells, but also entices the tumour cell to engage with stroma cells and invade, since cadherins interact with the exact same cadherin receptor on neighboring cells. Evidence for this theory can be gleamed from a clinical study where the gain of N-cadherin/loss of E-cadherin expression is seen in high-grade human prostate cancer tissue, but no N-cadherin expression was found in the surrounding

normal prostatic tissue, and less N-cadherin was seen in lower grade prostatic tissue (Tomita 2000). Furthermore, when immunofluorescence analysis of cadherin-11 was performed on prostate tissue, all of the prostate cancer specimens showed expression of cadherin-11 at the interface of the stroma and tumor cells, whereas no expression of cadherin-11 was found in nonmalignant prostate tissue (Tomita 2000). This study indicates that the cadherin switching in high-grade prostate cancer is related to the interaction between cancer cells and the stroma and could contribute to the invasiveness of these tumours.

Disruption of E-cadherin promotes Actin cytoskeletal reorganization and cell migration through Rho GTPases

Another role that cadherins play in the migration of cancer cells is through their association with Rho GTPases. As mentioned previously, disassembly of the cadherin-catenin-complex leads to the disruption of E-cadherin, which results in a loss of association with the actin cytoskeleton through the impedance of actin binding to α-catenin. This implies that the loss of E-cadherin could also play a role in forcing the actin cytoskeleton to reorganize itself. Rho GTPases play a key role in the organization of the actin cytoskeleton and thus, Rho GTPases can also modulate cell-cell adhesion by their association with cadherins (Cavallaro and Christofori 2004).

Rho GTPases and adhesion junctions have been shown to participate with one another through the association of E-cadherin and p190GAP, the RhoA inhibitory molecule. For example, L. Asnaghi and colleges have shown that E-cadherin inhibits RhoA activation through p190GAP to suppress cell migration and proliferation by demonstrating that the suppressive affects of E-cadherin can be alleviated through the siRNA inhibition of all three molecules (RhoA, p190GAP or E-cadherin) (Figure 1.2.4) (Asnaghi 2010).

In summary, cadherins participate in the progression of tumours and their invasive capacity through a cadherin switch from tumor suppressing E-cadherin to tumour promoting N-cadherin and cadherin-11. E-cadherin loss disrupts the cell-cell adhesion contacts allowing cells to move away from one another and causing tissue disorganization and N-cadherin and cadherin-11 gain allows cells to better interact with their surroundings so that they can

invade. Cadherins also participate with the actin cytoskeleton to inhibit cell migration and proliferation through the inhibition of RhoA. E-cadherin loss relieves this inhibition and many invasive cancers may use this strategy.

The fundamental requirements of cell migration: cytoskeletal reorganization, protease matrix degradation and cellular adhesion molecule-mediated cell adhesion and signaling, can be generally described in terms of two different and yet overlapping arms of cell migration, protease dependent and protease independent.

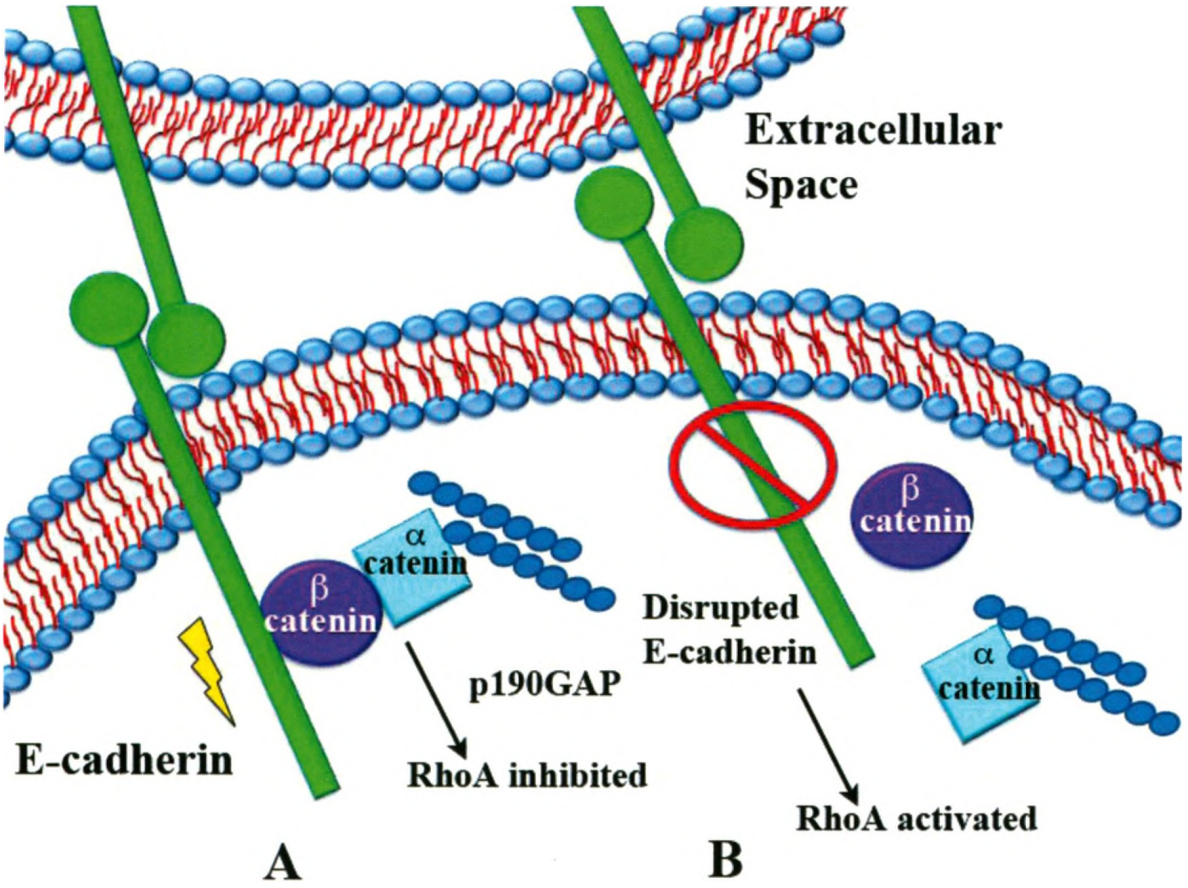

Figure 1.2.4: Loss of E-cadherin and cell migration

Loss of E-cadherin is associated with cancer cell migration. Cadherins bind to the same subtype on neighboring cells at cell adherence junctions and mediate cell-cell adhesion by signal transduction through catenins. The cytoplasmic tail of the cadherin molecule binds β-catenin, which connects the cadherin signal from the neighboring cell to the actin cytoskeleton through α-catenin. α-catenin binds both β-catenin and the actin cytoskeleton by directly binding to α-actinin (actin bundling protein). The E-cadherin subtype can play a role in both tissue organization and controlling cell migration through its interaction with Rho GTPases. **A.** Intact E-cadherin can signal to p190GAP to inactivate RhoA and keep migration in check. **B.** Destabilization of E-cadherin is commonly observed in cancer and can facilitate migration through multiple pathways including loss of RhoA regulation by p190GAP.

1.2.2 Types of Cancer Cell Migration Machinery

Cancer cell migration has been loosely categorized on the basis of two proposed mechanisms: protease dependent or protease independent. Furthermore, the same cell can employ these distinct mechanisms at different times by preferentially switching between the two. Protease dependent migration is also termed 'mesenchymal' migration and depends on the release of proteases to create a space in the ECM to move through (Rowe and Weiss 2008 and Hanahan and Weinberg 2011). Protease dependent, mesenchymal-elongated cell migration is mediated by Rac stimulated actin protrusions and does not have a requirement for Rho or ROCK (Sahai and Marshall 2003). Protease independent migration also called 'ameboid' migration is a type of migration that occurs in the absence of proteases and relies on the cell's capacity to 'squeeze' itself through the ECM (Rowe and Weiss 2008 and Hanahan and Weinberg 2011). Rho/ROCK signaling mediates this form of cell migration without the need for proteases (Sahai and Marshall 2003 and Wyckoff 2006). Wyckoff *et al.* demonstrated that metastatic breast tumour cells (MTLn) migrate through a complex ECM without proteolysis (Wyckoff 2006). Although the pharmacological inhibition of proteases does not prevent the 'deformation' of collagen, pharmacological inhibition of myosin ATPase or ROCK does. These results clearly implicate a protease-independent form of migration, related to actomyosin contraction, in order to contort through substrata. E. Sahai and C. Marshall elegantly point out the ability of cancer cells to switch during metastasis by demonstrating that cells with 'rounded' ameboid-like morphology invade using the protease-independent form of migration and inhibitors against Rho GTPases or ROCK or both synergistically, deplete invasion (Sahai and Marshall 2003). Conversely, elongated-mesenchymal type cells do not show the same decrease in invasion upon addition of these inhibitors alone or in combination, and invasion was even enhanced in one cell type. Subjection of both rounded and elongated cells to protease inhibitors does not lead to decreased invasion, but surprisingly, the combination of protease inhibitors and a ROCK inhibitor reduces their migration in all cases. From this data, Sahai and Marshall suggest that blocking the ability of cells to switch between the two forms of migration ultimately ceases cell invasion, a necessary component of migration.

1.2.2.1 Cortactin and RhoA, Examples of Proteins Involved in the Two Arms of Migration Machinery

RhoA and Cortactin are examples of proteins involved in the two different mechanisms used in cell migration. RhoA is involved in protease-independent cell migration machinery such as: formation of focal adhesions, cell contraction and pushing the cell forward from the rear. Conversely, cortactin is involved in protease-dependent migration machinery such as: actin polymerization in the formation of invadopodia used for matrix degradation and assists in pulling the cell forward at the leading edge. RhoA and cortactin are also frequently over-expressed or amplified, respectively, in many human cancers, conferring poor patient prognosis (Fritz, Just and Kaina 1999; Horiuchi 2003; Schuuring 1995; and Cai 2010). Elucidation of the roles rhoA and cortactin have on conferring metastatic potential to cancer cells *in vivo*, would help in the indication of the type of migration machinery critical for fully metastasized cells, and would assist in further defining the steps in metastasis where migration is rate limiting.

Role of RhoA in Cellular Migration

RhoA, a member of the Ras homology super family of small guanosine triphosphatases (RhoGTPases), acts as a molecular switch to turn on protease-independent, amoeboid cell migration machinery such as: formation of focal contacts at the leading edge of the cell, actin polymerization and stabilization, actomyosin mediated contraction and cell-cell contact destabilization.

RhoA mediated formation of focal adhesion contacts at the leading edge

RhoA activation has been described in numerous publications to promote the formation of nascent focal contacts during the initiation of migration. Focal contacts, as discussed in the previous section, are clusters of integrin cell- adhesion molecules that allow the cell to come into contact with the ECM. It is hypothesized by many that focal adhesion contacts are necessary to provide traction for the cell at the leading edge so that the cell can grab hold of the ECM to push itself forward using RhoA mediated actomyosin contraction, discussed below.

RhoA mediated actin polymerization and actomyosin contraction at the rear

To initiate cell motility, RhoA-GTP binds and activates its effector, Rho-associated coiled-coil forming kinase (ROCK1,2) (Narumiya, Tanji and Ishizaki 2009). ROCK 1 and 2 show sequence-similarity and both act to increase actomyosin contraction by phosphorylation of the myosin II light chain (MLC), rendering it in a conformation that associates with nearby F- actin filaments (Somlyo and Somlyo 2000). When multimeric myosin interacts with F-actin, myosin uses ATP to walk towards either end of two opposing growing ends of actin filaments and creates contractile force necessary for cell motility (Olsen and Sahai 2009). ROCK also antagonizes myosin light chain phosphatase (MLCP) to render myosin in an active state during contraction (Somlyo and Somlyo 2000). The RhoA-ROCK mediated cell migration drives the amoeboid arm of migration whereby tumor cells generate sufficient actomyosin contraction to push through the extracellular matrix (ECM) independent of degradation enzymes or cell protrusions. For example, treatment with a ROCK inhibitor in cells that rely on amoeboid migration increases cell protrusions yet these cells are unable to invade (Wyckoff 2006). Conversely, the same cells, when treated with ECM protease inhibitors, have fewer protrusions and still invade as the control cells (Wyckoff 2006).

Role of Cortactin in Cellular Migration

During metastasis, cells can form specialized, peripheral protrusions, called invadopodia, that assist with invasion into the ECM or endothelium during protease-dependent mesenchymal migration. Cortactin acts as a master switch, and upon phosphorylation, forms functional and mature invadopodia structures through the activation of actin polymerization in the direction of cell migration.

The role of Cortactin in mature invadopodia formation

Invadopodia formation can be broken down into stages from initiation of small invadopodium precursors to mature structures. Precursors contain actin, and actin polymerization regulators such as cortactin, N-WASP and cofilin (Yamaguchi 2005 and Artym 2006). Although cortactin is not a requirement for precursors, phosphorylation of

cortactin is absolutely necessary to stabilize and allow formation of mature invadopodia (Yamaguchi 2005 and Artym 2006). Cortactin relies on precise interactions at each of its distinct binding domains to complete the invadopodia maturation process. The acidic region at the N-terminus of cortactin harbors a binding site for the actin-polymerizing Arp2/3 complex. Upon phosphorylation of cortactin, the Arp2/3 complex actively begins to polymerize actin, forming branched networks extending the cell membrane outward (Mader 2011 and Pollard 2007). Following this domain is the site for F-actin binding, which allows for the actin fiber to come into close proximity to the Arp2/3 nucleating complex. At the C-terminus of the molecule is the location of Src-homology 3 (SH3) domain, which recruits additional components that are also necessary for initiation of invadopodia formation and provides additional Arp2/3 mediated actin polymerization, such as N-WASP (Neural Wiskott-Aldrich syndrome protein) family proteins (Yamaguchi 2005). Finally, there is a proline rich region that contains phosphorylation sites for Src family kinases which kick starts the aforementioned maturation and stabilization of invadopodia but also allows for progression of mature invadopodia to functional invadopodia.

The role of Cortactin in functional invadopodia formation

The final stage of invadopodia maturation confers functionality to these structures. This function is delivery, followed by secretion, of extracellular matrix-degrading enzymes such as type1 matrix metalloprotease (MT1-MMP) (Yamaguchi 2005 and Artym 2006). For example, when cortactin was depleted from MD-MBA-231 cells, gelatin matrix-degradation was blocked due to failure of cells to form invadopodia. Conversely when MT1-MMP was inhibited, invadopodial structures were only slightly decreased but cells were unable to degrade the matrix (Artym 2006). These findings indicate that cortactin is required to stabilize mature invadopodia, but cannot deform the ECM alone, and therefore requires MMPs for functional invasion. Cortactin has been shown to orchestrate invadopodia formation and ECM degradation events following stimulation with epidermal growth factor (EGF), via signaling through Arg and Src kinase (Mader 2011). This EGFR-Arg-Src-cortactin mediated pathway triggers actin polymerization by Arp2/3 complex and matrix proteolysis-dependent tumor cell invasion and provides a link between the external

matrix conditions and functional invadopodia formation (Mader 2011).

A side by side study, where both the protease-independent or protease-dependent arms of migration are inhibited, would allow for the question of whether one is more important than the other, for cell migration and metastasis, to be asked. Knockdown of genes such as rhoA or cortactin would represent both arms of the migration machinery and is a quick way to begin looking at this question. Migration machinery of both arms, however, can be overlapping, and additional validation would be required to tease out these overlapping functions. Gene knockdown can be mediated by short-interfering or short-hairpin RNA molecules that target mRNA transcripts in a sequence specific manner, depleting mRNA expression and protein expression of the gene of interest.

1.3 RNA Interference

RNA interference, or RNAi, is a conserved response to double-stranded RNA (dsRNA) utilized by most, if not all, eukaryotic organisms (Cullen 2004). This form of post-transcriptional gene silencing was originally discovered in *Caenorhabditis elegans* after the administration of dsRNA resulted in an increase in sequence-specific gene knockdown that was 10-fold more potent then single stranded RNA alone (Fire 1998). A hallmark of the dsRNA silencing machinery is the production of 21-25 base pair dsRNAs called small interfering RNAs (siRNAs) by Dicer, an enzyme that essentially 'chops up' long dsRNAs (Hannon 2002). In this form, siRNAs specifically and efficiently target transcribed genes using exact Watson-Crick base pairing to mRNA transcripts, by association with RISC (Hannon 2002). Targeted mRNAs experience degradation or inhibited translation, ultimately silencing the gene associated with the transcript. Endogenous dsRNA, called microRNA, can also be processed in the RNAi pathway as a method of gene regulation (Lochmatter and Mullis 2011). MicroRNAs, like exogenous dsRNA, also trigger formation of siRNA, however due to incomplete Watson-Crick base pairing to the targeted mRNA, the translation is stalled rather than degraded, as is normally encountered with long dsRNA processing (Lochmatter and Mullis 2011). This section summarizes the RNAi response used by mammalian cells to process both long dsRNA for resistance to exogenous pathogenic nucleic acids, and endogenous microRNAs to regulate expression of their own

coding genes. The application to which the RNAi response has been applied in research and the types of synthetic molecules used in this process is also highlighted.

1.3.1 Function of RNAi in Nature

Mediation of Resistance to pathogenic dsRNAs by the RNAi response

The RNAi pathway can be initiated by long pieces of dsRNA that can arise exogenously, as in the case of pathogenic virus infection or by injection of long dsRNA into the cell cytoplasm, as shown previously with murine oocytes (Lochmatter and Mullis 2011 and Wianny, and Zernicka-Goetz 2000). The antiviral response includes processing dsRNA into siRNA through the RNAi pathway and ultimately targeting viral gene products for destruction-halting viral propagation. Degradation of dsRNA is facilitated by Dicer, an RNase III endoribonucease enzyme, that is located in the cytoplasm. Dicer cleaves dsRNA into hallmark 21-25 nucleotide RNA duplexes, or siRNAs, each with a 2-nucleotide overhang at the 3' end (Lochmatter and Mullis 2011). The cleavage is thought to be cyclic so that Dicer binds dsRNA and repeatedly cleaves 22 bp until the entire dsRNA is obliterated (Lochmatter and Mullis 2011). Following cleavage, the ~22bp siRNA duplex remains associated with Dicer and one strand of the duplex is loaded into the RNA induced silencing complex (RISC) (Cullen 2004).

RISCs are ribonucleoprotein complexes made up of Argonaute proteins and contain the siRNAs for targeting of mRNA transcripts with complimentary sequences. The Argonaute protein family members all contain a PAZ domain that can bind siRNA and a PIWI domain to provide 'slicer' or nuclease activity (Valencia-Sanchez 2006). The main enzyme that confers RISC with its endonuclease or 'slicer' activity for target mRNA is Ago2 (Liu 2004). Ago2 coexpression also substantially increases sequence specificity of siRNA to its target as demonstrated by increased EGF receptor knockdown upon addition of Ago2 except for in the case where the EGFR mRNA has been mutated (Diederichs 2008).

MEDIATION OF GENE EXPRESSION USING RNAI RESPONSE AND MICRORNAS

The discovery that small, noncoding RNAs (20–30 nucleotides) can regulate the expression of genes was first made in C. elegans. Researchers found that a small, 21-nt RNA molecule, called *lin-4,* regulated *lin-14,* a developmental gene in C. elegans (Lee, Feinbaum and Ambros 1993). More intriguing to these researchers, was that the lin-4 molecule did not code for a protein, and instead, contained complementary sequences to the lin-*14* mRNA, targeting lin-*14* for translational inhibition through the RNAi pathway (Lee, Feinbaum and Ambros 1993). These RNA regulatory molecules, termed microRNAs, are now known to be abundant in the human genome where at least 1000 of these microRNAs (miRNAs) are hypothesized to have a key role in regulating many biological processes, including 30% of coding genes (Lochmatter and Mullis 2011).

The biogenesis of miRNA differs from siRNA because siRNA is cleaved from long dsRNA in the cytoplasm by Dicer, and does not require any prior processing. Conversely, miRNAs are transcribed from genes, introns or separate transcription units, all of which are located in the nucleus, and to facilitate Dicer cleavage in the cytoplasm, additional processing of miRNAs is necessary. The miRNA biogenesis pathway is comprised of RNA intermediates: primary-miRNA, pre-miRNA hairpin and the miRNA duplex (Figure 1.3.1). To initiate the biogenesis of mature miRNA, RNA polymerase II transcribes a several hundred-nucleotide primary-miRNAs (pri-miRNAs) from the genome (Lochmatter and Mullis 2011). Pri-miRNAs have a hairpin-shaped stem-loop that lacks perfect base pairing and can lead to 'bulges' in the initial secondary structure, which are often carried into the mature miRNA (Lochmatter and Mullis 2011). Within the nucleus, pri-miRNA hairpin associates with a large nuclear microprocessor complex composed of Drosha (RNase III endonuclease) and an essential cofactor, DiGeorge syndrome critical region gene 8 (DGCR8) (Lochmatter and Mullis 2011). DGCR8 binds the stem-loop structures of pri-miRNA and Drosha, like Dicer, cleaves the pri-miRNA about 70 nucleotides away from the hairpin loop leaving a 2-nucleotide 3' overhang (Lochmatter and Mullis 2011). The 60-80 nucleotide hairpin-RNA duplex that is released from Drosha is termed the pre-miRNA and is further processed in the cytoplasm, however since pre-miRNA resides in the nucleus, it must associate with Exportin-5 nuclear exporter protein, to be translocated out

of nucleus (Cullen 2004). Similar to the fate of dsRNA, once pre-miRNA is in the cytoplasm, the molecule is subjected to Dicer cleavage. Dissimilar to dsRNA, however, pre-miRNA cleavage serves in the removal of the hairpin loop to liberate the mature miRNA, a 22 nucleotide RNA duplex with 2-nt 3' overhangs (Cullen 2004). Once cleaved by Dicer, the rest of the RNAi pathway is similar to that of dsRNA whereby miRNAs are unwound and one strand is incorporated into the RISC complex to induce gene silencing (Lochmatter and Mullis 2011). Since siRNAs are almost perfectly complementary to target mRNA, siRNA gene silencing is usually facilitated by endonucleolytic cleavage of the mRNA transcript. However, if mismatches and bulges are present during base pairing, as observed in most naturally occurring miRNA, translational repression generally occurs (Lochmatter and Mullis 2011).

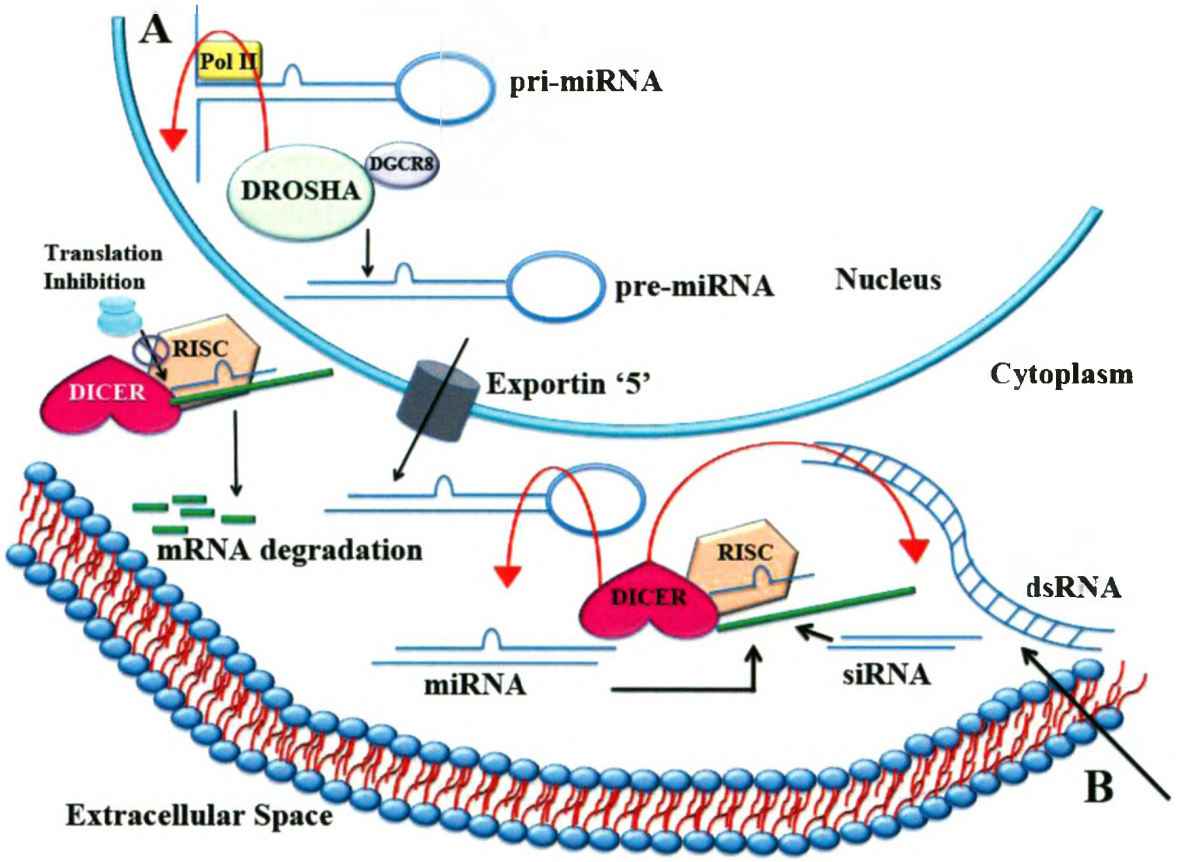

Figure 1.3.1: The RNAi pathway

A. RNA Polymerase II (Pol II, yellow) transcribes the several hundred-nucleotide long pri-miRNA from the endogenous genes in the nucleus. DROSHA (RNase III endoribonuclease), in association with an essential co-factor, DGCR8, cleaves the pri-miRNA about 70 nt from the hairpin, liberating a pre-miRNA. Pre-miRNAs are transported out of the nucleus and into the cytoplasm by the nuclear export factor, Exportin '5'. In the cytoplasm, the hairpin-loop is excised by DICER (RNase III endoribonucease), and this yields a 22-nt mature miRNA duplex. One of the strands from miRNA can be incorporated into RISC for translational inhibition of the mRNA (green) possibly by preventing the ribosome from entering. **B.** The exogenous entry of dsRNA into the cytoplasm triggers the RNAi pathway. Long dsRNA is recognized by DICER and cleaved into 22-nt siRNA duplexes. One strand of the duplex is loaded into RISC and the target mRNA (green) is degraded.

1.3.2 RNAi and Genomics

Synthetic RNAi Molecules and Delivery Methods: Benefits and Drawbacks

Synthetic siRNA, shRNA, or shRNA-microRNA molecules can be artificially expressed in cells and enter the RNAi pathway for RISC-associated mRNA degradation or translational suppression. This section provides the benefits and drawbacks for using these synthetic molecules in experiments requiring gene knockdown.

Synthetic small interfering RNA (siRNA) molecules

A. Fire *et al*, demonstrated that the introduction of long dsRNA (>500 nt) can induce specific gene silencing in C. elegans (Fire 1998). In mammals, however, introduction of such large RNA molecules activates an interferon response normally used in viral infections, and ultimately results in cell apoptosis (Lee and Esteban 1994). At first, this led to a roadblock in RNAi-mediated gene silencing in mammalian cells, however, a breakthrough was made upon the discovery that short (<30 nt) synthetic dsRNAs, termed siRNAs, could initiate RNAi-induced gene knockdown without eliciting the interferon response (Elbashir 2001). Several studies have since used synthetic siRNA, or similar versions, to elicit specific gene knockdown through the RNAi pathway, proving this genetic tool to be a powerful means of studying mammalian gene function (Simpson 2008; Bric 2009; Smolen 2010 and Lara 2011).

One advantage of siRNA molecules is that due their small size (~22nt) requirement, the chemical synthesis of synthetic siRNA is quick and easy for manufacturers (Sandy, Ventura and Jacks 2005). This is a major bonus when utilizing these molecules in gene knockdown experiments because the turn around time is quick and the costs are low. Another bonus of siRNA is that these molecules generate quick and robust knockdown in cells in vitro, because they can immediately associate with the RISC complex in the cell cytoplasm following delivery, negating Dicer (Lochmatter and Mullis 2011). Despite their rapid trigger of gene knockdown, siRNA molecules are diluted out in rapidly dividing cells and gene knockdown is only transient (maximum 1 week) in this context and costs could increase if the knockdown is needed over a longer time course, presenting major drawbacks to these molecules (Sandy, Ventura and Jacks 2005). Another potential

drawback is that siRNA must be delivered in a liposomal carrier, such as a transfection reagent, that will interact with the cell membrane and be taken up by the cell. While liposomal transfection agents can be user friendly, they often come at a high cost and further drive up the price of gene silencing in experiments where prolonged gene knockdown is necessary. Furthermore, not all cells are permissive or 'easy to transfect' and so gene knockdown in this fashion would not be feasible (Sandy, Ventura and Jacks 2005). These drawbacks of siRNA can be overcome by the introduction of short-hairpin RNAs (shRNAs) and viral transduction methods.

Plasmid short-hairpin RNA (shRNA) molecules

Short-hairpin RNAs are produced from single-stranded molecules of 50-70 nts that form a stem-loop, or hairpin, when the single strand folds back onto itself. A loop is formed because the molecule is designed to have two complementary 19-29 nt RNA fragments (the stem), leaving 5 to 10 nucleotides to form a loop from a lack of complementary base pairing in this region. The shRNA-encoding DNA fragment is almost always ligated into a DNA plasmid for ease of delivery. Once inside the nucleus, the shRNA-encoding DNA is transcribed into RNA, with the hairpin secondary structure intact, using RNA polymerase III promotors (for example; tRNA-val[33], U6 and H1) (Sandy, Ventura and Jacks 2005). A benefit to transcription using Pol III promotors is that they are active in all cell types providing continuous expression of the shRNA (Sandy, Ventura and Jacks 2005). Following transcription, the shRNA is transported to the cytoplasm and recognized by Dicer. Dicer essentially cleaves off the loop portion of the hairpin and the resulting product is identical to siRNAs (made of ~22nt and with 2-nt 3' overhangs) and is subsequently incorporated into RISC (Lochmatter and Mullis 2011). One huge advantage of using shRNAs incorporated into plasmid vectors is that gene knockdown can persist over time from stably transfected plasmids carrying an antibiotic resistance gene. Also, the introduction of an shRNA into a retro-or lentiviral vector allows for the stable integration of shRNA and antibiotic resistant genes into the genome for indefinite expression under antibiotic pressure (Dickins 2005). The use of viral vectors to carry shRNAs into the cell also circumvents the issue of the transfection-resistant cells since virus particles can infect many cell types including non-dividing, primary cells. A potential fallback of the viral

vector shRNA delivery system is that there is more start-up time for experiments because the shRNA must first be cloned into the viral vector, which could also introduce shRNA sequence errors, followed by 'packaging' of the vectors into virus particles for cellular transduction. Another fallback of the viral vector delivery system is the risk of shRNA integration into the host genome at undesirable locations. Retroviruses prefer to integrate near transcriptional start sites and this enhances the possibility for gene perturbation in host cells (Liu and Berkhout 2011). Self-inactivating (SIN) vectors have been developed to rectify this problem by removing regions on the viral vector that may interfere with cellular gene expression (Liu and Berkhout 2011). Also, lentiviruses have been used for shRNA delivery more frequently due to their preference to integrate within introns of active transcriptional units, which limits their ability to interfere with coding genes (Liu and Berkhout 2011).

Plasmid short-hairpin RNA-microRNA (shRNA-mir) based molecules

This new class of synthetic RNAi triggering molecules improves upon previous shRNA designs by taking into account the expanded knowledge of the RNAi pathway in mammalian cells. Initially, shRNA constructs were based upon a somewhat simple hairpin RNA, identical to the pre-miRNA intermediate (Silva 2005). When these constructs were made, understanding of the miRNA maturation process was still incomplete, in particular, the involvement of primary or pri-miRNA and the interaction it has with Drosha. In light of the advances made in our understanding of miRNA maturation, a new generation of shRNA constructs (shRNA-miR) have been developed and are modeled after more naturally occurring miRNAs, specifically, the primary miR-30 backbone. The actual design of the microRNA-30 based hairpin design evolved from the fact that endogenous primary miRNAs require a long flanking sequence (Silva 2005). MicroRNA-30 based hairpin design, therefore, incorporates a 125 nt flanking sequence on both the 5' and 3' ends of the hairpin that was derived from the human miR-30 primary transcript sequence (Silva 2005). The hairpin stem consists of 22 nt of dsRNA, complementary to the gene target of interest, and a 19nt loop from human miR30 (Silva 2005). This design adds a Drosha processing site to the hairpin construct and results in 12-fold increase in Drosha and Dicer processing of the expressed hairpins when compared with conventional shRNAs

(Silva 2005). Furthermore, gene suppression is more effective in this new 'natural' redesigned molecule in comparison to the simple hairpin design, possibly because miR-30 based design is more effective in producing mature synthetic miRNAs (Boden 2004 and Silva 2005). For example, in mammalian cells infected with laboratory strain of HIV-1, the miR-30 design was 80% more effective in knocking down the HIV tat protein than conventional shRNAs (Boden 2004). The majority of primary miRNAs are transcribed by RNAse II polymerase at Pol II promotors (CMV, MSCV) (Silva 2005). A comparison of the knockdown efficiency of shRNA-miRs, driven by various promoters, demonstrated that shRNA-miRs are more highly expressed by the pol II promotor CMV or, interestingly, the U6 pol III promotor (Silva 2005). Therefore, the incorporation of either a U6 or CMV promoter is often used in the design of shRNA-miR vectors to give the most consistent repression.

These second generation shRNA molecules, shRNA-miRs, can be delivered either by transfection or transduction, both of which introduce the stable expression of shRNA and mediate long term gene knockdown in many cell types. The same drawbacks of conventional shRNA are applied to the new design, since the effect of genome integration following viral infection is not guaranteed to provide insertion into inert locations and spare host cell gene expression. However, as mentioned above, precautions have been taken to avoid such events. Some added benefits of the newly designed molecules, aside from the obvious enhanced gene knockdown, are that many companies are offering viral particles with pre-packaged constructs, at an added cost, but allowing for less start up time for experiments. Also, since mir-30 shRNA designs are more naturally occurring in the cell, they are less likely to interfere with endogenous gene regulation unlike shRNAs and siRNAs that skip Drosha processing, and siRNAs that also skip Dicer processing, and can effectively 'monopolize' the RISC complexes and halt endogenous gene regulation by microRNA (Lochmatter and Mullis 2011).

GENOME- WIDE GENE KNOCKDOWN USING SHRNA LIBRARIES

Since the phenomenon of RNAi was first discovered 13 years ago, progress has been made in understanding the biosynthesis of molecules within the pathway, and this knowledge has been used to generate effective gene silencing. Today, RNAi is a useful genetic tool to study the function of individual genes in the context of many experimental conditions. In addition, collections of RNAi effector molecules, whether siRNA, shRNA or shRNA-miR, have been pooled together to represent almost all annotated genes in both the human and mouse genomes. In this manner, an abundance of screens for loss-of-function phenotypes have been reported, many using one of the commercially available 'libraries' in mammalian cells. All of the RNAi screens to date are based on the method of integrating one shRNA expression vector per target cell, subsequently leading to knockdown of one gene per clone, and reducing confounding results of multiple gene silencing (Boettcher and Hoheisel 2010; Lara 2011; Simpson 2008 and Smolen 2010). Identification of the shRNA template sequence in each cell, by means of a molecular tag, can then be easily performed in smaller screens by PCR amplification of the molecular tag, followed by sequencing or in larger screens by microarray hybridization techniques. The published RNAi screens to date are representative of the feasibility of these shRNA libraries and have contributed to major improvements and rigorous quality control measures made on these commercially available libraries over the last 6 years. Pooled shRNA libraries have proven to be effective tools for performing high-quality, high-throughput screens both in cell culture end point assays and when applied to screening for phenotypic attributes of cells *in vivo.*

Commercially available shRNA libraries

Due to the demand for RNAi technology, at least three shRNA-based libraries have been made commercially available. These libraries differ with respect to the amount of human genes they can target, the amount of shRNAs covered each gene, the means by which shRNAs are identified, the type of shRNA molecule and even the vector backbone used to carry the shRNA cassette.

Two of the commercially available libraries were selected to compare in this discussion as they were used to carry out two distinct aspects of the thesis project: 1) the Hannon and

Elledge library (H&E) and 2) The RNAi Consortium (TRC). A substantial portion of the H&E library was used to carry out a screen for mediators of migration in a cancer cell line, while individual constructs from the TRC library were used to establish a proof of principle for the migration screen.

Hannon and Elledge

The Hannon and Elledge (H&E) library has gone through considerable changes over the past 6 years beginning with the construction of their first generation library to the creation of a second-generation library covering 32,216 human genes (as of June 2006) (Chang, Elledge and Hannon 2006). H&E first generation libraries are composed of 29 nt shRNAs, made to mimic pre-miRNAs. Conversely, second-generation shRNA expression libraries consist of >125 nt shRNA-miRs, modeled after the naturally occurring primary miR-30 transcript (Silva 2005). The new libraries are substantially improved over their first-generation counterpart and are 12 times more effective in producing siRNA molecules (Silva 2005).

For construction of the second generation library, 'Ink Jet' synthesis (Agilent Technologies, Inc.) was used to make 22-24 thousand oligonucleotides per microarray, each containing a different shRNA-miR construct (Cleary 2006). In this manner, >195 000 oligonucleotides, representing more than 32, 000 known and predicted genes in humans, was generated (Silva 2005). The shRNA inserts were eluted from the glass array and amplified by polymerase chain reaction (PCR) so that they could be inserted into the pSM2 retroviral vector in pools (Cleary 2006 and Silva 2005). Altogether, 87,283 shRNAs targeting 32,216 human genes and 76,896 shRNAs targeting 30,629 mouse genes have been created using ink jet synthesis for the second generation library (Chang, Elledge and Hannon 2006). While 34% of the human genes represented in the library are covered by 3 shRNAs, the goal is to generate at least three shRNAs for each target gene (Chang, Elledge and Hannon 2006). The full collection of mouse and human shRNAs can be accessed at RNAi Codex (http://codex.cshl.edu/).

A U6 promoter drives expression of the shRNA-miR, however shRNA inserts can be easily moved into different vectors with alternative promoters, such as CMV, via a

recombination strategy (Silva 2005). This modification has been performed by Open Biosystems to create the lentiviral pGIPZ construct, and uses the CMV promoter to drive shRNA-miR expression.

Immediately following each miR-30 cassette is a RNA polymerase III termination signal and a randomly generated 60-nt 'barcode' region to identify individual shRNAs in large populations (Silva 2005). In general, molecular tags such as the H&E 'barcodes' work by PCR amplification of sequences unique to the shRNA construct but using primers common to all constructs (Boettcher and Hoheisel 2010). In this manner, all genomic DNA is collected, following infection of a population of cells, and the PCR product amplified from the genomic DNA contains multiple tags, representative of many different shRNAs introduced into the population. The PCR products are ubiquitously labeled with a fluorescent dye and each labeled tag will hybridize to complementary sequences spotted on the oligonucleotide microarray (Boettcher and Hoheisel 2010). Each spot is of a known sequence and so identifies the shRNA linked to the fluorescent tag. In this way, the abundance of given shRNAs in a cell population are indirectly analyzed by signal intensity as a complementary tag binds. This is a quick technique to detect the gain and loss of signal for shRNAs, and thus the genes with positive and negative effects on a cell population.

The molecular tag used by the H&E libraries are external 60 nt barcode, present in every shRNA-miR expression vector, and are an exclusive feature of the H&E library (Boettcher and Hoheisel 2010). Although other libraries have molecular tags to identify the encoded shRNA inserts, the H&E barcode is unique because it is located downstream from the shRNA template and was sequence validated, linking each barcode to a given shRNA expression construct (Boettcher and Hoheisel 2010). In contrast, the H&E libraries that are used to perform smaller scale screens can, like other commercially available libraries, use the actual shRNA hairpin sequence, with the forward primer upstream of the hairpin, and the reverse primer downstream, so that the actual shRNA is sequenced for gene identification (Boettcher and Hoheisel 2010).

The RNAi Consortium (TRC)

The RNAi Consortium (TRC) library was in production at the same time as the H&E library, however, this library has taken a different approach: resulting in far less genome coverage than the H&E library, but double the number of shRNAs covering each individual gene. Specifically, the TRC library covers 14, 538 human genes, however, the amount of shRNAs created between the two groups are almost the same: 77,301 shRNAs for TRC (July, 2006) and 87,283 for H&E (June 2006) (Root 2006 and Chang, Elledge and Hannon 2006). The significance of taking such an approach is to increase the confidence in positive hits by avoiding 'off-target effects', or occasions where shRNAs will bind unintended sequences, thereby knocking down the wrong gene. In this respect, the H&E library falls short with half the number of shRNAs/gene target compared to the TRC library.

To the dismay of the scientists involved in the design of the TRC library, their library was constructed using the pre-miRNA model, containing 21-nt stems and a 6 nt loop, as an RNAi trigger. Although engineers of the H&E library showed a significant increase in siRNA production using more 'natural' shRNA-miR-30 constructs, the TRC library does not contain this technology and the scientists involved explain that it is "important to determine whether improved knockdown is due to the miRNA context, or whether other shRNA design and vector attributes are more important for enhanced gene suppression" (Silva 2005 and Root 2006). TRC library shRNAs were originally produced using conventional oligonucleotides synthesis, but have since been produced in a similar manner to H&E library using chip synthesis of oligomers to reduce cost. Harvested shRNA oligomers were then amplified and cloned into the pLKO.1 vector (Root 2006).

The TRC library is composed of a simple vector design, containing the shRNA cassette in the pLKO.1 vector. pLKO.1, like the pGIPZ vector, is a third generation, self-inactivating lentiviral based vector. Self inactivating (SIN) vectors are designed so that the viral particles can package the shRNA containing vector for delivery to cells, however once inside the cell, the viral particles do not have the capacity to replicate and so the cell will not harbor a viral infection and user safety is enhanced (Root 2006). Furthermore, third generation lentiviral vectors are generated using a three-plasmid packaging system that

separates essential viral assembly genes: gag, pol and rev and the gene encoding VSV-G envelope or viral coat protein into separate vectors (Root 2006). This minimizes the possibility of these sequences recombining into viruses that have the capacity to replicate. Also, as mentioned previously, SIN vectors are designed to insert into non-coding regions of the genome, to reduce the risk of interfering with endogenous gene expression (Liu and Berkhout 2011). In both H&E and TRC libraries, the U6 promoter is used to drive expression of the shRNA cassette, and the PKG promoter is responsible for expression of the puromycin resistance gene to allow selection of transduced cells. An exception is the pGIPZ version of the H&E library, which relies on the CMV promoter to drive expression of both the shRNA-miR and the puromycin resistance gene, however there is an internal ribosomal entry site or IRES before the puromycin resistance gene to help ensure its expression. The TRC library uses half-hairpin tags as a method to identify shRNA constructs. Half-hairpin tags are made useful by PCR amplification of the antisense strand of the shRNA sequence itself.

Finally, it should be noted that in both libraries 1 out of 3 shRNA expression constructs, targeting a given gene have been verified to knockdown gene expression by at least 70% (Boettcher and Hoheisel 2010). However, this information must be taken with a grain of salt, as not all cell lines will behave in a similar manner to the cell lines used for validation by the commercial suppliers.

Table 1: Comparison of Key Features of Hannon and Elledge (H&E) and The RNAi Consortium (TRC) Commercially Available shRNA Libraries

	Hannon and Elledge (H&E)	The RNAi Consortium (TRC)
Distributor	Open Biosystems, Thermo Scientific	Open Biosystems, Sigma-Aldrich, Partnered with Ontario Institute of Cancer Research (OICR)
Retroviral Vector	pSM1 (1st generation) pSM2 (2nd generation) Self-inactivating	None
Lentiviral Vector	pGIPZ Third generation, Self-inactivating	pLKO.1 Third generation, Self-inactivating
Number of Genes Covered	As of June 2006: 32,216 human genes 87,283 shRNAs	As of July 2006: 14,538 human genes 77, 301 shRNAs
Average Number of constructs/gene	2.5 pGIPZ 2.8 pSM2	5
shRNA insert	shRNA-miR-30 (primary-miRNA RNAi trigger): 22 nt stem, 19 nt loop, flanked by 125 nt of miR-30 sequence on both 5' and 3' end of stem	shRNA (pre-miRNA RNAi trigger): 21 nt stem, 6 nt loop
Molecular Tag	60 nt external barcode or hairpin	Half -hairpin

Adapted from Boettcher, M. and Hoheisel, J.D. *Current Genomics* (2010),11:162-167

Screening for mediators of migration using shRNA libraries

Genetic screens to identify genes involved in a phenotypic outcome are becoming increasingly popular ever since the introduction of highly efficient, commercially available RNAi libraries for mammalian cells. Many of the screens in the literature are aimed at understanding molecular pathways involved in human cancer cells. These screens have focused on the hallmarks of cancer including, but not limited to: cell proliferation pathways, tumor suppressor genes, genes involved in metastasis and genes required for cell migration. These screens have greatly increased our understanding of the progression of cancer and identified novel markers of cancer for further study. RNAi screens for cell migration in human cancer constitute a relatively small subset of cancer related genetic screens and 100% of RNAi screens for cancer cell migration are performed *in vitro*. In this section I will introduce a few key genetic screens that have been performed in human cancer cells, to identify mediators of migration, with a focus on the methods used to measure cellular migration, and one genetic screen that has been performed *in vivo*, however, not directly looking at cancer cell migration.

Screening for mediators of migration *in vitro*

Wound healing

One of the early cell migration-based RNAi screens published, was performed in MCF-10A cells, an immortalized, yet non-tumorigenic, breast epithelial cells using a 'scratch wound' or wound healing assay (Simpson 2008). The scratch wound assay involves plating cells to confluence, after which a wound is made in the layer of cells. The cells are imaged at time zero, and a given time after the wound is made, and the rate at which the wound closes is related to the migration capacity of cells as they move towards the center. One parameter that must be normalized, or at least taken into account when performing this assay, is the cell proliferation status between the cells containing various siRNA constructs. An siRNA that causes cell proliferation or decreases cell proliferation could influence the number of cells breaching the wound area, therefore, the assay would represent a measurement of proliferation rather than migration. To accommodate for this, some groups have characterized the rate of proliferation for cells prior to experimental

testing using chemical based assays such as MTT. MTT or 3-(4,5-Dimethylthiazol-2-yl)-2,5-diphenyltetrazolium bromide, is a yellow tetrazole that, when in living cells, is reduced to purple formazan by mitochondrial enzymes (Scudiero 1988). The intensity of the purple is read by a spectrophotometer and corresponds to the amount of live cells per well. However, another method was employed by J.A Brugge's group and includes the use of another chemical reagent, Alamar Blue to test the cytotoxicity, or reduction in cell numbers upon addition of each siRNA on the MCF-10A cells just prior to wounding the cells (Simpson 2008). Alamar blue is a membrane permeable, non-toxic dye that upon reduction by living cellular enzymes, produces a measurable fluorescent signal and is, therefore, a measure of cell viability, proliferation and metabolism (Simpson 2008). Two siRNA libraries, targeting a total of 1,081 human genes, were used to perform the screen for migratory genes in MCF-10A cells. One library of siRNAs covered the human phosphatase and kinases and the other was a migration and adhesion related (MAR) library, targeting known or predicted genes involved with migration (Simpson 2008). Transient knockdown of siRNAs that reduced or accelerated migration were then validated using a second trial of scratch wound assays, however with individual shRNAs from TRC targeting the same genes. In this respect, knockdown of genes identified as being important to migration from the first scratch wound assay, were confirmed by stable gene knockdown in a second scratch wound assay.

This 2008 screen, performed by J.S. Brugge's group, paved the way for future screening for cell migration mediators, identifying 66 validated and high confidence genes involved in migration, 42 of which were not previously associated with motility or adhesion. However, this screen is still lacking a measure of physiological cell migration since the screen is performed as cells randomly migrate across a rigid substratum, without a matrix to recapitulate cell movement *in vivo*. As discussed in the cell migration section, cell adhesion molecules (CAMs) signal to internal regulators of migration based on their interactions with the ECM and environmental cues such as chemoattractants, resulting in the release of proteases, invasive structures, and exhibiting directional cell migration in realistic 3D environments. In a plastic dish, the invasive structures, such as invadopodia, may not form due to the lack of substratum to 'burrow' into. In addition, proteases may not exert their normal functions in a plastic dish or their secretion may be downregulated due

to the lack of invadopodia formation. In addition, CAMs, such as integrins, initiate signaling upon binding to collagen or fibronectin and receive signals from neighboring receptors associated with growth factor ligands. Without such matrices and external stimuli, the cell migration witnessed in this initial screen may not reflect true mediators in an *in vivo* context, whereby cells move with directionality towards a stimulus using structures necessary to manipulate 3D environments.

Boyden Chamber

In the two years following the scratch wound-based screen for migration-associated genes, at least two additional screens for cell migration emerged, however they were both based upon migration through a boyden chamber. Boyden chamber assays measure the ability of cells to move across a perforated plastic membrane, usually with pores about 8.0 um in size. Cells are suspended in serum free, chemoattractant-free media in the upper chamber, above the membrane. Over a time course of about 18-48 hours, cells that have the capacity to migrate will move through to the opposite side of the membrane, thus the membrane acts as a physical barrier between the less migratory and more motile cells. Furthermore, the cells travel towards a lower chamber containing a chemoattractant, such as serum, so that the migration is directional. The physical separation between the migratory vs non-migratory cells is an attractive feature for RNAi screening because cells that make it across the membrane can be harvested, and the hairpins identified by conventional PCR (Finlayson and Freeman 2009 and Smolen 2010). Individual shRNAs can also be introduced into separate cell populations that are then placed in their respective chambers followed by a quick staining of the bottom of the membrane for a direct comparison of migration between cells infected with various shRNAs (Smolen 2010). In their study, G.A Smolen *et al.* performed an RNAi screen using 55, 000 pooled lentiviral shRNAs from the TRC library targeting ~11,000 genes using MCF-10A cells (Smolen 2010). They performed a primary screen, allowing cells to migrate through the transwell of a boyden chamber, towards a chemotactic stimulus, following infection with the shRNA library (Smolen 2010). Cells that migrated were considered 'highly migratory' and they were harvested for shRNA identification (Smolen 2010). shRNAs identified through this primary screen could then be individually infected into MCF-10A cells so that

confirmation of the increased migratory capacity could be re-examined by staining the bottom of transwell membranes for direct comparison between various shRNAs (Smolen 2010). A.E. Finlayson and K.W. Freeman also performed a cell motility screen using boyden chambers, however in these chambers, the membranes were overlaid with Matrigel ™ to select for pro-invasive genes (Finlayson and Freeman 2009). Matrigel ™ is a proprietary basement membrane extract composed of extracellular matrix proteins and thus acts as an *in vitro* 3D-model of cell migration, recapitulating the *in vivo* phenotype to a higher degree than the membrane-only boyden chamber and the scratch wound assay.

Screening for mediators of migration in vivo

Although the boyden chambers, with Matrigel™ inserts, are a better representation of the 3D environment cells normally migrate in and provide matrix proteins to facilitate downstream signaling by CAMs, they are still lacking a true *in vivo* setting. An *in vivo* setting includes interactions between not just the migrating cells in question, but also the surrounding stroma cells, immune cells, blood vessels and the multitude of components in the ECM including ligands acting as triggers of downstream signaling. An elegant study for the identification of tumor suppressors in a spontaneous lymphoma mouse model highlights the ability to perform large RNAi screens *in vivo* (Bric 2009). In their study, A. Bric *et al.* took fetal mouse liver hematopoietic stem cells (HSCs) with a E_u-Myc background, so as to facilitate lymphoma progression, and infected them with the 'Cancer' 1000 set (collection of shRNA-miR-30 molecules targeting 1000 cancer related genes from the H&E library) (Bric 2009). To establish a phenotype for screening, irradiated, syngenic recipients were injected by tail vein with the shRNA-miR-30 containing stem cells and onset of lymphoma was monitored in the animals receiving shRNA-containing cells versus control shRNA-containing cells (Bric 2009). In this study, the phenotype was tumourogenesis instead of cell migration, however this screen invites others to try an *in vivo* screen where the phenotype is cell migration. The caveat is that mouse models are not transparent and so witnessing a phenotype for cell migration is not straightforward. Furthermore, to perform a representative screen of a large portion of the *human* genome, not only would an exorbitant amount of animals need to be used, but also the animals would need to be tolerant to human cancer cells. In the next section, I will introduce an

animal model that is conducive to witnessing cell migration phenotypes using intravital imaging, is cost effective when performing large-scale RNAi screens and can tolerate human cells: the ex-ovo chicken embryo model.

1.4 A Model of Human Cancer Cell Migration: The Ex-Ovo Chicken Embryo

The chicken embryo model offers many advantages for performing cell migration and metastasis assays including: (1) an immunodeficient host that is permissive to transplantation of foreign tissues, including human cancer cells, (2) a platform for analysis of the different stages of metastasis using either an experimental or a spontaneous mode of cancer dissemination, (3) accessible membranes that are external to the embryo and contain vasculature, stroma cells and extracellular matrix components to recapitulate the tumour microenvironment and provide a 'window' into visualizing cancer cell movement, and (4) is inexpensive and establishes tumorogenesis and metastasis within 7 days, saving time and labor.

At the heart of the chicken embryo model is the chorioallantoic membrane or CAM. This specialized tissue is attached to the eggshell and can be liberated by removal of a 'window' of shell for experimental manipulation and observation. The ex-ovo chicken embryo model provides even easier access to the CAM by allowing the embryo to develop outside of the egg. In this manner, the CAM is fully exposed and can be utilized for cancer cell growth, invasion and migration studies.

1.4.1 Anatomy of the Chicken Embryo Used to Study Cell Migration

The chorioallantoic membrane (CAM) is a versatile organ for studying cancer cell migration and invasion due to its capacity to support human tumour cells and the ease at which cancer cells can be monitored. The CAM is formed between days 5 and 6 of embryo development by the fusion of the chorion and allantois for the purpose of gas exchange between the blood vessels within the CAM and the porous eggshell (Ribatti 2010). The CAM is an extremely thin organ (100um thick) and is composed of three, distinct layers (Figure 1.4.1) (Deryugina and Quigley 2008). The ectoderm is a one or two-cell epithelial layer that attaches to the shell membrane or at the air interface in ex-ovo models (Deryugina and Quigley 2008). At day 10 of development, the ectoderm is fully developed and contains a capillary plexus (network of capillaries), which serves as one of the most important features of the CAM in regards to invasion and metastasis (Ribatti 2010). The

ectoderm capillary plexus supports transplantation of human cancer cells and promotes tumour progression through the formation of new blood vessels (neoangiogenesis) that feed the growing tumor (Deryugina and Quigley 2008). Underlying the ectoderm is the mesoderm that contains blood vessels, terminal capillaries, fibronectin, laminin and type IV collagen fibers, and stromal cells (Deryugina and Quigley 2008). Finally, the endoderm, composed of a monolayer of cells, along with the ectoderm effectively 'sandwiches' the mesoderm. (Deryugina and Quigley 2008). Since the CAM is thin, transparent, and is the outermost layer of the embryo, experimental injection of fluorescently labeled human cancer cells into the vasculature of the embryo permits cancer cell visualization using a standard upright fluorescent microscope. Following injection, cancer cells are seen first within vessels, and later, post-extravasation, the cells can be observed within the stroma. Alternatively, cancer cells can be inoculated directly onto the ectoderm of the CAM and in this spontaneous model of invasion; cancer cells can be directly visualized at the tumour cell border invading into the stroma.

1.4.2 Methods Used to Study Cell Migration and Metastasis in the Chicken Embryo

Experimental Metastasis Model

The experimental model of metastasis in the ex-ovo chicken embryo involves the injection of human cancer cells directly into the vasculature, after which, the cells will circulate throughout the embryo and transmigrate into tissues at the site of extravasation. The tissues that tumour cells arrest in post-extravasation include not only the CAM, but also organs such as the lung, liver, and brain. When cells arrest in the ectoderm of the CAM, however, they have extravasated out of the capillary plexus and migrated through the stroma, oftentimes towards arterioles in which they wrap themselves around before proliferating into micrometastases (Chambers 1995). In the experimental model of metastasis, the formation of micrometastases begins within hours of injection and although growth of micrometastases are dependent on the proliferation rate of the cell line, most aggressive cancers achieve sizable colonies within 7 days. The downside to the experimental model is that the early steps of metastasis, such as invasion and intravasation into the blood vessels

are eliminated, however, local invasion of cells from progressing micrometastases can still be observed as well as the capacity for these cells to colonize different tissues.

Spontaneous Metastasis Model

Topical administration of cancer cells

The CAM model for spontaneous metastasis takes into account the early steps of metastasis, tumor cell invasion from the primary tumour and intravasation into the vasculature. This model involves the topical inoculation of 20-30ul of human cancer cells onto the surface of the ectoderm following the abrasion of this membrane to promote local angiogenesis. Depending on the number of cells inoculated and their rate of proliferation, most primary CAM tumours are in the range of 200-600 mg after 7 days post transplantation. Simultaneous to tumour growth, aggressive tumour cells can invade the surrounding stroma and intravasate into blood vessels, causing their dissemination to distant organs. At these organs, cancer cells can grow into micrometastases that are visible by fluorescence microscopy of fluorescently labeled cells or by histological analysis. In this manner, all of the steps of the metastatic cascade are performed, however, this process is over 6-7 days rather than the typical 4-10 weeks for murine models (Ribatti 2010).

Bolus administration of cancer cells

The spontaneous model of metastasis can also be accelerated by the inoculation of tumour cells directly into the mesoderm. This procedure is reminiscent of the subcutaneous injection of tumor cells in murine models and introduces a 'bolus' of cancer cells that generate an immediate mass of cells mimicking the primary tumour. Cells that have been inoculated into the CAM by 'bolus' injection can be imaged immediately, however after 3 days, most boli resemble similar sized tumour to topically administered cells and are more appropriate for study (Deryugina and Quigley 2008).

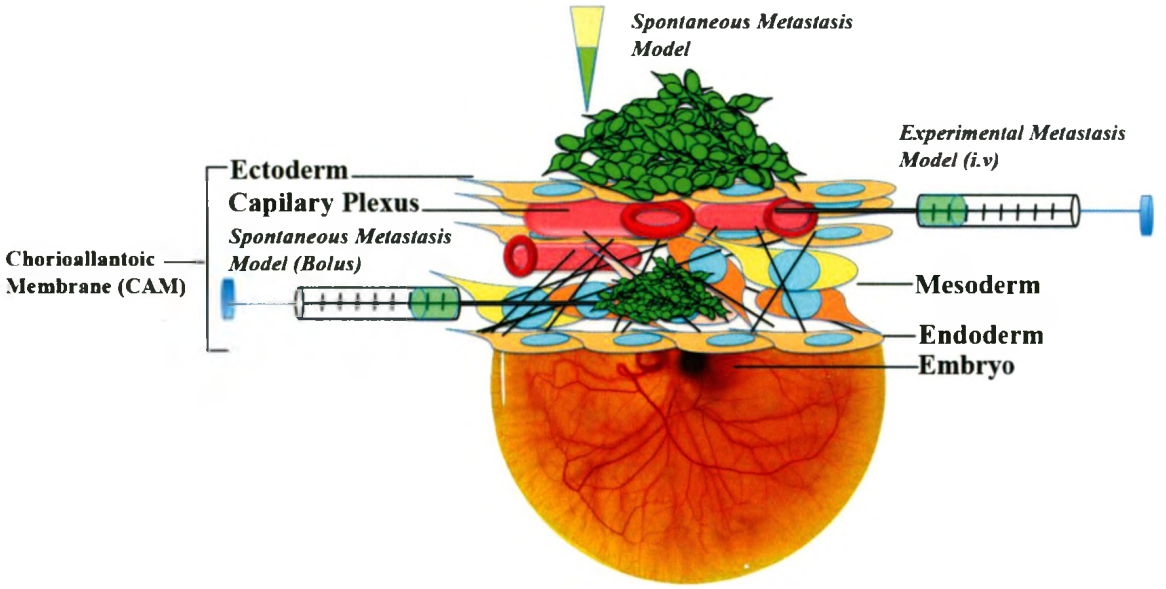

Figure 1.4.1: The ex-ovo chicken embryo model

The chorioallantoic membrane (CAM) is utilized by the embryo for gas exchange between blood vessels and the porous eggshell. The ex-ovo chicken embryo model allows for the embryo to develop outside of the egg, providing full exposure of the CAM for cancer cell growth, invasion and migration studies. The CAM is composed of three layers as depicted by a cross-sectional view: the ectoderm, a one or two-cell epithelial layer that contains a capillary plexus (network of capillaries), the mesoderm that contains blood vessels, terminal capillaries, fibronectin, laminin and type IV collagen fibers, and stromal cells and finally, the endoderm, composed of a monolayer of cells. Experimental injection of fluorescently labeled human cancer cells into the vasculature of the embryo (*Experimental metastasis assay)* permits cancer cell visualization following injection, first within vessels, and later, post-extravasation, the cells can be observed within the stroma. Alternatively, cancer cells can be inoculated directly onto the ectoderm of the CAM (*Spontaneous metastasis assay)* and can be directly visualized at the tumour cell border invading into the stroma. Another means to perform the spontaneous assay is injection of a 'bolus' of cells directly into the mesoderm of the CAM, forming primary tumours (*Spontaneous metastasis assay (Bolus)).*

Intravital Imaging of Cancer Cell Migration

In addition to evaluating the capacity for cells to metastasize to distant organs by tissue harvesting, the experimental mode of metastasis can be used to visualize cancer cells within the stroma, post-extravasation, to monitor their motility. Similarly, the spontaneous mode of metastasis can also be used to monitor early events of metastasis, such as invasion and migration, by intravital microscopy of cells at the transplanted tumor border (Deryugina and Quigley 2008 and Wyckoff 2000). A. Chambers *et al.* explain that intravital video microscopy (IVVM) allows cancer cells to be 'watched', *in vivo,* thus proving inferences about cancer cell migration and metastasis that were previously inferred from histological samples or end-point animal assays (Chambers 1995). Intravital video microscopy uses a camera attached to an epifluorescent or light microscope to visualize and record cell movement whether it be within the CAM or another animal model. The drawback of intravital video microscopy is that tissues have to be inherently thin and remain immobilized in order to transilluminate them as well as keep the cells within them in focus. The chicken embryo ex-ovo model, is the ideal model for witnessing cancer cell migration using intravital imaging because of how thin and accessible the CAM is. Using a modified immobilizing-incubation chamber, fitted with a coverslip that is placed over the area of interest, the CAM, and the cancer cells within it, are easily immobilized for the production of focused videos. A fluorescent microscope can be used to illuminate the CAM and excite fluorescently labeled cancer cells within the tissue without any background signal.

In other animal models, imaging cancer cell movement is not as straightforward because the organs to be imaged are not transparent, or the animal must undergo surgery, anesthetization or both. Although intravital imaging of cancer cell migration has been demonstrated in murine models, the technique involved is invasive and laborious (Morris 1993 and Wyckoff 2000). In mouse models, the labeled cancer cells are either injected into the blood circulation, which may require surgery to reach a vessel of interest, or injected subcutaneously. Tumour progression then occurs to the desired stage: immediately, if capturing extravasation events from cells injected into the vasculature, and up to 3 weeks if capturing invasion events from cells implanted subcutaneously (Morris 1993 and Wyckoff

2000). In either event, the mouse must be anesthetized and undergo surgery to reveal the cancer cells underneath the skin (skin flap surgery) or in the desired organ. Most concerning is the possibility of disrupting the vasculature, which could have profound influences on cell migration and metastasis during these surgeries. Also, the organs and tissues must be perfused with saline to maintain hydration, which is not only time consuming, but without careful manipulation, may influence the pressure in the surrounding tissues containing the cancer cells. Oftentimes, these murine intravital experiments can only be performed in limited occasions, and this not only increases the amount of animals used, but also contributes to variation amongst animals.

Another model used to capture cell migration using intravital, real-time imaging is the zebrafish embryo model (Stoletov 2010). The zebrafish is immunodeficient, transparent and can be transgenic to express fluorescent protein throughout the entire embryo. These qualities make the zebrafish an excellent candidate to image cancer cell migration in action, however, there are still drawbacks to using this model. For instance, animals must still be anesthetized prior to imaging and cancer cells may not be located near the exterior of the fish, resulting in the requirement for confocal microscopy to acquire a high resolution image, which is more complex and not as ubiquitously found in laboratories.

Alu *Polymerase Chain Reaction (PCR): A quantitative measure of metastasis*

In both spontaneous and experimental metastasis models, inoculation of cancer cells would normally not occur any earlier than day 9 of development. Since the embryos 'hatch' on day 21 of development, this leaves at the very most 12 days to complete a metastasis assay, whereby the organs are harvested and analyzed for micrometastases. Even the most aggressive cells do not usually form macroscopically visible colonies in the secondary organs in this short amount of time, making the detection of micrometastases the most difficult part of the assay. To remedy this situation, investigators have modified and tested the *alu* Polymerase Chain Reaction (*alu* PCR) method to detect very small populations of human cancer cells in secondary organs (Zijlstra 2002).

This extremely sensitive and quantitative method of analysis is based on the PCR amplification of human-specific-*alu* sequences in a background of chicken embryo cells.

The organs are harvested following a metastasis assay, and the mixed populations of human cancer cell DNA and chicken embryo cell DNA (from the particular organ) is extracted directly. Utilizing real-time PCR, the amount of human *alu* events are recorded per sample and permits comparison between highly metastatic cell populations inoculated into one embryo and low metastatic cell populations inoculated into another embryo (Zijlstra 2002). Creation of a standard curve, or known amount of human cancer cells mixed with the naïve organ of interest, facilitates in the quantification of *alu* signal release from the samples by comparison to the standard curve.

This method of quantification has been shown to detect as low as 25 cells/lung in the chicken embryo model of metastasis demonstrating the sensitivity of the technique (Zijlstra 2002). In addition, this method requires no processing past the PCR step, handles a large number of replicates, does not require the specialized microscopy seen with IVVM, and can be applied to both the spontaneous and experimental models of metastasis.

1.4.3 Screening for Mediators of Cell Migration in the CAM

RATIONALE

Metastasis is the cause of 90% of cancer related mortalities (Hanahan and Weinberg 2000). Therefore, the primary motivation behind this project is to halt the metastatic cascade through the discovery of targets for anti-metastasis therapies. Compelling evidence that migration is a key player in metastasis was demonstrated by previous studies performed by our group whereby the inhibition of migration with a monoclonal antibody against human tetraspanin CD151, a transmembrane protein previously published to be involved in cell motility and metastasis, abolished metastasis (Johnson 2009 and Ke 2009). In this study, the systemic treatment of anti-CD151 mAb decreased in rear detachment of human adenocarcinoma and fibrosarcoma cells at the invasive tumor border, halting migration and metastasis for both cell lines in spontaneous models of metastasis for both the chicken embryo and the SCID mouse (Zijlstra 2008). These results highlight migration as an important step to focus on out of the various steps in metastasis.

In the same study, the human cancer cells were introduced into the chicken embryo via experimental metastasis assay. In this context, the tumour cells still proliferated to form

micrometastasis in the stroma of the CAM, however, when treated by systemic administration of anti-CD151 antibody, the cells failed to invade into the CAM and remained tightly clustered (Zijlstra 2008). In other words, compared to 'diffuse' tumour colonies seen in the CAM with control cells, the tumor colonies seen upon treatment with the migration-blocking antibody established a 'compact' tumour phenotype in the CAM, consistent with a loss in cell migration.

Based on these findings, I propose that an experimental metastasis approach can be taken to perform an *in vivo* shRNA screen for targets that inhibit tumour cell migration in the CAM. Injection of fluorescently tagged, human epidermoid adenocarcinoma (HEp3) cells, harboring shRNAs against migration, can be screened using fluorescent microscopy and visually searching the CAM for the compact, migration-inhibited tumor phenotype. Since the CAM is transparent and exposed, it is straightforward to identify and retrieve non-migratory tumour cell colonies under a fluorescence stereomicroscope. Compact colonies or 'hits' will be cultured for PCR analysis of the shRNA hairpins corresponding to genes required for migration (Figure 1.4.2).

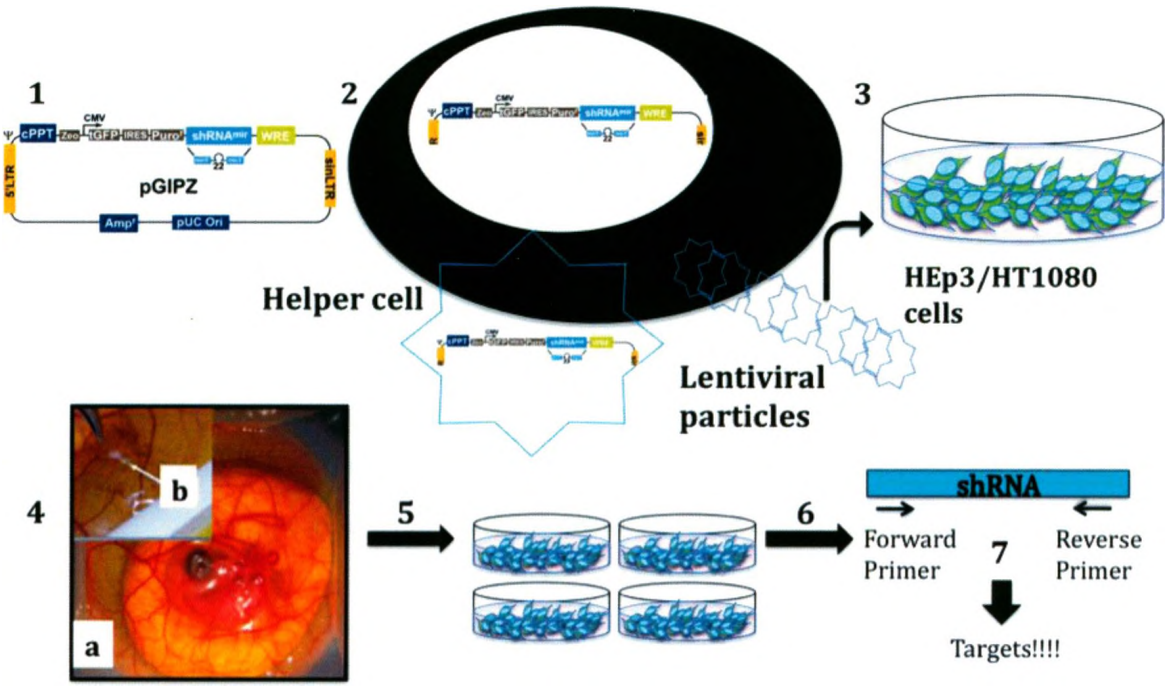

Figure 1.4.2: Screening Strategy.

1. pGIPZ lentiviral vector containing shRNA-miR cassette. Contains puromycin selection marker and turboGFP for ease of detection upon infection. **2.** Transfection of the helper cell with pGIPZ and accessory plasmids permits packaging of the pGIPZ construct into lentivirus particles. **3.** A library of virus particles containing 10,000 shRNAs are purchased from Open Biosystems and are ready-to-infect into the cell of interest, HEp3. **4.** The transduced cells are injected as a pool into the vasculature of the ex-ovo chicken embryo model (a) where they will extravasate into the stroma of the CAM and form many micrometastases (b). **5.** Individual compact colonies are extracted from the CAM and sub-cultured in separate dishes under the selection of puromycin. **6.** The genomic DNA is extracted from the each dish that pertains to an individual extracted colony. **7.** PCR-mediated amplification of the shRNA, followed by sequencing, identifies the shRNA responsible for the compact colony phenotype.

Hypothesis

1) Genes that are required for the migration of HEp3 cancer cells can be identified using a random, shRNA library screen for compact tumour phenotypes, using an *in vivo* chicken embryo metastasis assay

2) The inhibition of cortactin or rhoA, which are associated with poor prognosis and metastasis in many human cancers, will result in decreased cell migration and lead to abrogation of metastasis in the chicken embryo model and serve as positive controls for the RNAi screen

Objectives

1) Establish optimal screening parameters *in vitro and in vivo*:

    a. Calculate the *functional* multiplicity of infection (MOI) of human HEp3 epidermoid adenocarcinoma cells for the Open Biosystems Decode RNAi viruses

    b. Determine the amount of cells to inject per animal for maximal arrest of shRNA-containing cells in the CAM

    c. Estimate the number of animals to provide 3X representation of the 5000 genes covered in the screen (1 gene represented per tumour colony)

2) Establish a proof of principle using positive control shRNAs that target known mediators of cell migration, RhoA and Cortactin:

    a. Knockdown of rhoA and cortactin mRNA transcripts using individual shRNAs in HEp3 cells

    b. Assess the level of RhoA and Cortactin protein levels following RNAi-mediated knockdown in HEp3 cells

    c. Determine the impact of rhoA and cortactin knockdown on cell migration for HEp3 cells *in vitro*

d. Determine the impact of rhoA and cortactin knockdown on cell migration for HEp3 cells *in vivo* using intravital imaging

e. Characterize the proliferation rate of cortactin and rhoa knockdown cells in comparison to control cells

f. Measure the presence of liver metastases using a spontaneous model of metastasis in the chicken embryo model using cortactin or rhoA inhibited HEp3 cells

3) Perform the RNAi screen for compact tumour colonies *in vivo* using HEp3 cells and a pool of 10 000 shRNAs covering 5000 distinct genes in the human genome

4) Identify targets of migration by performing polymerase chain reaction on sub-colonies of extracted 'hits', using primers unique to the shRNA, followed by sequence analysis.

The preliminary results from the RNAi screen performed in this study indicate the feasibility of this screen, in particular, the ability to locate compact tumour colonies in the CAM following gene inhibition. Although the data is ongoing, it provides a basis for a larger scale screen, covering more genes in the human genome. The efforts made here ultimately contribute to the overall goal to identify targets whose loss-of-function recapitulate a non-migratory phenotype, and will allow for the discovery of novel targets required for migration.

Chapter 2

2 Results

2.1 Objective 1: Establish Optimal Screening Parameters *In vitro* and *In vivo*

CALCULATION OF THE FUNCTIONAL MULTIPLICITY OF INFECTION (MOI) OF HEP3 CELLS *IN VITRO*

A titration assay of pGIPZ-empty lentivirus particles reveals the 'cell counting method' to be comparable to flow cytometry as a measure of percent GFP and demonstrates an increase in transduction efficiency upon increasing amounts of virus

The pGIPZ containing lentivirus particles provided in the Open Biosystems Decode ™ RNAi viral screening libraries have been titered using a highly permissible version of human embryonic kidney cells (HEK293T) and are verified to contain at least 5×10^8 transducing units/milliliter (TU/mL). Transducing units are not virus particles *per se* and instead, represent the only virus particles that are successful in producing a phenotype, whether it be puromycin resistance, GFP expression, or capacity to clear a cell monolayer in the case of lytic viruses. The concentration of *effective* virus particles (TU) is necessary to calculate the multiplicity of infection (MOI) and achieve a desired number of pGIPZ-shRNA-miR integrations per cell. MOI is calculated by the following equation:

$$\text{MOI} = \frac{\text{number of effective virus particles (TU/ml)}}{\text{number of cells to be infected}}$$

For RNAi screening, only one shRNA-miR construct should be integrated per cell and according to Poission's distribution (Table 2), the predicted probability of multiple integrants is almost 10% of the cell population over an MOI of 0.4. To minimize the percentage of cells with more than one shRNA-miR, cells should not be infected with an MOI greater than 0.4 in RNAi screening studies to avoid additional screening of confounding results. For example, identification of a compact tumour phenotype with more than one shRNA contributing to that phenotype would require additional testing to determine if the multiple gene knockdown is synergistic in decreasing cell migration or if

only one of the genes is an effector. At the same time, viral infections should be maximized to obtain a high number of cells that harbour a pGIPZ-shRNA-miR construct. Taking these principles into consideration, the optimal MOI would theoretically be 0.4 as the percentage of cells with multiple integrants is within an acceptable range, yet 33% of cells will become infected with pGIPZ-shRNA-miR.

The MOI is a vital ratio to take into consideration when performing RNAi screens to prevent confounding results, however, the MOI is an inherent property of the cell line used for viral infection. Determination of an appropriate MOI using the viral titer obtained from using HEK293T cells, as in the case of the Open Biosystems Decode™ library, therefore, may not necessary represent the same outcome in another cell line. To account for the differences, the calculation of a *functional* MOI will need to be calculated for HEp3 cells. A *functional* MOI is calculated based on the number of transduced cells as reported by a phenotype in the cell line of interest and can be compared to a *non-functional* MOI which is calculated based on the MOI that is derived from the titer value reported by the supplier (as calculated in HEK293T cells).

Calculation of the *functional* MOI necessary transduce cells and elicit a phenotype such as GFP expression, has been performed by flow cytometry and microscopic analysis of GFP positive cell counts (Sastry 2002 and Lyva 2011). Since the pGIPZ lentiviral construct contains turbo GFP as a marker of cell infection (Figure 2.1.1A), the percentage of GFP positive cells is proportional to the ratio of virus particles that successfully produce GFP phenotype in cells (MOI). Taking advantage of these properties, the *functional* MOI for HEp3 cells was calculated by a microscopic 'cell counting method' whereby the number of GFP positive cells are counted and divided by the total cell number, yielding the percentage GFP. Alternatively, flow cytometry was used as an automated method to calculate the percentage of GFP positive cells within in the infected population.

To test the accuracy between the two methods for calculating the *functional* MOI, both flow cytometry and cell counting were performed on HT1080 cells and the percent GFP positive cells were compared between each method. To provide a range of viral concentrations to test, HT1080 cells were infected with serially diluted amounts of non-silencing control virus (pGIPZ-empty). This construct is identical to the pGIPZ-shRNA-

miR vectors used for the RNAi lentiviral screening libraries, however, the non-silencing control is 'empty' and does not contain the shRNA-miR cassette (Figure 2.1.1A). Following infection, HT1080 cells were allowed to express turbo GFP so that the percentage of GFP positive cells could be quantified using the cell counting method. Immediately after cell counting, cells were fixed and subjected to flow cytometry. Comparison of the cell counting method versus flow cytometry revealed no significant difference between the two methods of analysis (Figure 2.1.1A, $p=0.1477$ as determined using a matched, 2-way ANOVA with Bonferroni Post test, of the mean ±SEM, N=2, 6 Fields of view (FOV)/well (microscopy) or 10,000 events (flow)). Details regarding materials and methods used in each experiment performed in the results section can be obtained in 'Chapter 4: Materials and Methods'. The change in percent GFP between dilutions, however, was statistically significant (Figure 2.1.1A, $p<0.0001$ as determined by a matched, 2-way ANOVA of the mean ± SEM, N=2, 6 FOV/dilution). These results conclude that either method is conducive to calculating the percentage of GFP positive pGIPZ-empty containing cells, and that increasing amounts of virus leads to an increase in transduction efficiency for HT1080 cells (Figure 2.1.1AB). Due to limited amount of occasions requiring the calculation of the *functional* MOI, the counting method was employed so that MOI calculations for any cell line could be quickly performed in house, without formal flow cytometry training.

Table 2: Poisson's Distribution of Multiple Integrants.

Distribution of the percentage of cells expected to contain multiple shRNA integrants per cell in response to increasing Multiplicity of Infection (MOI). The shRNA construct confers GFP expression upon integration and is therefore an indirect measurement of MOI.

Integrants	0	>1	>2	>3	>4	
MOI	Percentage of cells with the given number of integration events					Percentage GFP positive cells
0.1	90	9	0	0	0	9
0.2	82	16	2	0	0	18
0.3	74	22	3	0	0	25
0.4	67	27	5	1	0	33
0.5	61	30	8	1	0	39
0.6	55	33	10	2	0	45
0.7	50	35	12	3	0	50
0.8	45	36	14	5	0.01	55
0.9	41	37	16	5	0.01	58
1.0	37	37	18	6	0.02	61

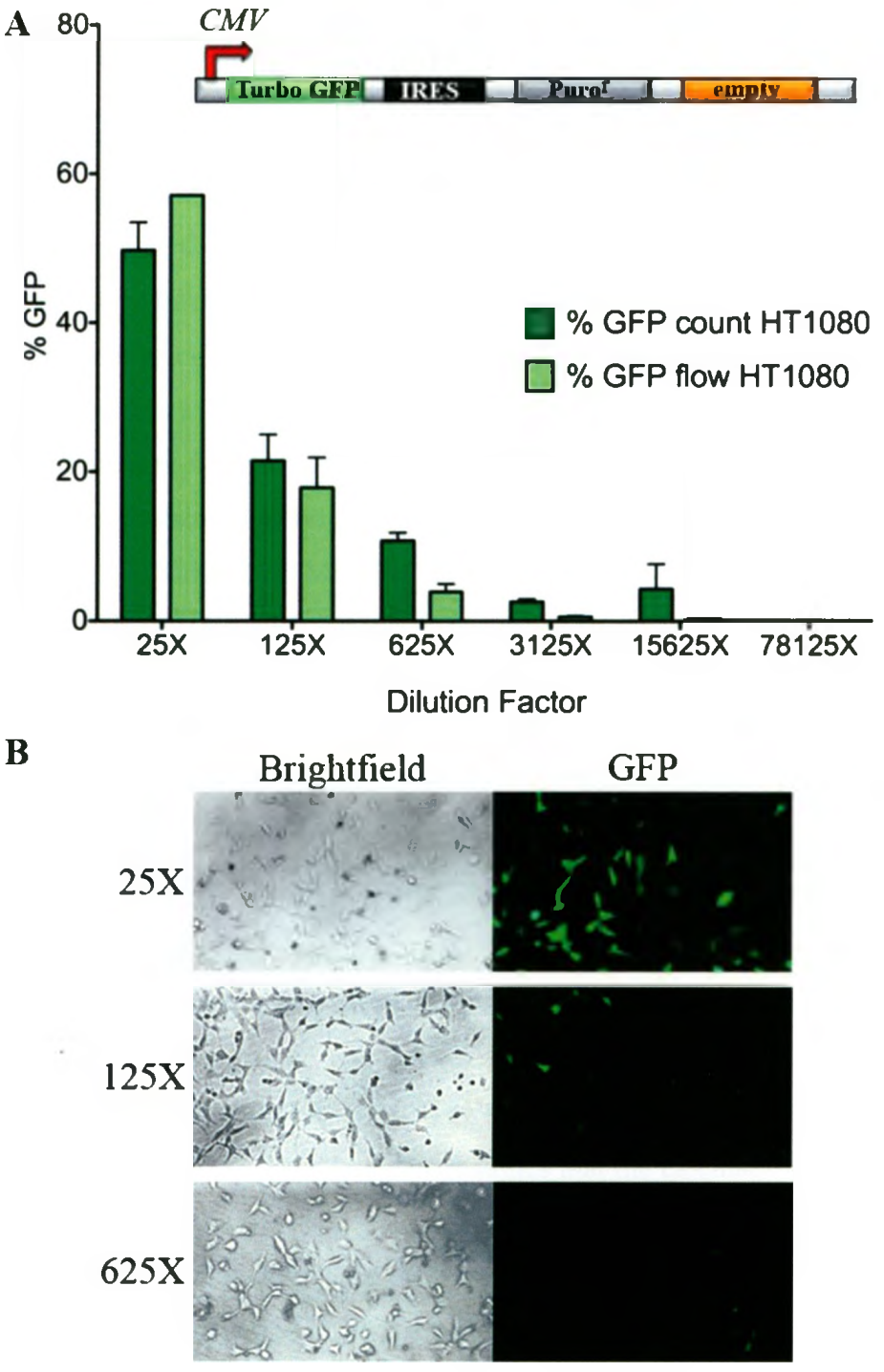

Figure 2.1.1: Quantification of percent GFP using 'cell counting' method is comparable to flow cytometry.

A. Quantification of the percentage of HT1080 cells infected with pGIPZ -empty (inset) as measured by GPF signal, either by the 'counting' method (% GFP count HT1080) or flow cytometry (% GFP flow HT1080), reveals there is no difference between the two methods. **B.** Representative images of HT1080- pGIPZ-empty cells, 48 hours following infection with various dilutions of virus taken with 100X magnification. As the dilution factor decreases (625X-25X), providing more transducing units (TU) per cell, the transduction efficiency, as measured by GFP signal, increases. *Columns,* represent the mean from duplicate experiments as determined by both counting and flow cytometry and *bars* represent the SEM.

The* functional *MOI is lower in HEp3 cells in comparison to the* non-functional *MOI reported by Open Biosystems, as measured by percent GFP expression

The *functional* MOI for HEp3 cells was calculated using the cell counting method in order to determine the amount of virus necessary to obtain an optimal number of integrants per cell and maximize the transduction efficiency. To perform *functional* MOI calculations, HEp3 cells were infected with the pGIPZ-empty lentivirus using three different MOIs (1, 5, and10), each calculated using the titer obtained by Open Biosystems in HEK293T cells and are referred to as *non-functional* MOIs. Read-out of the percentage GFP positive cells for each of the *non-functional* MOIs (1, 5, and 10) represents the *functional* MOI in the cell lines of interest when cross-referenced to the Poisson distribution curve (Table 2). Interestingly, the *functional* MOI for HEp3 cells was lower than the corresponding *non-functional* MOI (Figure 2.1.2 AB). This suggests that the HEp3 cell line is less permissive to the vesticular-somatis virus G protein (VSV G)-pseudotyped lentiviral particles than the highly permissive HEK293T cells, however without testing the virus on HEK293T cells in house, it can only be concluded that the *functional MOI* is less than the titer reported by Open Biosystems. At *non-functional* MOIs of 1, 5 and 10, the corresponding percentage of GFP positive HEp3 cells is: 8%, 30% and 46% which represent *functional* MOIs of 0.1, 0.4 and 0.6 respectively (Figure 2.1.2 AB). Furthermore, the percentage of GFP positive cells increased with increasing MOIs, similar to what was seen in HT1080 cells (Figure 2.1.1AB) and by other groups, and this was statistically significant ($p < 0.0001$, as determined by 1-way ANOVA, and Tukey's post test, of the mean ±SEM, N=3, 6 FOV/MOI) (Lyva 2011). This data demonstrates that the calculation of a *functional* MOI is possible for HEp3 cells using the counting method and the *functional* MOI is at less for HEp3 cells than the *non-functional* MOI, as quoted by Open Biosystems in HEK293T cells. Furthermore, increases in MOI are able to illicit increases in transduction efficiency, however this increase is not linear as GFP signal appears to increase by a smaller percentage at higher MOIs. From these experiments, it was determined that a *non-functional* MOI of 5 would be used for future experiments as this corresponds to a *functional* MOI of 0.4 in the cell line of interest and will not only keep the number of cells with multiple integrants at an acceptable level, but also maximizes transduction efficiencies.

A

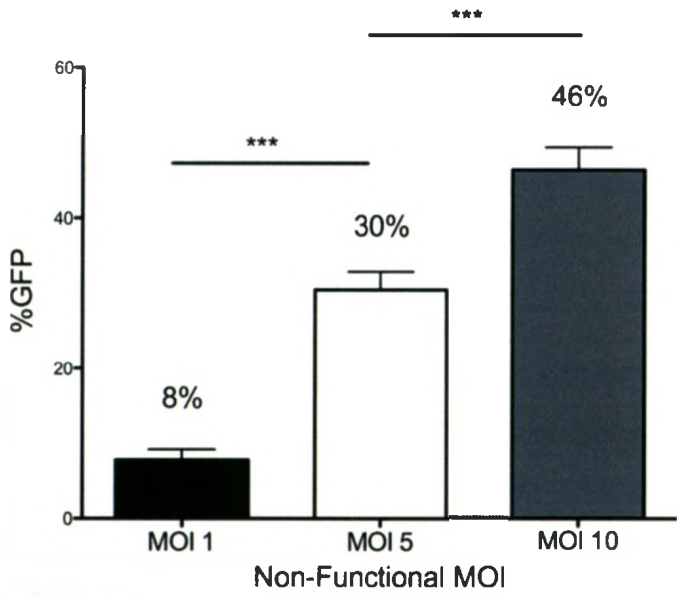

B

HEp3 cells	Non-Functional MOI		
	1	5	10
% GFP	8	30	46
Functional MOI	0.1	0.4	0.6

C

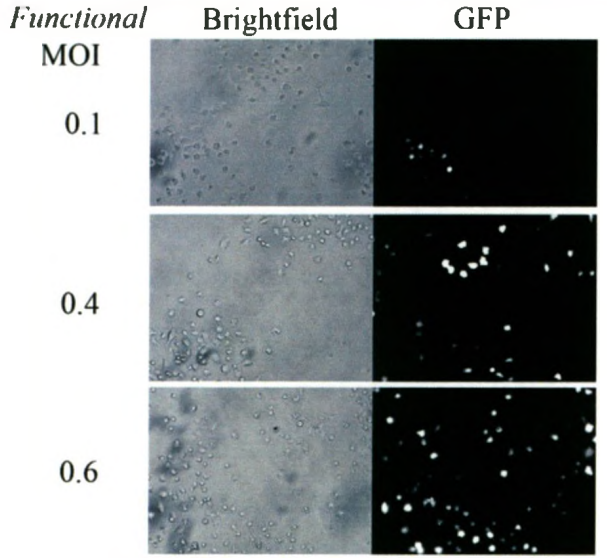

Figure 2.1.2: The *Functional* MOI of HEp3 cells is less than the *non-functional* MOI reported in HEK293T cells

A. HEp3 cells were infected with pGIPZ-empty lentivirus at various *non-functional* MOIs (1, 5, and 10) that were calculated using the titer quoted by the supplier. 48 hours post-infection, cells expressing GFP were counted and divided by the total number of cells in a field of view to achieve a percent GFP per MOI. **B.** The percent GFP for each *non-functional* MOI was compared to the Poisson distribution curve in order to evaluate the *functional* MOI. The *functional* MOI is up to 10-fold less than expected in comparison to the quoted MOI calculations. **C.** Representative images of one field of view used to calculate the percent GFP in HEp3 cells at 100X magnification. As the MOI increases (1-10 or 0.1-0.6), more virus is used to infect HEp3 cells resulting in increased transduction efficiency, as measured by GFP signal. *Columns,* represent the mean from triplicate experiments and *bars* represent the SEM, ***$p<0.001$.

OPTIMIZATION OF SHRNA-CONTAINING COLONIES IN THE CAM AND ESTIMATION OF THE NUMBER OF ANIMALS TO PROVIDE 3X GENE REPRESENTATION FOR RNAI SCREENING

Administration of 100, 000 HEp3-pGIPZ cells into the vasculature of the chicken embryo yields an optimal number of colonies within the CAM and allows for 3X coverage of the 5000 genes in the RNAi screen using 168 animals

The discrete number of HEp3-pGIPZ colonies the CAM can sustain is an important question to address since this will ultimately determine the total number of animals needed to perform the screen. A single tumour colony within the CAM represents the outgrowth of an individual cell that has been optimized to harbour only one shRNA or gene knockdown. This relationship dictates that a total of 5000 colonies must be present in the cumulative number of CAMs across 'X' number of animals to represent the 5000 genes in the library. The total number of colonies that arise in the CAM, in response to a given concentration of cells, must be known in order to determine 'X'. To answer this question, two different concentrations of HEp3-pGIPZ-empy cells were injected into the vasculature of day 9 embryos. Before day 12, the basal lamina of endothelial cells, pericytes and smooth muscle cells are discontinuous, allowing for greater vessel permeability (Ribatti 2010). The percentage of cancer cells that undergo extravasation and arrest in the stroma of the CAM is, therefore, lower when injected into the vasculature of older embryos (day 13) in comparison to cells injected into younger animals (day 9) due to these decreases in vessel permeability. To prevent the possibility of inhibiting cell extravasation by knocking down a gene important to this function when performing an RNAi screen, day 9 animals should be used when administering cancer cells into the bloodstream since the extravasation barriers are limited. Using day 9 animals, therefore, is ideal for the purpose of witnessing cell migration post-extravasation since even cells whose migration machinery has been inhibited, can still extravasate into the stroma with high efficiency (Figure 2.2.5-2.2.6).

Upon i.v injection of two different concentrations of HEp3-pGIPZ-empty cells into day 9 animals, tumour cells arrested in the stroma of the CAM (Figure 2.1.3 B, day 0) and tumour colonies were allowed to form (Figure 2.1.3B, day 8) prior to manually counting the number of colonies per animal. The first concentration of 100,000 HEp3-pGIPZ-empty cells per animal (50ul injection) yielded a total mean of 192 ± 34 colonies per animal

(N=4), when quantified 8 days post injection (Figure 2.1.3A). Colonies were quantified by scanning the entire surface of the CAM using a fluorescent microscope and 'stitching' individual fields together to form one complete image of the CAM and the Turbo GFP colonies within the CAM (Figure 2.1.3B). Some of the colonies, however, did not have a sufficient amount of spacing between them, which is a requirement for their extraction and further processing (Figure 2.1.3B, inset). The total number of 'extractable', or distinct colonies that could be removed, was 91±10 colonies (N=4 animals). This means that upon injection of 100,000 HEp3-pGIPZ-shRNA-miR cells, ~192 genes will be represented by the colonies within the CAM but only 48% of the total colonies in the CAM are relevant for the screen, and only ~ 90 genes will be represented per CAM. In an attempt to increase the number of 'extractable' colonies per CAM, injection of a lower concentration of HEp3-pGIPZ-empty cells, 50,000 cells per 50ul injection, was administered, also on day 9 embryos. This concentration achieved a total mean of 59± 8 colonies per animal (N=4 animals), 8 days post-injection. Although there was greater spacing between colonies when 50,000 HEp3-pGIPZ cells were administered per injection, only 68% of the total number of colonies (38±8 colonies, N=4 animals) were extractable, yielding less usable colonies per CAM than the 100,000 cells/injection group.

Since the total number of extractable colonies was greater per animal in the 100,000 cells per injection group, it was determined that this would be an optimal number of HEp3-pGIPZ cells to inject per animal for the screen. Understanding that 100,000 cells yields ~90 extractable colonies in the CAM, allows for the number of animals needed to cover all 5000 genes in the screen to be estimated:

100,000 HEp3-pGIPZ cells/animal= 90 extractable colonies/animal

1 colony=1 shRNA=1 gene knockdown

10, 000 shRNAs ÷ 2 shRNAs/gene= 5000 genes

5000 genes ÷ 90 extractable colonies/animal=~56 animals

56 animals × 3= ~168 animals for a 3X representation of the screen

It is estimated above that 56 animals will be needed to cover the 5000 genes represented in the library if 100,000 HEp3-pGIPZ-shRNA-miR cells are injected per animal. In order to increase the confidence of the screen, it is necessary to perform a 3X representation of the total genes in the library. The total number of animals needed for a 3X representation of the screen is, therefore, 168 animals.

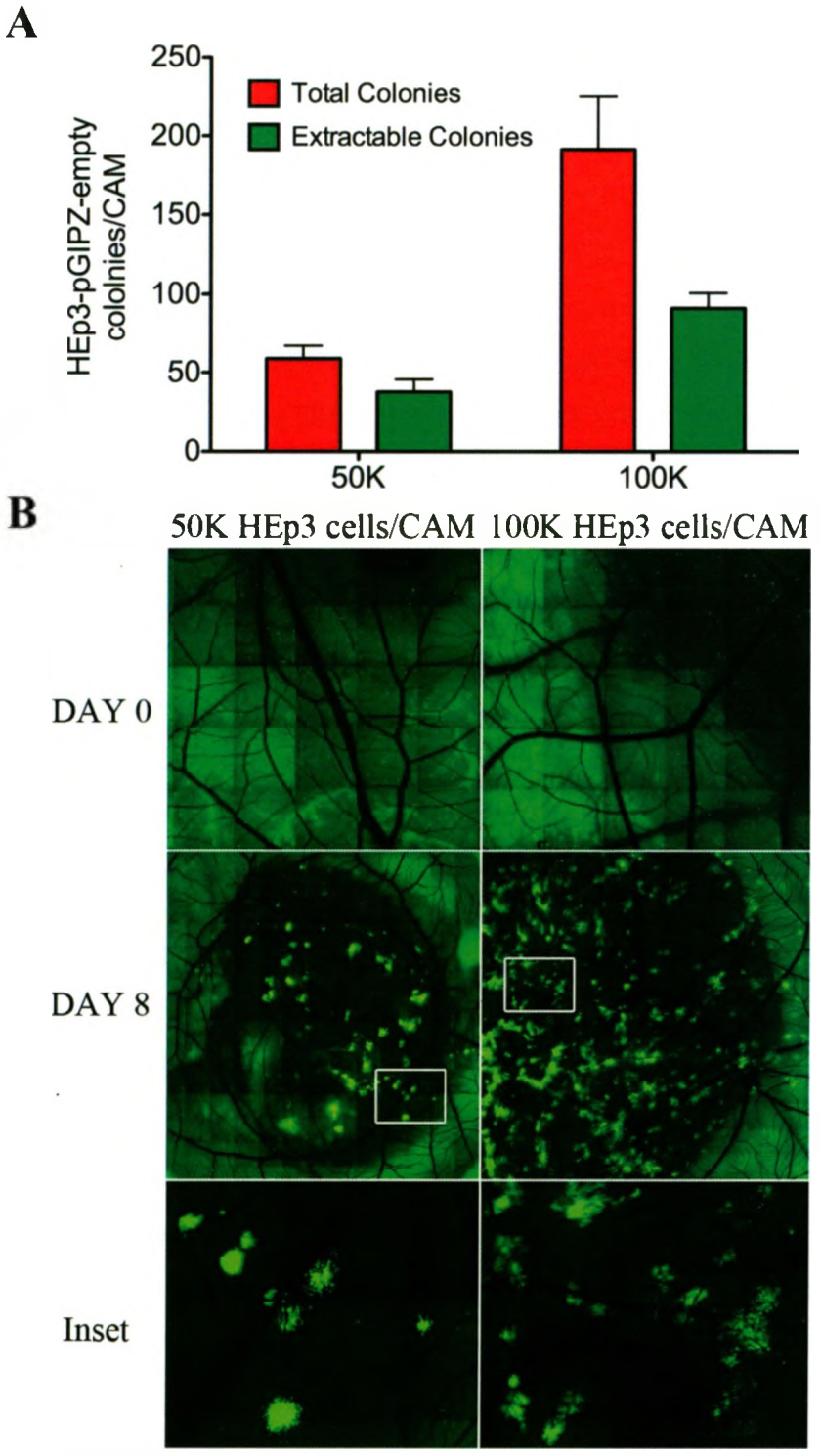

Figure 2.1.3: Total and 'extractable' number of HEp3-pGIPZ-empty colonies in the CAM
A. Quantification of the total number of HEp3-pGIPZ colonies seen in the CAM 8 days post injection of either 50,000 or 100,000 cells per animal (green bars) versus the number of colonies that can be 'extracted' for further processing (red bars). **B.** 'Stitched' images of a section of CAM immediately following injection with either 50,000 or 100,000 HEp3-pGIPZ-empty cells at 25X magnification (DAY 0). Stitched images of the entire CAM 8 days post injection of either concentration of cells at 25X (DAY 8). Zoomed in image of colonies from the white box in DAY 8 (Inset) detail the spacing between colonies that is necessary for proper extraction.

2.2 Objective 2: Establish a Proof of Principle Using Positive Control shRNAs Targeting Known Mediators of Cell Migration: RhoA and Cortactin

Prior to performing an RNAi screen to identify novel migratory genes, it was first necessary to demonstrate the behavior of cancer cells when known mediators of migration are inhibited both *in vitro* and in the chicken embryo model. Individual shRNAs against the cortactin and rhoA genes, shCTTN and shRhoA respectively, were infected into HEp3-GFP cells using a lentiviral delivery system to test if RNAi-mediated knockdown of known migratory genes cause decreased migration, invasion and metastasis.

KNOCKDOWN OF THE RHOA AND CORTACTIN MRNA TRANSCRIPTS AND PROTEIN USING INDIVIDUAL SHRNAS IN HEP3 CELLS

The RNAi Consortium lentiviral shRNA delivery system can be used to deliver individual shRNAs against cortactin and rhoA mRNA transcripts and quality control measures to test for recombination confirmed the correct shRNA-containing plasmid orientation prior to virus production

To establish the chicken embryo model as a predictable model to measure cell migration, a proof-of-principle was established using two known mediators of migration: RhoA and Cortactin. In another *in vivo* screen, A. Bric *et al.* demonstrated the feasibility of providing a positive control while screening to demonstrate the phenotype they were screening for (Bric 2009). To inhibit RhoA and Cortactin, RNAi was utilized to further emulate the actual screening parameters. The shRNA constructs used were designed by The RNAi Consortium, and unlike the Open Biosystems RNAi library, virus particles, harboring either shCTTN or shRhoA hairpins are made in house. Construction of virus particles involves transfer of the pLKO.1-hairpin plasmid, contained in glycerol bacterial stocks, to Luria broth supplemented with carbenicillin to ensure amplification of the hairpin-pLKO plasmid. As lentiviral plasmids have a high frequency of recombination in bacteria, quality control measures must be taken in house to ensure the correct plasmid sequence is replicated. Although the pLKO.1 vector has been shown to have a rate of recombination below 0.05% following growth from bacterial glycerol stocks, it is necessary to retest the

vectors in house for recombination events (Root 2006). Restriction enzyme-mediated DNA digestion was performed on various pLKO.1 plasmids containing shRNAs against genes of interest: green fluorescent protein (shGFP) and luciferase (shLUC) as negative controls and cortactin (shCTTN) and rhoA (shRhoA) as positive controls for migration, prior to production of viral particles, to ensure the successful transduction of shRNA into HEp3 cells. The restriction enzymes EcoRI and Kpn1, specifically, were used to digest each pLKO.1 plasmid and yield the predicted DNA fragments of 7 Kb and 1.4 Kb if the shRNA is contained within the plasmid and recombination has not occurred (Figure 2.2.1A). Digestion of the pLKO.1 plasmids, isolated from more than one bacterial clone for each shRNA, all yielded the appropriate size bands when subjected to DNA electrophoresis, suggesting that these plasmids are in the correct orientation and have not undergone recombination events, as predicted by D.E Root *et al* (Figure 2.2.1B). More than one shRNA construct was tested for each gene and are represented by individual numbers 77-145. Clones 145, 146 (shGFP), 77, 78 (shLUC), 134, 135, 136, 137, 138 (shCTTN), 45, 46, 47, 48, and 49 (shRhoA) were used to make lentivirus for infection of HEp3 cells.

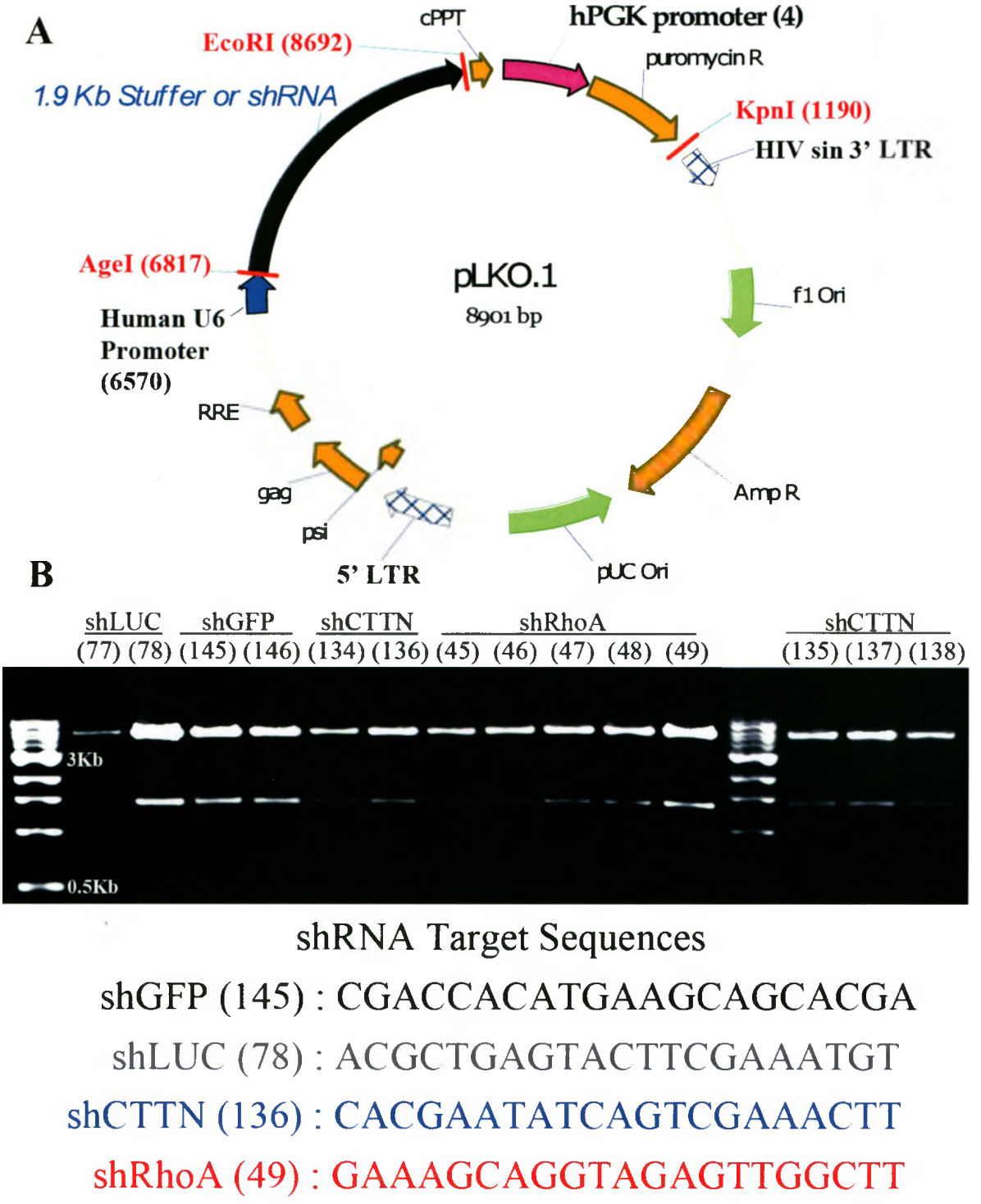

shRNA Target Sequences

shGFP (145) : CGACCACATGAAGCAGCACGA

shLUC (78) : ACGCTGAGTACTTCGAAATGT

shCTTN (136) : CACGAATATCAGTCGAAACTT

shRhoA (49) : GAAAGCAGGTAGAGTTGGCTT

Figure 2.2.1: pLKO.1 construct and the mRNA target sequences of shRNA clones.
A. pLKO.1 construct, designed by The RNAi Consortium, contains a 1.9Kb stuffer sequence that can be excised in exchange for a shRNA (22-mer hairpin) using the AgeI and EcoRI restriction enzyme sites. **B.** Restriction enzymes EcoRI and KpnI were used to digest the shRNA containing pLKO.1 plasmid to check for recombination events. The DNA was run on 0.7% agarose gel containing ethidium bromide and visualized for the appearance of the correct size bands (7Kb (top band) and 1.4Kb (lower band)). Target sequences contained in the mRNA for the given genes are listed next to the corresponding shRNA clone used in the study.

Quantification of the mRNA expression level for rhoA and cortactin following RNAi-mediated knockdown revealed that the mRNA transcripts were depleted for both genes by more than 80%

To test the efficacy of shRNA constructs for specific gene knockdown, HEp3-GFP cells were stably transduced with individual shRNA clones targeting either the cortactin or rhoA mRNA transcripts, followed by quantification of the mRNA levels of each gene using real time quantitative polymerase chain reaction (RT-PCR). Gene-specific primers were utilized for amplification of rhoA or cortactin mRNA transcripts and were normalized to the 'house-keeping' gene glyceraldehyde-3-phosphate dehydrogenase (GAPDH) mRNA transcript levels (Figure 2.2.2A). mRNA expression levels in HEp3-GFP-shRhoA (shRhoA) and HEp3-GFP-shCTTN (shCTTN) cells were compared to control HEp3-GFP cells that harbor an shRNA for either GFP (shGFP) or luciferase (shLUC) genes, both of which are not normally expressed by human cancer cells and thus have no natural, endogenous mRNA target. RT-PCR analysis of mRNA transcript levels revealed that the shRNA constructs: 48, 49 and the combination of both 45 and 49, all had significantly reduced rhoA mRNA transcript expression in comparison to the control HEp3-GFP cells. In particular, the rhoA mRNA expression was reduced by $> 80\%$ in comparison to shLUC cells for these shRNA constructs ($p<0.05$ for constructs 48 and 49 and $p<0.001$ for combination of constructs 45+49, N=3, as determined by a 1-way ANOVA and Tukey's post test and reported mean ±SEM). shRhoA cells harboring constructs 45 and 47 demonstrated a reduction in the mean rhoA mRNA expression level, however this was not significant, while rhoA shRNA construct 46 did not reduce the rhoA mRNA levels (Figure 2.2.2C). The combination of constructs 45+49 did not have a significant synergistic effect on rhoA mRNA transcript level, as there is no significance between construct 49 and 45+49. Cells containing the combination of shRNA constructs, although they provided good knockdown of rhoA mRNA, were not used for further study as the control cells do not harbor two different shRNA constructs. Due to the excellent rhoA mRNA repression seen upon addition of shRNA constructs 48 and 49, cells harboring construct 49 were selected for further study.

In contrast to the shRhoA cells, only two constructs were tested for the shCTTN cells because the other shCTTN constructs were eliminated by a prior western blot analysis of the Cortactin protein levels (Appendix A). For the shCTTN constructs tested by RT-PCR, cortactin mRNA expression levels were also reduced by greater than 80% when compared to shLUC cells (Figure 2.2.2C (inset), $p<0.05$ for construct 136, N=3, as determined by an unpaired, two-tailed, student's T-test, reported the mean ±SEM). shCTTN cells harboring construct 134 also demonstrated a reduction in the mean CTTN mRNA expression level, however this was only performed in a single cursory experiment and significance cannot be determined (Figure 2.2.2B). In summary, knockdown of rhoA and cortactin gene expression through specific RNAi-mediated mRNA silencing resulted in significant, stable repression of mRNA transcripts by greater than 80% when either shRhoA constructs 48,49, and 45+49 or shCTTN construct 136 were introduced into HEp3-GFP cells. For subsequent studies, the HEp3-GFP cells containing shCTTN construct 136 or shRhoA construct 49 were used to test the loss-of-function phenotype in the context of cell migration and metastasis. Although mRNA transcript levels are specifically targeted and repressed, this finding does not always translate to a decrease in the protein. To test the impact of rhoA or cortactin mRNA repression on the level of RhoA and Cortactin protein expression, shRhoA (49) and shCTTN (136) cells were probed for protein expression using antibodies specific to both RhoA and Cortactin protein by western blotting.

A

Primer Sequences

Gene	Forward	Reverse	References
rhoA	5'-ATGGCTGCCATCCGGAAGAA-3'	5'-TCACAAGACAAGGCACCCAGA-3'	(Simpson, K., *et al.*, 2004)
CTTN	5'-GCGTCAACCTTTGAGGATGT-3'	5'-CTCCTCCAGCTTCCTCCTG-3'	(Luo, M.L., *et al.*, 2006)
GAPDH	5'-CCTGGCCAAGGTCATCCATGAC-3'	5'-TGTCATACCAGGAAATGAGCTTG-3'	(Lipscomb, E.A.,*et al.* 2005)

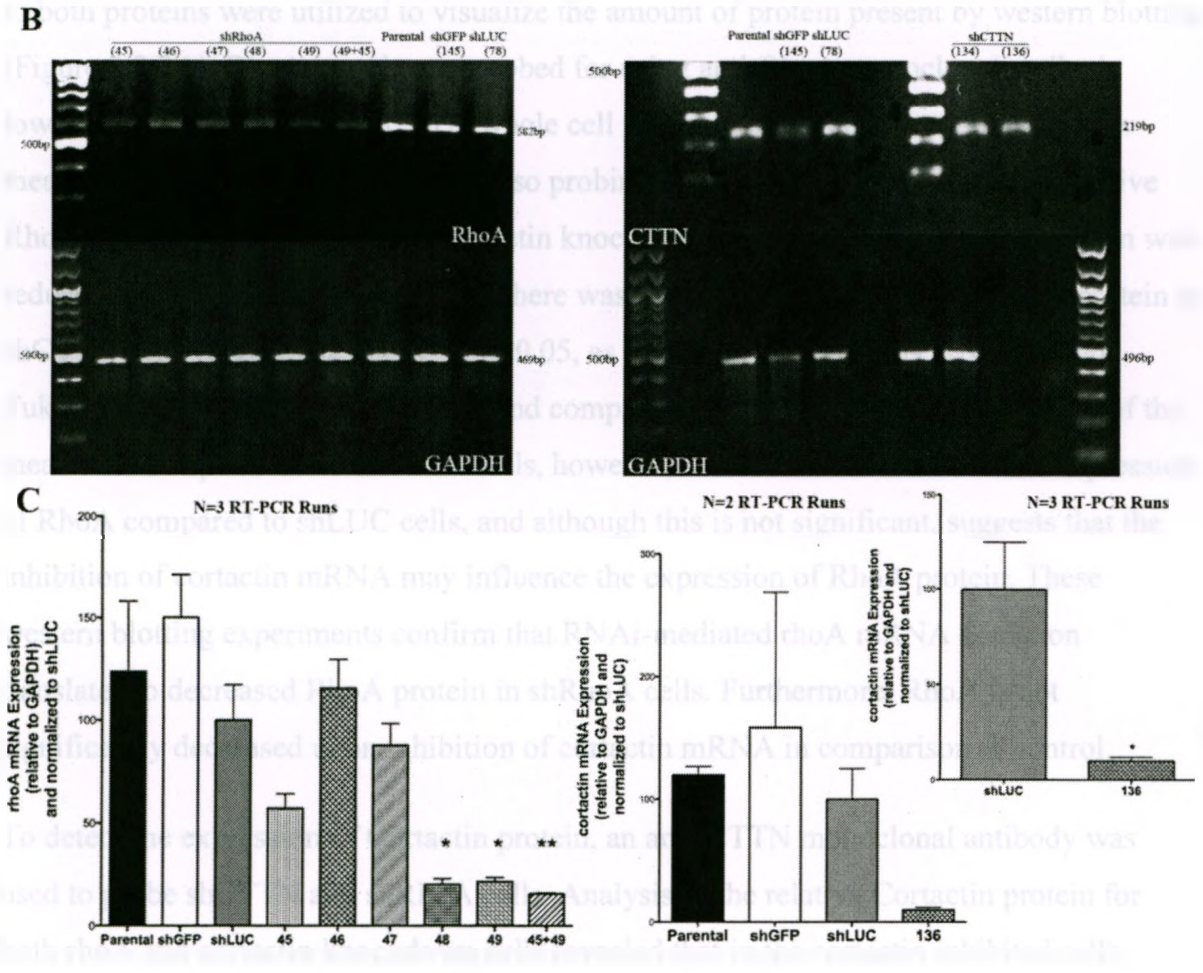

Figure 2.2.2: Relative mRNA expression of rhoA and cortactin transcripts following knockdown
A. Primer sequences used to amplify specific mRNA transcripts from the total RNA extracted from HEp3-GFP-shRNA cells during simultaneous quantification of mRNA expression levels by RT-PCR. **B.** Representative images of amplified mRNA transcripts following RT-PCR processing that were run out on a 1% agarose gel stained with ethidum bromide and visualized using UV light. **C.** Results of N=3 RT-PCR runs for rhoA mRNA expression levels for each shRhoA construct (left panel) and the quantification of cortactin mRNA expression level for shCTTN construct 136 (right panel) compared to controls. Inset is the quantification of cortactin mRNA levels for N=3 RT-PCR runs for shCTTN (136) as compared to shLUC (78). *Columns* represent the mean of triplicate experiments (**C** and **B** (inset)) and duplicate experiments (**C**, right panel). *Bars* represent the SEM, *$p<0.05$ and **$p<0.01$.

Quantification of protein expression levels for RhoA and Cortactin following RNAi-mediated inhibition revealed that RhoA was depleted by 80%, and Cortactin by more than 95%

To directly test if the inhibition of rhoA and cortactin transcript repression translated to decreased RhoA and Cortactin protein levels, monoclonal antibodies specifically targeted to both proteins were utilized to visualize the amount of protein present by western blotting (Figure 2.2.3A). RhoA protein was probed for using anti-RhoA monoclonal antibody towards both shRhoA and shCTTN whole cell protein lysates, and the expression was measured relative to total protein by also probing for β-Tubulin. Analysis of the relative RhoA protein for both rhoA and cortactin knockdown cells revealed the RhoA protein was reduced by 80% in shRhoA cells, but there was no significant reduction of RhoA protein in shCTTN cells (Figure 2.2.3B. $N=3$, $p<0.05$, as determined by a 1-way ANOVA and Tukey's post test of the mean ±SEM and compared to shLUC). Careful observation of the mean RhoA expression in shCTTN cells, however, revealed a decrease in mean expression of RhoA compared to shLUC cells, and although this is not significant, suggests that the inhibition of cortactin mRNA may influence the expression of RhoA protein. These western blotting experiments confirm that RNAi-mediated rhoA mRNA depletion translates to decreased RhoA protein in shRhoA cells. Furthermore, RhoA is not significantly decreased upon inhibition of cortactin mRNA in comparison to control.

To detect the expression of Cortactin protein, an anti-CTTN monoclonal antibody was used to probe shCTTN and shRhoA cells. Analysis of the relative Cortactin protein for both rhoA and cortactin knockdown cells revealed that in the cortactin inhibited cells, Cortactin protein was reduced by more than 95% in comparison to shLUC cells (Figure 2.2.3C (inset), $N=3$, $p<0.05$, as determined by an unpaired, two-tailed student's T-test, of the mean ±SEM). There was a large variation in the level of Cortactin protein across western blots for shRhoA cells and, therefore, the significance of Cortactin protein expression upon rhoA inhibition could not be determined. It can be speculated, however, that rhoA depletion may contribute to decreases in Cortactin protein expression since the mean expression of Cortactin in shRhoA cells is lower than control cells. This relationship between rhoA and cortactin was also seen in the opposite case where cortactin was

inhibited and RhoA protein levels were decreased. Further analysis would need to be performed to test this hypothesis such as use of additional means to inhibit RhoA and Cortactin protein and mRNA by inhibitors or by employing different shRNA constructs for rhoA and cortactin mRNA, respectively. Understanding that both the rhoA and cortactin genes are inhibited through knockdown of mRNA transcript expression and moreover, RhoA and Cortactin protein expression is repressed, allows for the comprehensive analysis of HEp3 cell migration both *in vitro* and in the chicken embryo model in the absence of these mediators of migration.

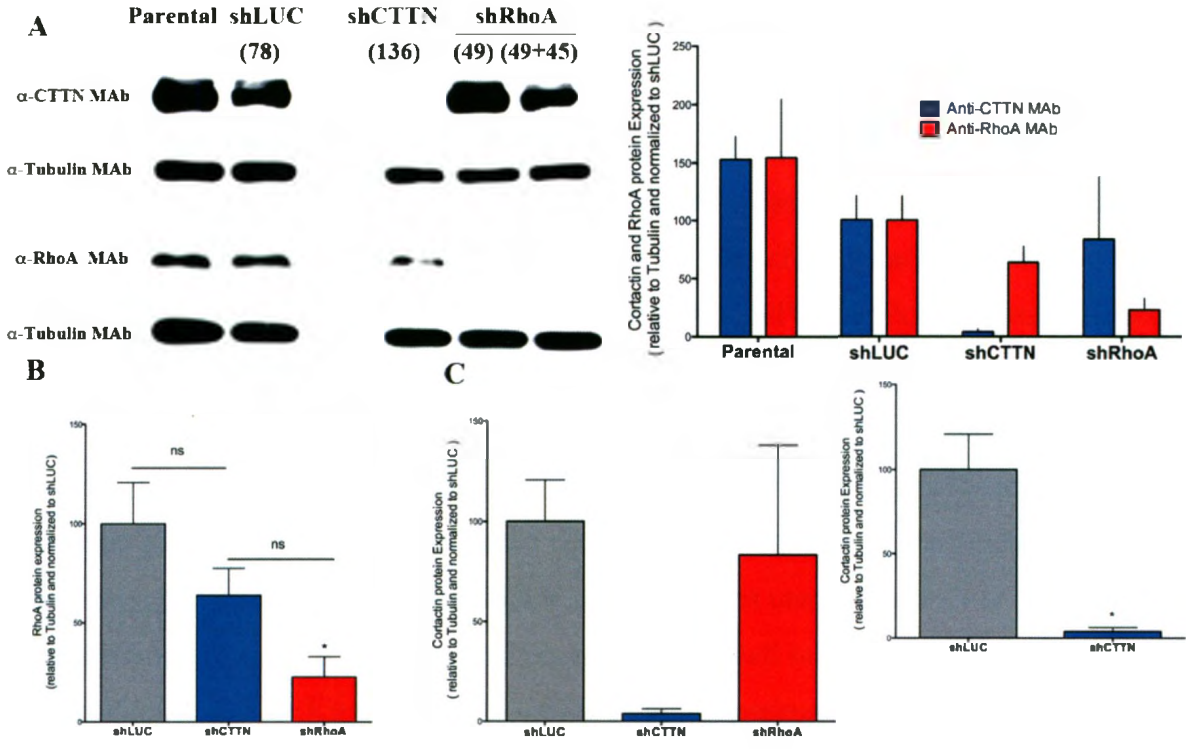

Figure 2.2.3: RhoA and Cortactin protein expression is repressed following RNAi inhibition

A. Detection of the RhoA and Cortactin proteins using Western blotting. The Cortactin protein (top row) and the RhoA protein (second row from the bottom) were detected using specific monoclonal antibodies (left panel) and their fold protein expression relative to α-Tubulin was quantified using densitometry and normalized to relative expression in shLUC cells (N=3) in both shCTTN and shRhoA cells (right panel). **B.** RhoA protein expression is significantly decreased in shRhoA cells in comparison to shLUC, however, there is no significant decrease in expression of RhoA protein for shCTTN cells, although the mean RhoA expression is repressed. **C.** Cortactin protein expression is decreased in shCTTN cells, however, in a 1-way ANOVA statistical analysis, this is not significant compared to shRhoA cells. A student's T-test reveals that the level of Cortactin is repressed by 95% in comparison to control cells (inset). *Columns,* represent the mean from triplicate experiments as determined by densitometry using ImageJ analysis tools and *bars* represent the SEM, *$p<0.05$.

Affect of RhoA and Cortactin Inhibition on Cell Migration In Vitro and Cell Migration and Metastasis In the Chicken Embryo Model

RhoA and Cortactin are required for cell migration and invasion in an in vitro *setting that resembles the tumour microenvironment*

Prior to testing the migration capacity of rhoA and cortactin knockdown cells in the chicken embryo model, these cells were first subjected to an *in vitro* cell invasion and migration assay. This assay involved the use of a Boyden chamber and the invasion and migration of shRhoA and shCTTN cells through a Matrigel™ matrix and porus membrane is measured over time in comparison to shLUC control cells (Figure 2.2.4A). In these experiments, the Matrigel™ is composed of matrix proteins that are found in the tumour microenvironment and thus, this is a good *in vitro* measure of cell invasion and migration in comparison to cell movement across a rigid substratum such as a plastic dish. Previously, cancer cell invasion through a 3D-matrix was used to identify an actin-polymerizing protein, mDia1, as a positive mediator of cell migration after siRNA-mediated knockdown (Kitzing 2010). Similar to this experiment, HEp3-GFP cells, following RNAi knockdown of positive mediators of cell migration, should demonstrate decreased levels of invasion through the Matrigel™.

The results of the invasion and migration experiments revealed that both RhoA and Cortactin are important for cell movement in this context as measured by manual counting of the migrated cells after 22 hours of incubation (Figure 2.2.4B. N=3 membranes/experimental condition, reported the mean number of cells that traversed the membrane for 5 FOV per membrane ±SEM, $p<0.0001$ as determined by 1-way ANOVA, Tukey's post test). The mean percentage of invaded cells for shCTTN and shRhoA experimental groups were 52% and 61% of the average number of shLUC control cells that invaded. These experiments indicate a role for both Cortactin and Rho in cell migration and invasion, however there was no significant difference between cells inhibited for either rhoA or cortactin suggesting that both proteins are equally important for this process in HEp3 cells *in vitro.* The next question asked was whether or not inhibition of rhoA or cortactin by RNAi also contributes to decreased cell invasion, migration and metastasis in

the chicken embryo model to demonstrate that the model is conducive to both the monitoring of cell migration and detecting metastasis following gene knockdown.

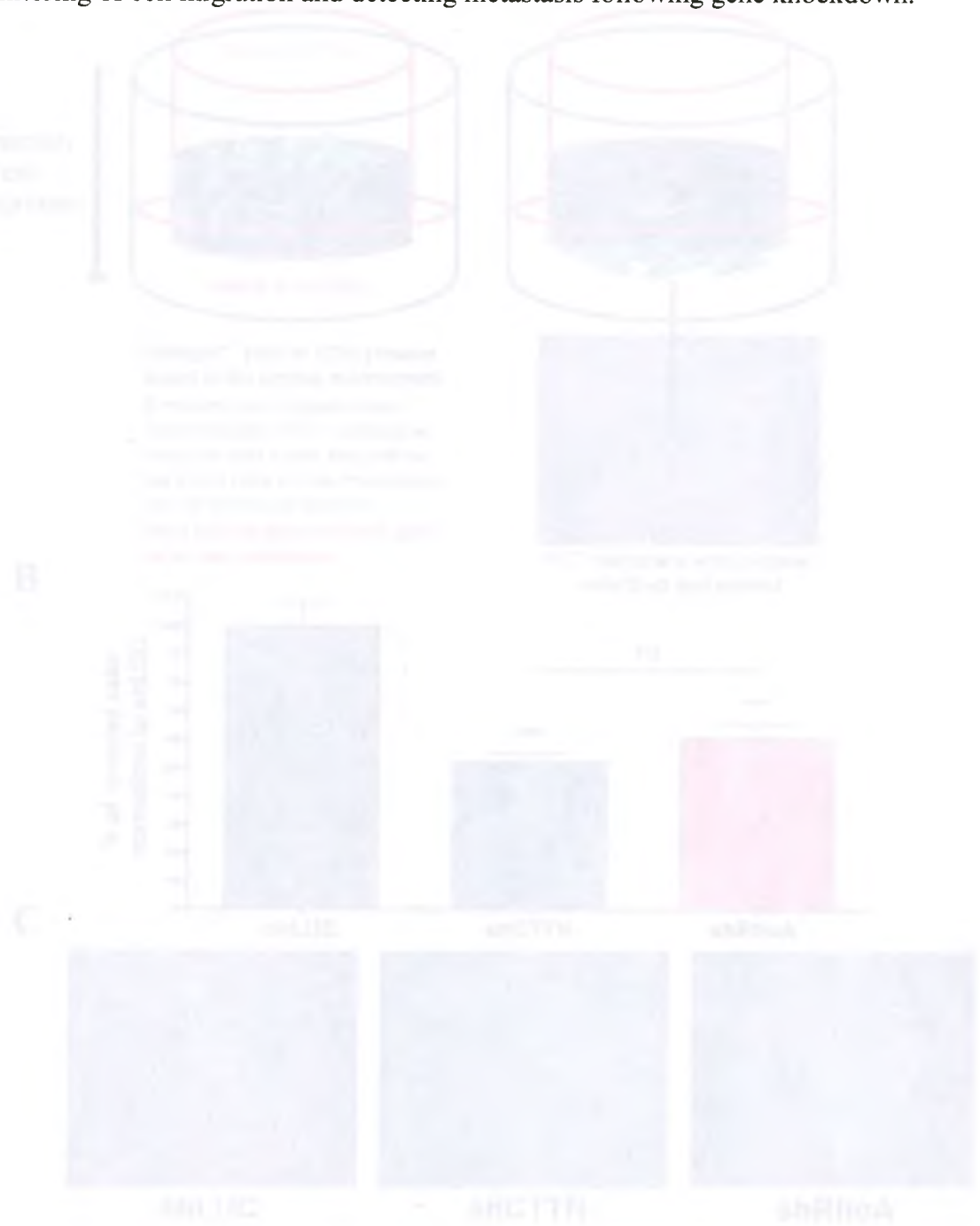

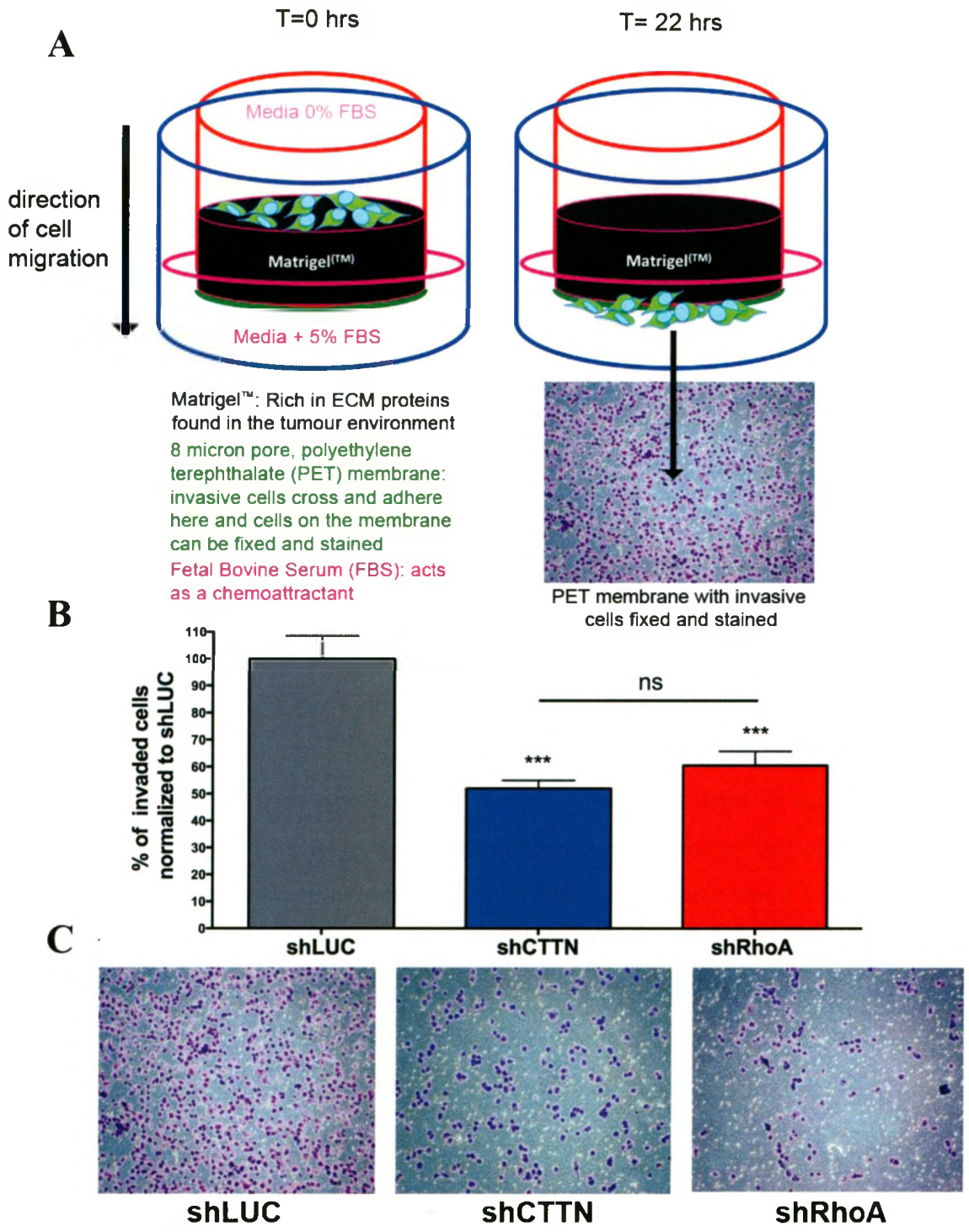

Figure 2.2.4: Cortactin and RhoA are required for cell migration and invasion *in vitro*
A. Cartoon of the Matrigel™ invasion chambers. The inner chamber (red) contains serum free media and cells on the surface of the Matrigel™. Cells are incubated for 22 hours and invasive cells that have migrated and invaded through both the Matrigel™ (black) and the PET membrane (green) are fixed and stained by removing the inner chamber. The outer chamber (blue) contains 5% serum so that the cells move in the direction of the chemoattractant. **B.** Counting the number of cells adhered to three PET membranes/group revealed that cortactin and rhoA are required for cell migration and invasion *in vitro* (***p<0.0001, 1 way ANOVA of the mean ±SEM, Tukey's Post test.). **C.** Representative images of the PET membranes depicting the invasive cells for each group.

RhoA and Cortactin are required for cell migration in the chicken embryo model and the inhibition of rhoA or cortactin by RNAi decreases cell migration by more than 50%

To test the affect of rhoA and cortactin knockdown on cell migration in the chicken embryo model, shRhoA or shCTTN cells were established in the CAM using an experimental metastasis approach. This model of metastasis involves the injection of cells directly into the bloodstream, effectively bypassing the initial steps of metastasis and allowing the cells to extravasate and arrest in the stroma of the CAM of day 9 embryos. Once cells have established a niche in the CAM stroma, they proliferate to form micrometastases composed of up to 100 cells per micrometastasis on average, after 3-5 days post-injection. Micrometastases are useful for studying cell migration because single cells can be easily tracked following time-lapsed, live cell imaging, using tracking software (ImageJ). A single micrometastasis also allows many cells (~30 cells) to be tracked over long time courses, but since the CAM can harbor many micrometastases, more than one of these colonies can be imaged during a single experiment by programming the microscope to toggle over each colony per time point. These properties of the experimental metastasis model in the chicken embryo CAM allow for more aggressive statistical analysis of cell migration in a single experiment. To compare the migration of shRhoA and shCTTN cells versus the shLUC control cells in the chicken embryo model, individual animals were injected per experimental condition on day 9 animals and imaged over a 10-hour time course, 3-5 days post-injection. At least 5 micrometastases were imaged per animal, however only cells from the best 3 of these colonies were used for quantification. Manual tracking of cells for the 3 individual micrometastases were averaged together for each group tested and the average cell velocity was compared to shLUC control cells. Velocity was calculated by the change in the X and Y cell coordinates between time points over a time span of 10 hours.

These experiments revealed that either RhoA or Cortactin is required for cell migration in the stroma of the chicken embryo model because knockdown of each of these genes resulted in reduced migration by more than 50% compared to shLUC control cells (Figure 2.2.5C, N=60 or more cells per animal, mean velocity is reported ±SEM, $p<0.001$, as determined by a 1-way ANOVA and Tukey's Post Test). These results are similar to the

observations made in the *in vitro* invasion and migration assays, where either RhoA or Cortactin was required for migration and invasion through the ECM, however, *in vivo*, there is no significance between shRhoA and shCTTN cell migration. These observations suggest that HEp3 cells do not preferentially utilize one protein over the other in cell migration and invasion. The ability of Cortactin and RhoA to work together to orchestrate cell migration was not tested. A key experiment to test if both Cortactin and RhoA work in the same pathway to enhance cell migration would be to simultaneously knockdown both genes and observe if this results in a synergistic decrease in cell migration. Although this experiment would have been feasible to perform by the methods used to test one gene at a time, these experiments are outside the scope of this project. The purpose of the project is to inhibit one gene at a time using genome-spanning shRNAs and screen for individual mediators of migration in the chicken embryo model.

The results from both the *in vitro* and *in vivo* migration assays demonstrate that known mediators of migration can be inhibited by RNAi to decrease cell migration and provide a proof of principle for the shRNA screen. When performing the screen for novel mediators of cell migration using the RNAi libraries, compact tumor phenotypes will be the selection criteria for decreased migration upon gene knockdown, and not cell velocity. To make a connection between decreased cell velocity and the appearance of less diffuse cells at the tumour border and better recapitulate the selection criteria of the screen, the shRhoA and shCTTN cell velocities were studied at the invasive border of tumours. In theory, compact colonies would be less likely to have invasive, motile cells at the tumour colony borders. If the cell velocities are reduced at the tumour border for rhoA and cortactin knockdown cells, this data would not only support previous findings in the current study, but would also relate cell migration in terms of velocity to the more compact tumour phenotypes where cells are not as motile at the tumour periphery.

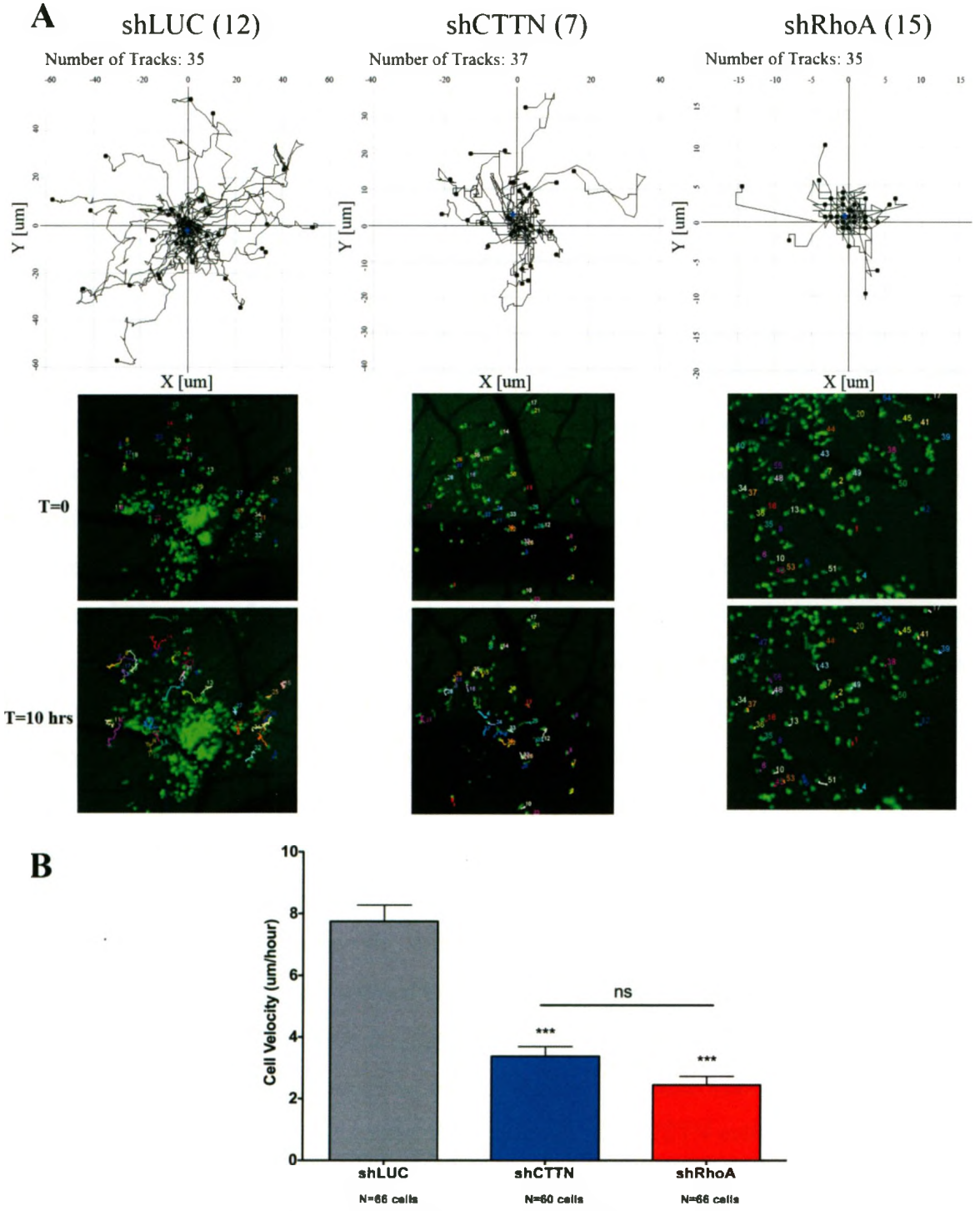

Figure 2.2.5: Cortactin and RhoA are required for cell migration as individual cells in micrometastases
A. Wind-Rose plots of the X and Y co-ordinates for cell tracks at each time point over 10 hours and the corresponding frames for each track at time 0 and 10hrs (50X magnification). Bracketed numbers represent the individual micrometastasis used to generate X/Y plots and images out of the three micrometastases that were averaged together to calculate the average velocity for each group in **B**. **B.** Cell velocity in micrometers per hour (um/hour) for individual cells (N=3 micrometastases/group). Cell velocities in the cortactin and rhoA knockdown groups are significantly lower compared to the control knockdown group, shLuciferase (shLUC). ***$p<0.0001$ compared to shLUC, 1 way ANOVA of mean±SEM, Tukey's Post Test.

RhoA and Cortactin are required for cell migration at the tumour border in the chicken embryo model and the inhibition of rhoA or cortactin by RNAi decreases cell velocity at the tumour periphery by 50% for shCTTN cells and by 37% for shRhoA cells

Previous studies performed by Zijlstra *et al.* have shown that decreased cell migration at the tumour border results in the formation of compact colonies and leads to decreased metastasis (Zijlstra 2008). To relate cell migration, in terms of cell velocity, to the appearance of compact colonies, shRhoA and shCTTN cell velocities were calculated at the invasive tumour border using a spontaneous model of metastasis in the chicken embryo model and intravital imaging. In contrast to previous studies performed by A. Zijlstra *et al.*, instead of using an antibody to block cell migration, shRNA against known mediators of migration, rhoA and cortactin, were used by injecting shRhoA or shCTTN cells directly into the mesoderm of the CAM. Injection of this 'bolus' of cells effectively bypasses extravasation events of metastasis and instead, cancer cells immediately begin to establish a niche in the stroma of the CAM by invading into the surrounding tissues. Decreases in cell motility at the tumour border have been explained by J.B Wykoff *et al* for protease-independent, amoeboid cell migration and demonstrate that RhoA mediated cell contraction, through its effector, ROCK, is responsible for the cell pushing itself through the ECM (Wyckoff 2006). Invasion into the surrounding tissues, as detected by histopathology, compounded by increases in Cortactin expression, also suggest a role for protease dependent invasion into the stroma (Mader 2011). In light of the possibility of cells to utilize protease dependent and independent programs in cell invasion and migration at the tumour border, in the current study, the roles of both arms of the migration machinery were examined by studying either RhoA or Cortactin knockdown cells at the tumour-stroma interface. In this experiment, shRhoA or shCTTN cells at the invasive border were imaged over time and cell migration was tracked to illustrate: 1) that less invasive tumours have decreased motility at their borders and 2) to uncover the type of migration machinery necessary to achieve less invasive, compact colonies.

Quantification of the average cell velocity at the tumour border for shCTTN cells revealed that the velocity was 4 um/hr, representing a 50% reduction of cell velocity compared to shLUC control cells that traveled at 8 um/hr (Figure 2.2.6B, N=55 cells, velocity

represents the mean cell velocity ±SEM of cells in 3 non-overlapping FOV per tumour, $p<0.01$, as determined by a 1-way ANOVA and Tukey's Post test). These migration results are identical to those discovered from the *in vitro* study and also corroborate with the reduction of cell migration seen with cells in a micrometastasis *in vivo.* The reduction of cell velocity seen with shCTTN cells at the tumour border also support the findings of A. Zilstra *et al.* who show that reduced cell migration at the tumour border leads to compact tumor phenotypes, thus strengthening this proof-of-principle study for the RNAi screen for migration mediators. Also, the lack of significance between shRhoA and shCTTN cells, indicates that both arms of the migration are necessary for motility at the tumour border.

Quantification of the average cell velocity at the tumour border for shRhoA cells revealed that the velocity was 5 um/hr, representing a 37% reduction of cell velocity compared to shLUC control cells (Figure 2.2.6B, N=71 cells, velocity represents the mean cell velocity ±SEM of cells in 3 non-overlapping FOV per tumour, $p<0.05$, as determined by a 1-way ANOVA and Tukey's Post test). This reduction in cell velocity is not significantly different from the shCTTN cells, however the mean cell velocity is higher for rhoA inhibited cells at the tumour border than the cells in a micromet (Figure 2.2.5B). The data for shRhoA cell migration, taken together, suggests that rhoA may be more important for single cell migration in the CAM over invasive cell migration at the tumour border for HEp3 cells.

In summary, cell migration is inhibited upon the RNAi-mediated knockdown of both cortactin and rhoA mRNA transcripts and protein both *in vitro* and in the chicken embryo model. The average cell velocity is decreased *in vivo* upon inhibition of rhoA or cortactin in the context of single cells in a micrometastasis. These decreases in cell velocity are carried over to cell migration at the invasive tumour border, suggesting that cell migration is responsible for more invasive tumour phenotypes as previously demonstrated by A. Zijlstra *et al.* Also, in both cases of migration, either as a single cell in a micrometastasis, or as a cell at the tumour-stroma interface, both protease-dependent and protease-depended cell migration machinery are required for migration. These studies provide a proof of principle for conducting the shRNA screen for compact tumor phenotypes to identify

mediators of migration, however, in this study, it has not yet been demonstrated how cells with inhibited mediators of migration will behave in the context of metastasis.

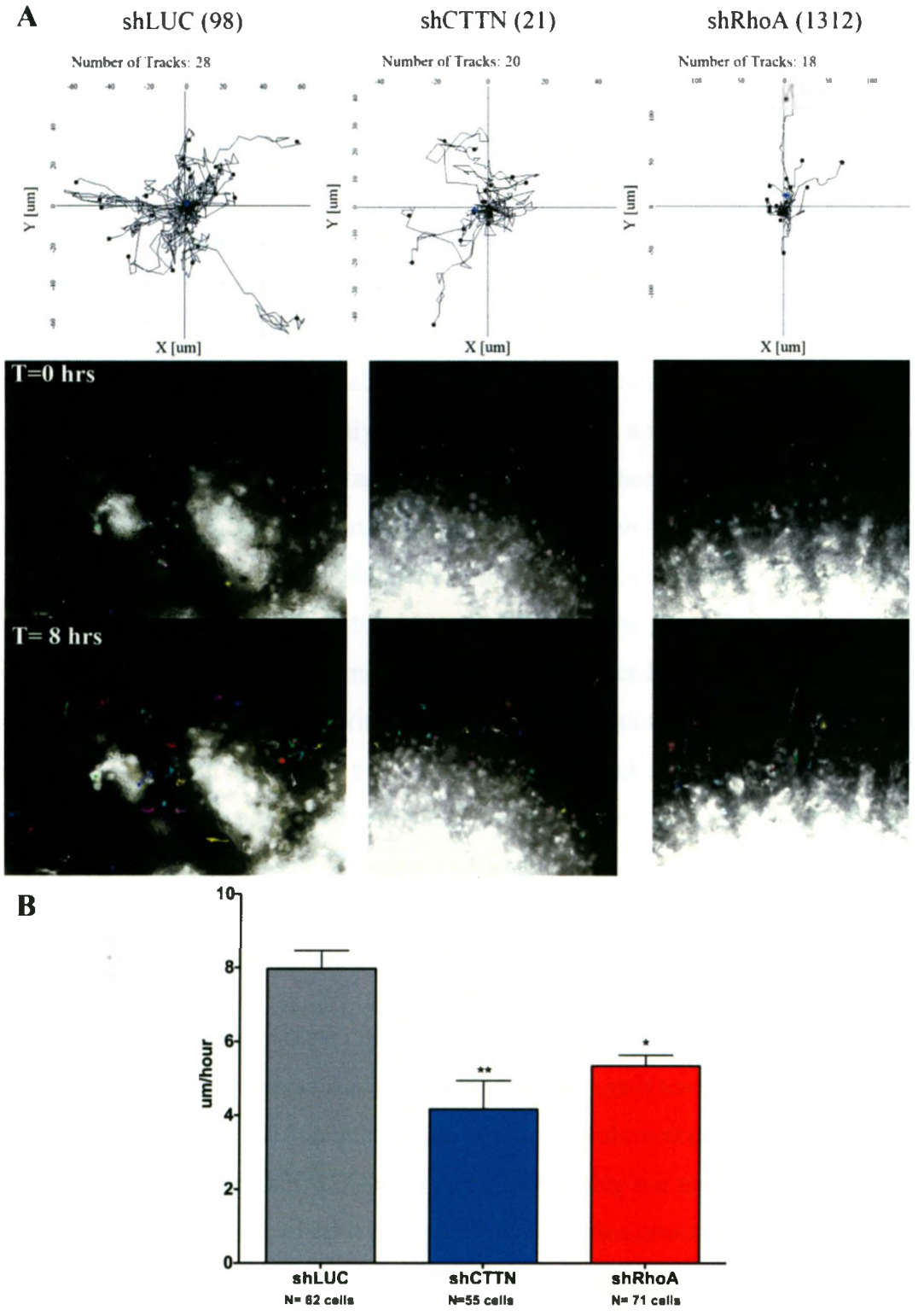

Figure 2.2.6: Cortactin and RhoA are required for cell migration at the invasive tumour border
A. Wind-Rose plots of the X and Y co-ordinates for cell tracks at each time point over 8 hours and the corresponding frames for each track at time 0 and 8hrs (100X magnification). Bracketed numbers represent the individual FOV per tumour used to generate X/Y plots. **B.** Cell velocity in micrometers per hour (um/hour) for individual cells at the tumour border (N=3 FOV/group). Cell velocities in the cortactin and rhoA knockdown groups are significantly lower compared to shLUC .*$p<0.05$ and **$p<0.01$ compared to shLUC, 1 way ANOVA of mean±SEM, and Tukey's Post Test.

Inhibition of migration mediators, RhoA and Cortactin, results in diminished metastasis

Due to the overexpression of rhoA and amplification of cortactin in many human cancers, and the accumulating amount of evidence detailing their effects on enhancement of cell migration and metastatic potential, animal studies have been performed to look at their direct effect on metastasis (Fritz, Just and Kaina 1999; Gou 2011; Cai 2010; Lai 2009; Chan 2010 and Yansong 2001). Most of the studies to date, however, are generated using experimental metastasis models and use only semi-quantitative methods to read out metastasis such as presence or absence of microscopic nodules, histology and/or imaging techniques. Also, the crude analysis of metastases does not take into account tumor cells that may lie dormant in organs and go undetected. Furthermore, these studies were done by manipulating either rhoA or cortactin in a cell line of interest, but never rhoA or cortactin in the same cell line and/or model. Due to the design of previous studies, rhoA and cortactin were not studied side by side, and therefore, the general mechanism of cancer cell migration, either protease-dependent or protease-independent, and whether RhoA or Cortactin is more important during invasion and intravasation, is still undefined. Execution of an experiment to look at the particular migration machinery important to all steps of metastasis, either protease-independent or protease-dependent, and whether these cells are addicted to one method over the other, is possible using a quantitative, spontaneous model of metastasis and would be a novel study to perform *in vivo*, in addition to providing a proof of concept for the RNAi screen.

Inhibition of migration has previously been shown to abolish metastasis *in vivo* using a spontaneous model of metastasis (Zijlstra 2008). To test if mediators of migration identified through an RNAi screen could possibly result in decreased metastasis upon inhibition, shRhoA and shCTTN cells were tested using the spontaneous metastasis model and the absolute number of cells present in the liver was quantified using the sensitive, *alu* RT-PCR technique (Zijlstra 2002). The spontaneous model of metastasis requires implantation of cancer cells directly onto the ectoderm of the CAM and incorporates all the steps in the metastatic cascade including invasion into the surrounding stroma and intravasation into nearby blood vessels, followed by extravasation into the secondary sites (Ribatti 2010).

In the assay, chicken embryo livers were dissected 7 days following implantation of shCTTN or shRhoA cells and the genomic DNA was extracted from all cells in the liver. Utilization of primers specific for human *alu* repeats, in a chicken embryo background, allowed for both the amplification and detection of human cancer cells present in the liver. A standard curve was run side-by-side in the *alu* RT-PCR experiment, and was used to interpolate the precise number of human cancer cells per liver in unknown samples (Zijlstra 2002). Primary tumours were also collected and weighed at the time of sacrifice, and were used to normalize the amount of metastases.

When the spontaneous metastasis assay was performed on rhoA and cortactin knockdown cells, quantitative RT-PCR analysis revealed that the average number of cells found in the chicken embryo livers was reduced for both experimental groups when compared to the control cells, however this was not significant (Figure 2.2.7A, N=1 experiment, at least 4 animals per experimental and control groups. Reported is the mean number of cells detected in the liver per milligram of primary tumour, relative to the amount of liver tissue present, as detected by chicken GAPDH specific primers. A 1-way ANOVA, and Tukey's post-test tested for significance). This data suggests that both arms of cell migration, as observed in previous assays performed in the study, are also important in metastasis. Upon analysis of this assay, it was necessary to normalize the amount of cells in the liver to the primary tumour size as the primary tumours that develop for rhoA and cortactin inhibited cells have a smaller average size than those for control cells, although this finding is insignificant when compared to shLUC tumour weights (Figure 2.2.7C (left panel), N=5 tumours, reported is the mean weight of tumours in milligrams, 7 days post-implantation ±SEM. *$p<0.05$ compared to parental cells, as determined by a 1-way ANOVA, Tukey's post test).

Cell proliferation assays have been performed by many groups to test the affect of a given treatment between experimental and control cells and have found that the knockdown of certain genes can lead to differential cell proliferation rates (Scudiero 1988and Simpson 2008). To exclude the possibility that that tumours of rhoA and cortactin inhibited HEp3 cells are proliferating at a slower rate than control cells, an MTT cell proliferation assay was performed to calculate the number of cells present for each group over 7 days. Results

from this experiment conclude that the knockdown cells are not proliferating at significantly different rates compared to shLUC cells (Figure 2.2.7B. N=3 experiments, duplicate wells per experiment for each cell type, shCTTN: p=0.089 and shRhoA: p=0.124 as determined by analysis of the differences between the slopes in a linear regression test and compared to shLUC). The fact that shRhoA and shCTTN cells do not proliferate slower than the control, suggests that the proliferation rate of rhoA and cortactin knockdown cells is not responsible for low tumour weights and instead, the inability of these cells to invade down into the mesoderm of the CAM, where blood vessels are located, is more likely. Evidence for this hypothesis comes from previous experiments in this study where the inhibition of rhoA and cortactin lead to decreased invasion through Matrigel™ (Figure 2.2.4).

To determine if increasing the number of rhoA or cortactin knockdown cells implanted onto the CAM would increase the tumour weight, 2 million cells per implant were used to form primary tumours with shRhoA or shCTTN cells, but only 1 million cells per implant were used to form primary tumours with parental and shLUC control cells. This experiment did not result in significantly larger tumours (See Appendix B), although the mean weight of the tumours for shRhoA cells did increase, bringing these tumours closer to the size of control and tumours (Figure 2.2.7C, right panel).

These results suggest that the knockdown of mediators of migration, rhoA and cortactin, decrease the motility and invasion of cells at the primary tumour, and contribute to an overall decrease in metastasis. Experimental evidence obtained from these known mediators of migration provide support for the execution of a genome-wide, RNAi screen for the compact tumour phenotype where novel mediators of migration can be identified and these genes may also be required for metastasis.

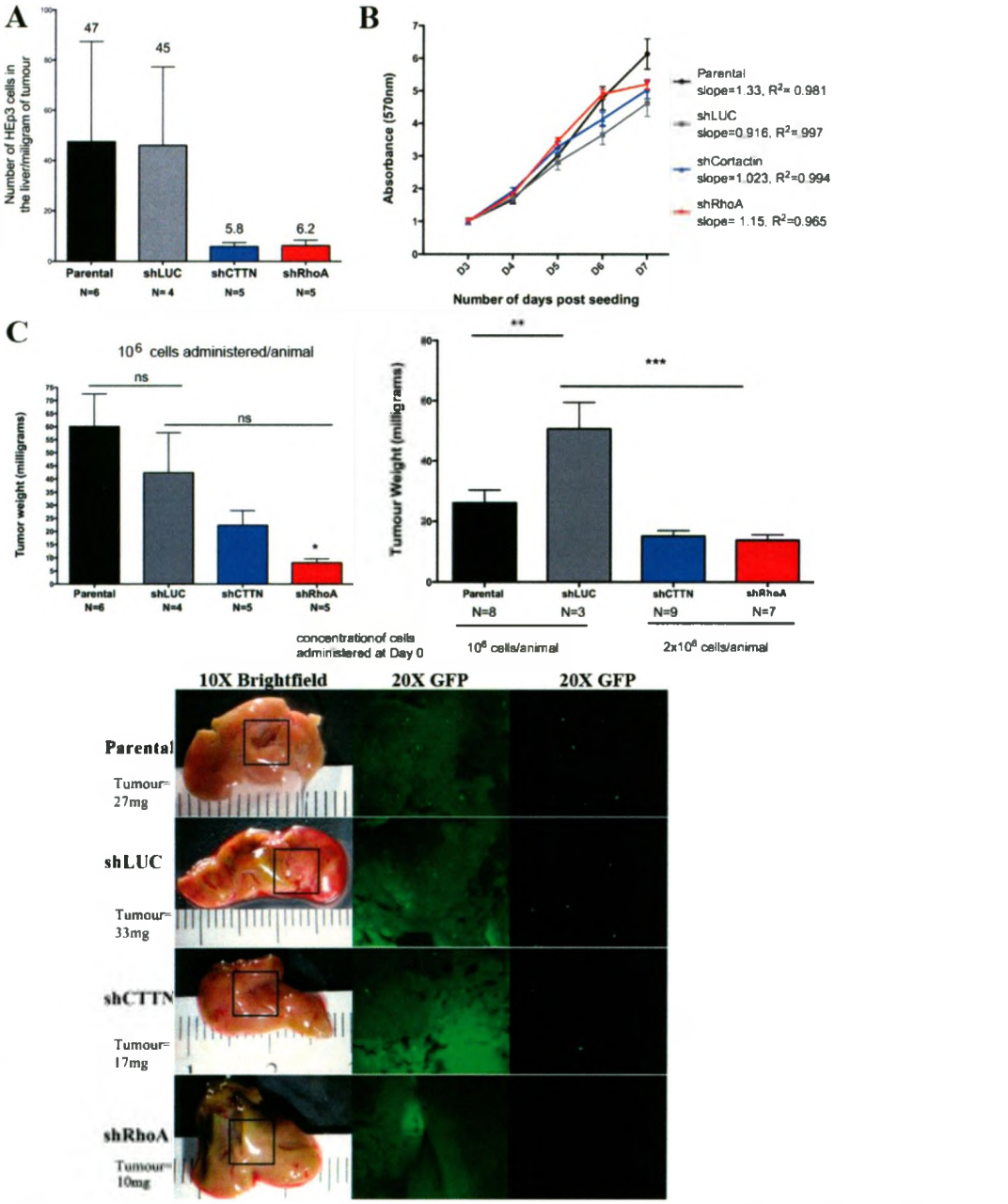

Figure 2.2.7: Inhibiton of RhoA or Cortactin prevents tumour establishment in the ectoderm of the CAM and decreases metastasis

A. The number of cells that metastasized to the liver per milligram (mg) of primary tumour as quantified by *alu* RT-PCR, relative to total amount of liver per sample (chicken GAPDH). The results of this experiment are not significant as determined by a 1-way ANOVA analysis, N=4-6 animals per experimental condition. **B.** Cell proliferation assay as measured by colourometric analysis of the conversion of MTT to formazan. The slopes are not significantly different as determined by linear regression analysis between shRhoA or shCTTN and shLUC cells (N=3, duplicate wells per cell type). **C.** *Left panel:* tumour weight (mg) for primary tumours of animals analyzed by *alu* RT-PCR. shRhoA tumours are significantly smaller than the parental cells (N=5 animals, *$p<0.05$, as determined by a 1-way ANOVA, Tukey's Post test). *Right panel:* tumour weight (mg) for primary tumours, 7 days post-administration of 2X cells onto the CAM for shRho and shCTTN cells (N=3-9 tumours/group *$p<0.01$, **$p<0.001$ as determined by 1-way ANOVA and Tukey's Post test). *Bottom:* Representative livers 7 days post implantation of 1 million cells/animal for each experimental and control group at 10X and individual fluorescent HEp3-GFP cells in the liver at 20X.

2.3 Objective 3: Perform an shRNA Screen for Novel Mediators of Cell Migration in the Chicken Embryo Model

Identification of compact tumour colonies *in vivo* using HEp3 cells and a pool of 10 000 shRNAs, covering 5000 distinct genes in the human genome and Identification of shRNA targets in individual compact colonies

To perform the RNAi screen, HEp3-GFP cells were first infected with the optimized *non-functional* MOI of 5 (*functional* MOI of 0.4) to reduce double integration events *in vitro* using the Open Biosystems Decode RNAi viral screening library. This library contains lentiviral particles that are packaged with 10, 000 individual shRNA containing pGIPZ vectors that target ~5000 genes in the human genome for knockdown (Figure 2.2.8A). Cells were selected in puromycin to eliminate non-infected HEp3-GFP cells and were subsequently expanded to provide a total of 20 million cells for the screen. Each animal was subjected to i.v injection of 100,000 HEp3-GFP-pGIPZ-shmiR cells and a total of 150 animals were injected within an 8 hour period of time to accommodate 3X coverage of the 5000 genes in the screen. The CAMs of chicken embryos were visualized using fluorescence microscopy for compact colonies beginning at 5 days post-injection. Discovery of compact tumour colonies were marked with filter paper and resected from the CAM (Figure 2.2.8B). Compact colonies continued to be identified, and resected up to day 7 post-injection (day 17 embryos). Dissected colonies were expanded in tissue culture in puromycin to select out chicken embryo tissue and contaminants. In this iteration of the screen, 12 compact tumour colonies were extracted from the CAMs of chicken embryos (Figure 2.2.8B and Appendix.C-E). These colonies were ranked as highly compact (score of 1) to diffuse (score of 5), and out of the 12 colonies: 5 were highly compact (1), 3 were compact (2), 2 were medium compact (3), 1 was somewhat compact (4), and another was diffuse (5). Unfortunately, out of all 12 colonies resected, only 3 colonies survived expansion in tissue culture (Figure 2.2.8B: colonies C, D and F). From these three colonies, sub-colonies were picked to reduce the chance of expanding two cells with different shRNAs that may have formed one colony. This step is necessary since only one short hairpin can be sequenced per sample. Genomic DNA was extracted from 5 sub-

colonies per tumour colony and using forward and reverse primers, unique to sequences flanking the shRNA, regions containing the shRNA were amplified using PCR (Figure 2.2.8A). Sequencing of these amplicons revealed three gene targets: MESDC1, KIF3B and ARHGAP12 (Figure 2.2.8D). These targets arose from colonies C and F, but not colony D, as amplicons from D did not yield interpretable sequencing results. An explanation for this is that there is more than one short hairpin in the sample, contaminating the PCR result. The additional shRNA could be present either by the multiple-integration of unique pGIPZ plasmids, or by the contamination of more than one cell per well during the selection of sub-colonies in cases where more than one cell forms a compact tumour.

In summary, the optimization of an shRNA screen has been performed for a small-scale screen and these optimization parameters can also be applied to larger scale screens for cell migration. The efforts made in this study contribute not only to the optimization of such large scale screens but also provides a proof-of-principle by describing how positive hits can be identified in the chicken embryo model through RNAi inhibition. In this smaller scale screen, three gene targets were discovered to be important for cell migration *in vivo*, however, many potential targets were lost through the screening process and clearly, there are still areas of the screen that need further optimization. Such areas include maximizing the survival of hits post-extraction or subjecting these cells to more sensitive PCR techniques that require less cells. Another area of improvement would be to sub-clone the shRNAs into individual cloning vectors from the collection of cells from the primary tumour instead of colony picking. This would provide faster processing time and prevent drop out of hits from muddled sequencing results when more than one shRNA is PCR amplified. In addition, further validation of the gene targets found in this initial screen, using cell migration assays described in this study is still necessary to elucidate and confirm the role of these genes in cell migration and metastasis.

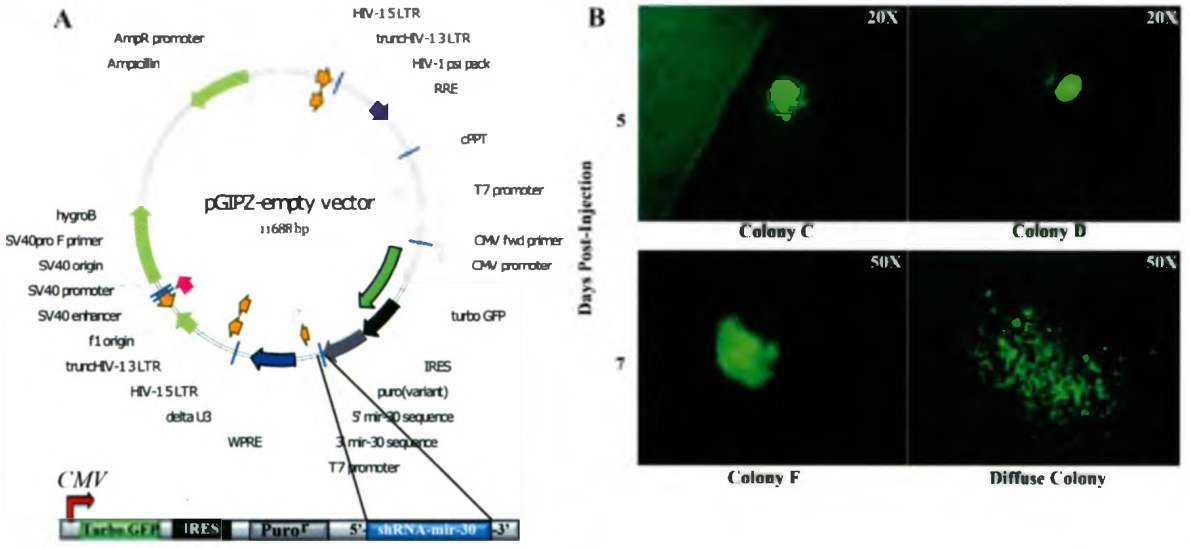

Colony	Sub-colony	Gene Symbol	Human Gene Description	Function	No. Articles (PubMed)	References
C	C	MESDC1	Mesoderm Development Candidate 1	Actin-binding Protein	2	Wines, M.E. *et al.*(2001) Gingras, A.R. *et al.* (2010)
C	E					
C	L					
C	F	KIF3B	Kinesin Family member 3B	Microtubule based movement/Matrix degradation	45	Zhang, Y. and Hancock, W.C (2004) Wiesner, C. *et al.* (2010)
F	A	ARHGAP12	Rho GTPase Activating Protein 12	GTPase activator activity/signal transduction	3	Zhang, Z. *et al.* (2002) Gentile, A. *et al.* (2008)
F	B					
F	R					
F	S					
F	Wii					

Figure 2.3.1: Identification of novel mediators of cell migration using an RNAi screen in vivo
A. Annotated pGIPZ construct and the region containing the shRNA-mir30 sequence (inset). The forward and reverse primers amplify the region containing the shRNA from compact colonies. **B.** Images of the compact colonies extracted for identification of the shRNA construct responsible for the loss of cell migration. Colonies C, D and F are ranked as highly compact and are a '1' on a scale of 1-5. The diffuse colony in the bottom right panel represents a colony that would not be considered a hit in the screen and is given a score of '5'. **C.** shRNA specific primers were used to amplify the short hairpin and flanking sequences (561bp) in order to sequence the shRNA and identify the gene target. 5 sub-clones from each individual compact colony were PCR amplified and sent for sequencing. **D.** Target genes of the shRNAs amplified from the compact colonies in **B.**

Chapter 3

3 Discussion

Cell migration is a well-documented phenomenon in the human body and typically results in a beneficial outcome, such as in the event of immune surveillance, wound healing, and reproduction (Walzer and Vivier 2011; Wang 2011 and Chen 2011). In contrast, cell migration in the context of cancer enhances the invasiveness of tumour cells, and leads to increased instances of metastasis, ultimately contributing to poor patient prognosis (Zijlstra 2008 and Shieh 1999). Many of the mediators of migration, including cytoskeletal reorganization proteins, matrix metalloproteases and cell adhesion molecules have been identified to be deregulated in cancer cells, and their aberrant expression is often found in advanced stage cancers (Horiuchi 2003; Toyoda 2009; Wang 2010; Cai 2010 and Alshenawy 2010). Although 1300 manuscripts linking migration to cancer were published as of 2010, the full repertoire of cell migration genes is incomplete and only a fraction of the mediators discovered have been tested clinically, and none are in clinical use (Palmer 2011). There is always a question of whether or not it is feasible to target motility in the clinic as most patients arrive post development of the primary tumour and cancer cells may have already disseminated. In the review by T.D. Palmer *et al.,* the authors make a strong case for why targeting motility could be a success in the clinic. They suggest that targeting motility could be a preventative measure taken while 'watchful waiting' so that the patient who presents biomarkers for metastasis or who has a higher grade tumour, may be treated less aggressively without putting them at risk for developing metastasis. Targeting migration in invasive cancers that cannot be resected, such as in the brain or pancreas, could also be another benefit for patients. Finally, the authors make the point that targeting migration in cancer early on may prevent more aggressive phenotypes from evolving, as invasive-programs are often associated with enhanced motility (Palmer 2011; Zuo 2011 and Alshenawy 2010).

Clearly, the known players in cell migration to date have not resulted in a successful treatment for cell migration and metastasis, providing a rationale for the identification of novel mediators of migration as additional druggable targets for metastasis (Palmer 2011 and Kessenbrock, Plaks and Werb 2010). Treating migration in the clinic requires targeting

the molecular mediators of cancer cell migration only, and not the mediators of inflammation and wound healing. A genome-wide screen for mediators of migration, *in vivo* would be a beneficial means to identify a multitude of diverse genes involved in cancer cell migration so that exclusion of genes critical to normal physiological processes would not significantly impinge upon the number of druggable targets that could be taken to the clinic.

RNAi screens for cell migration in human cancer constitute a relatively small subset of cancer related genetic screens and 100% of RNAi screens for cancer cell migration are performed *in vitro*. Therefore, this study fulfills the need for a high throughput method to identify relevant migration mediators *in vivo*. The screen performed in this study is a modified H&E shRNA-miR-30 based library, purchased from Open Biosystems, and packaged in the form of lentiviral particles. Individual particles deliver single shRNA-miR-30 cassettes and integrate them into the host genome. To corroborate with other RNAi screens that are based on the method of integrating one shRNA expression vector per target cell, so that confounding results of multiple gene silencing are reduced, the RNAi screen in this study was optimized to introduce the bare minimum amount of double integration events (Boettcher and Hoheisel 2010; Lara 2011; Simpson 2008 and Smolen 2010). Optimizing the amount of virus particles delivered to each cell is an important measure to take in the cell line of interest (HEp3) to ensure only one shRNA is integrated per cell. Since Open Biosystems uses a different cell line to titer viral particles, the MOI would need to be calculated in the HEp3 cell line as HEK293 cells yield notoriously higher viral titers than most cell lines when tested by GFP expression or by quantifying the amount of DNA transcripts within the cell (Sastry 2002). P. Salmon *et al.* point out two independent reasons why different cell lines have varying amounts of permissibility. First, variation between cell lines could reflect changes in the expression levels of pro-viral genes, or genes necessary for the many steps required in the infection process from viral entry to genomic integration. Secondly, as viral titers are based on the expression of exogenous genes such as GFP or puromycin resistance, the assay used to determine cell infectivity would also rely on the capacity of the particular cell line to produce the protein being measured (Salmon and Trono 2006).

To address the question of how HEp3 cells compare to HEK293 cells in terms of viral infectivity, a measure of the *functional* MOI had to be determined though a biological assay on HEp3 cells. Open Biosystems, as well as other groups, calculate viral titer using flow cytometry analysis for HEK293 cells, however it is suggested by the supplier and other groups that manual cell counting of GFP signal can be used to obtain titer and MOI values for the cell line of interest (Sastry 2002 and Lyva 2011). To test if manual counting is accurate compared to flow cytometry analysis, in house, the percentage of GFP positive cells was counted using both methods. Comparison of the two methods of analysis showed no statistical difference in the way cells are titered for MOI determination. However, as the dilution of virus becomes greater, the titers begin to diverge between the two methods, lending to the fact that dim cells are not detected by flow cytometry and are therefore gated out of the calculations (Sastry 2002). As the two methods are identical at the low dilutions, which most closely resemble the amount of virus that was be used in the actual study, the cell counting method was implemented for MOI calculations on HEp3 cells. Another observation taken from this study was the significant decrease in GFP positive cells calculated by both the cell counting and flow cytometry methods as the dilution of virus increases. Other groups using different cell lines have also made this observation, and so the data obtained in this study corroborates with current literature on lentiviral infectivity (Lyva 2011).

Calculation of the *functional* MOI for HEp3 cells was performed using the counting method for GFP positive cells since this was determined to be comparable to flow cytometry. Results from this experiment demonstrate that HEp3 cells have a lower *functional* MOI than the expected MOI based on the viral titers calculated by the supplier in HEK293T cells. The low transduction efficiency of HEp3 cells could be a result of their capacity to express proteins necessary for viral gene delivery or could be a reflection of their ability to express Turbo GFP. Large differences in cell permissively have been reported for the same cell type when infected with the same MOI when different methods are used for cell differentiation, and thus gene expression profiles may be altered between the two cell types. In these reports, however, infectivity was measured by GFP or EGFP (flow cytometry) and although this demonstrates how gene alterations could account for the lower MOI values in HEp3 cells than expected, it still does not uncover whether or not

these changes in gene expression result in less viral permissively or less fluorescent protein production (Lyva 2011). Differences in cell permissiveness between cell types, however, has been reported when directly measuring viral infectivity without relying on expression of an exogenous genes such as GFP, supporting the need for pro-viral genes that support the virus life cycle (Cooi 1988). Although HEp3 cells demonstrate a lower infectivity for the VSV-G peudotyped lentivirus particles, they still exhibit the same kinetics seen in HT-1080 cells and by other groups and the increase in virus particles (MOI) causes increases in transduction (Cooi 1988; Lyva 2011 and Sastry 2002). Surprisingly, this increase in transduction was not a linear relationship in accordance with MOI, as seen by L. Sastry *et al.* and instead, appeared to have 'decreasing amounts of increase' as moving from *non-functional* MOIs of 1 to 5 had a greater increase in GFP expression than moving from 5 to 10. The method used to detect increases in viral infection by L. Sastry *et al.* however involved a more sensitive technique using PCR amplification of viral DNA vectors present within cells, that gives 10-fold higher transduction efficiency readings than GFP measurement and therefore the could be an artifact of the assay used (Sastry 2002). Finally, it cannot be discounted that the virus received from Open Biosystems may have exhibited a lower titer on HEK293T cells, had they been tested for viral infectivity in house. The permissibility of HEp3 cells, therefore, cannot be concluded to be lower HEK293T cells, however there is evidence to prove that HEK293 cells are a highly permissive cell type in comparison to most cells (Sastry 2002).

Discovering how the cell line of interest behaves in terms of viral infectivity is a necessary first step to performing RNAi based screen. The next step in this process is to ensure that all genes represented by the RNAi library are represented in the model of interest whether *in vitro* or *in vivo*. The RNAi screen performed in this study was initially infected into cells *in vitro* and the cell population used for infection was enough to accommodate all genes within the library. An MOI of 5 was discovered to be effective for transductions and renders 30% of cells infected. Since 300, 000 cells were used for RNAi infection, this means 90,000 shRNAs will be represented *in vitro.* These figures allow for the 10,000 shRNAs in the library to be represented 9X and the genes in the screen to be represented 18X. Moving *in vivo*, however, this representation needs to be maintained to a level of at least 3X. Expanding cells from *in vitro* RNAi infections in cell culture allows for any

number of cells to be administered to animals for maintenance of gene representation *in vivo.* The *in vivo* model system employed, however, cannot be oversaturated with cells as this would interfere with both screening for compact tumour phenotypes as well as extraction of hits. To obtain a desirable number of cells in the CAM, that represents genes in the library at 3X, and more importantly, represents genes that can be properly extracted without contaminating colonies, the number of cells administered to each animal must be optimized. Optimization parameters included: 1) maximization of the amount of colonies in the CAM, to reduce the number of animals needed, for more high-throughput screening and 2) minimization of the amount of colony overlap for a clean isolation of hits. The results from this study describe that upon administration of 50,000 HEp3 cells, the number of colonies that are also easily extracted, without contaminating colonies, is still less than the number of colonies that can be cleanly isolated by the administration of 100, 000 cells. This observation led to the selection of 100,000 HEp3 cells to use for the screen and also allowed for a broad estimation of the number of animals the screen would need to be performed on in order to represent the genes in the screen three times over. In other model systems used for *in vivo* RNAi screening, there can be up to a 20-week end point for tumour development to occur and so screening in this manner can be arduous and does not facilitate entire genome screening (Bric 2009). The feasibility of entire genome screening within the chicken embryo CAM, demonstrated by the high number of tumour colonies and the short time course for tumour development seen within the CAM, is an exciting opportunity to explore the entire genome for cell migration, *in vivo*, which has never been done before.

Others have used positive controls when conducting RNAi screen *in vivo* and have demonstrated the importance of these controls, not only to prove that phenotypes can be measured by the system, but also to set a baseline to which RNAi knock down can illicit a particular phenotype *in vivo* (Bric 2009). In this study, known mediators of migration and metastasis, RhoA and Cortactin, were selected to serve as positive controls in an RNAi screen for novel mediators of migration *in vivo.* These proof-of-principle studies have laid the ground work for not only a small scale RNAi screen in the chicken embryo model, but have also contributed to the overall goal of screening the entire human genome to create a comprehensive library of potentially therapeutic targets of cell migration. RhoA and

Cortactin were chosen as positive controls because in addition to their association with cell migration, metastasis and poor patient outcome, these proteins also encompass all requirements of cell migration through the two distinct arms of cell migration, protease-independent and protease-dependent, respectively (Gou 2011; Cai 2010; Wyckoff 2006 and Artym 2006). In addition to providing a proof of principle for the screen, testing the cell migration patterns in either cortactin or rhoA knockdown cells, could provide insight into the types of cell migration machinery most often used by HEp3 cells for migration and predict the type of genes that might be identified in the screen. In this respect, inhibition of cortactin, would depress protease-dependent cell migration through a decrease in mature, invadopodia structures that assist in locating collagen IV proteases to the site of cell invasion and 'pave the way' for migration into the ECM (Artym 2006 and Rowe and Weiss 2008). Inhibition of RhoA, on the other hand, would depress protease-independent movement through the ECM through ROCK-myosin II actomyosin contractility (Wyckoff 2006 and Row and Weiss 2008). The results from this study show that there is no preference for the use of protease-independent versus protease-dependent migration machinery in HEp3 cells since inhibition of either rhoA or cortactin led to similar decreases in cell migration both *in vitro* and *in vivo*. Furthermore, this depression of migration contributes to obliteration of metastasis as reported by other groups (Palmer 2011 and Zijlstra 2008). These positive controls, therefore, demonstrate that knockdown of migratory genes should demonstrate the less invasive phenotype seen by less motile cells, and that the baseline decrease in cell migration in HEp3 cells upon inhibition could be as low as 50% (Zijlstra 2008). These results also conclude that the type of cell migration mediators uncovered by the screen could involve players of either arm of migration machinery. One hypothesis for why both arms of cell migration might be important to establishing migration, invasion and metastasis, has been suggested in the literature. This hypothesis emphasizes that since events in metastasis-cascade require many barriers to cells, cancer cells may preferentially switch between the two arms of cell migration to accommodate for any situation they may encounter (Sahai, and Marshall 2003). Results from this study show that knockdown of either rhoA or cortactin inhibits metastasis and this could be accounted for by the inability of HEp3 cells to switch between the two mechanisms when one is inhibited. Another explanation for the similar requirements for

both RhoA and Cortactin in all of the steps in the migration cascade including migration, invasion, intravasation, and extravasation could be that rhoA and cortactin function in the same pathway. Evidence for this hypothesis comes from discovery that cortactin modulates rhoA activation in 11q13-amplified head and neck cancer cells, where 11q13 represents the chromosome on which the cortactin (*EMS1)* gene is located, to promote cell cycle progression and enhanced cell proliferation (Croucher 2010). This observation could explain why knockdown of cortactin behaves similarly to knockdown of rhoA since, in this hypothesis; rhoA could be a downstream effector of cortactin. The amplification status of *EMS1* is unknown for HEp3 cells, however, because the proliferation rate of cortactin knockdown cells is not significantly different from the control, it is not likely that cortactin is amplified in HEp3 cells lines, as a decrease in cortactin expression in 11q13 amplified cells should show a decrease in proliferation. Furthermore, Cortactin has been shown to signal through Cdc42, but not RhoA, to potentiate migration in mouse embryonic fibroblasts suggesting that the connection between Cortactin and RhoA may only be applicable for proliferation and not migration (Lai 2009).

One drawback to the experiments performed with RhoA and Cortactin is that the RNAi mechanism by which these genes were silenced is, in theory, specific for the cortactin and rhoA transcripts only, however, since only a few nucleotides, or seed region, on the shRNA need to match the mRNA, there is a chance for off-target or unwanted gene knockdown, confounding the results (Dua 2011). To add confidence to these experiments, additional shRNA constructs targeting these genes could be used to confirm the results; alternatively, inhibitors of these proteins could also be used to treat these cells prior to experimentation. These results are strengthened, however, by the fact that not only one, but two mediators of migration were knocked down independently, and each resulted in decreased invasion, migration and metastasis, and in an indirect way this is similar to the addition of two shRNAs per one migratory gene. Furthermore, knockdown of each of these genes exhibited a decrease in migration, invasion and metastasis in a number of different experiments testing for migration, emphasizing that the decrease in migration is not an artifact of one particular testing method.

Taken together, the knockdown of cortactin and rhoA, as tested by measuring both mRNA transcript levels and protein, demonstrates that inhibition of migration mediators will exhibit a decreased migratory phenotype in multiple experiments, including experiments in the chicken embryo model. These experiments look at genes responsible for both arms of migration machinery, and thus, allude to the type of genes that could be uncovered for HEp3 cells. These genes could represent both arms of the migration machinery, either because HEp3 cells 'switch' between the two types of migration, or use both protease-independent and dependent genes in the same pathway at once. Understanding and predicting the type of hits could be found in large-scale screening allows for the rationalization of such gene targets and the planning of appropriate validation experiments.

Performing an iteration of the Open Biosystems, H&E pGIPZ-shRNA-miR-30 RNAi library, containing 10,000 hairpins covering ~5000 genes, led to the discovery of three mediators of migration: MESDC1, KIF3B, and ARHGAP12. MESDC1 or mesoderm development candidate 1, recovers two PubMed articles when input into the database: the first describes the identification of MESDC1 as an embryonic lethal deletion in mice, located on mouse chromosome 7, and has a highly conserved sequence from humans to *Xenopus* to *Drosophila* (Wines 2001). M. Wines *et al.* also identifies the mouse Talin protein to have similar sequence identity to the protein encoded by MESDC1 (Wines 2001). Talin is responsible for connecting the ECM to the actin cytoskeleton through integrins and is, therefore, a key component to cytoskeletal reorganization and cell adhesion molecules, both of which are requirements of cell migration (Aplin 1998). The second publication identifies MESDC1 as a novel F-actin binding protein that has homologous residues to a portion of Talin, and binds actin to a higher extent than Talin. The authors suggest that MESDC1 is a novel F-actin binding protein and that it may play an important role in the function of Talin (Gingras 2010). The lack of publications directly looking at the role of MESDC1 in cell migration provides an open opportunity to explore this protein for potential drug targeting to potentially block migration and metastasis.

KIF3B yields 45 publications when searched for in PubMed and while most demonstrate this protein as a kinesin II motor, used for microtubule motility and intracellular trafficking, KIF3B has recently been identified as a player in transport of MT1-MMP

(MMP-14) along microtubules to the cell surface for both adhesion protein shedding and ECM degradation (Zang and Hancock 2004; Wiesner 2010). Furthermore, knockdown of KIF3B and KIF5B led to decrease in migration for MT1-MMPs along microtubules and more importantly, the siRNA-mediated knockdown of KIF3B led to less matrix degradation by these macrophages (Wiesner 2010). The suggestion of KIF3B as an important mediator of ECM degradation through MT1-MMPs could provide an upstream target of MT1-MMPs for the reduction of cell migration and improve upon previous failed clinical trials using MMP inhibitors (Kessenbrock, Plaks and Werb 2010). The implication of the immune system requirements for KIF3B however, would have to be addressed in further detail to risk detrimental impairment of the immune system using KIF3B blocking drugs.

The final gene identified through the screen was ARHGAP12, and while there are many publications in PubMed regarding ARHGAPs, only 3 are specifically addressed to ARHGAP12. One of these publications identifies ARHGAP12 as a Rho-inactivating protein expressed at high levels in many tissues including tumour cell lines, while another investigated further to discover that the ARHGAP12 interacts with Rac1 to decrease it's activity, but not RhoA (Zhang 2002 and Gentile 2008) In this study by A. Gentile, *et al.*, the silencing of ARHGAP12 and simultaneous hepatocyte growth factor stimulation, led to an increase in cell migration through a Matrigel™ transwell chamber, increased cell spreading on fibronectin and increased cell adhesion (Gentile 2008). This study contrasts with the findings of the current screen, which show ARHGAP12 as a requirement for cell migration and the invasive tumour phenotype and upon shRNA-mediated inhibition, cell migration is blocked. The discrepancy between the study by A. Gentile, *et al.*, and the current study could be accounted for by the fact that ARHGAP12, while inactivating Rac1, may allow for the expression of other pro-migratory proteins in the cell. Evidence for this comes from the fact that p190RhoGAP, while inactivating RhoA, allows FAK to activate Rac1 to proceed with migration (Tomar and Schlaepfer 2009). In order to definitively conclude the role of ARHGAP12 in the context of cell migration *in vivo* follow up assays of migration will need to be performed.

Although the RNAi screening technique allows for high throughput analysis of genes involved in many processes including cell migration, there are drawbacks associated with this technique that are important to take into consideration when interpreting the results of RNAi based screens. One point of concern is that although the RNAi library has been validated so that 1 out of 3 shRNA knockdown gene expression by at least 70%, not all cell lines will behave in a similar manner to the ones used for these validation studies (Boettcher and Hoheisel 2010). In fact, there are even discrepancies between the cell lines tested by the commercial suppliers for knockdown of the same gene (Boettcher and Hoheisel 2010). Since HEp3 cells have not been validated for >70% knock down for each of the 5000 genes represented in the library, it is plausible that a portion of the migration genes may not be knocked down to a level that would result in a compact tumour phenotype. In this respect, migration mediators may be missed in this cell line. One means to remedy this situation would be to apply the same screening parameters on another cancer cell line that thrives in the chicken embryo model, such as HT-1080 fibrosarcoma, to observe if additional migration mediators are identified.

Another parameter that must be taken into account when performing the screen, is the cell proliferation status between cells containing various shRNA constructs (Simpson 2008). An shRNA that causes decreases in cell proliferation could influence the number of cells that form colonies in the CAM. Although genes directly related to proliferation is not the goal of the screen, some genes that influence proliferation, may also influence cell migration (Croucher 2010). To account for this, extraction of colonies from the embryos is spread over 3 days, and since the genes are represented 3X, these slower growing colonies may be caught at later extraction dates, however, the cells that cannot proliferate at all could have already dropped out prior to *in vivo* administration because cells are expanded in culture for a week prior to administration. Alternatively, these slow-proliferating cells could be eliminated from the screen following colony extraction where the colonies must be expanded to facilitate PCR processing. This could have been the reason why many hits were identified in the screen, however after transfer to cell culture, they did not thrive and therefore could not be identified by PCR and sequencing. Another reason, other than cell proliferation, for lack of cell survival when moved from the *in vivo* setting to an *in vitro* setting could be that the cell migration genes lost in these cells may also be important for

cell adhesion. Cell adhesion is a requirement for migration and genes associated with adhesion could be identified as hits in the screen. If cell adhesion genes are lost, the cells may not be able to establish contact with the cell culture dish and experience anoikis, or cell death due to loss of anchorage to the ECM. To remedy the loss of hits post extraction, moving forward, an all-in-one DNA PCR extraction kit could be used to extract genomic DNA out of as many as 10 cells immediately following extraction (Applied Biosystems®Arcturus®PicoPure® DNA Extraction Kit). Due to the possibility that the screen may cause the dropout of cell migration genes related to proliferation, the screen at hand will only identify mediators of that influence migration, and not both migration and proliferation.

A technical consideration that was relevant in the single shRNA studies using pLKO.1 TRC library clones for cortactin and rhoA, also applies to the pGIPZ, H&E shRNA-mir30 based library. The issue is that of off-target effects, or knockdown of unintended genes. Although the new generation of self inactivating lentiviral vectors like pLKO.1 and pGIPZ have been designed to preferentially integrate into the intronic sequences of the human genome, and therefore endogenous gene expression deregulation is spared, unwanted mRNA sequences that are similar to the intended mRNA, could still bind to an shRNA-miR, silencing gene expression (Liu and Berkhout 2011 and Lochmatter and Mullis 2011). In this scenario, genes that actually cause the compact tumour phenotype may not be identified through PCR amplification of the shRNA, because the shRNA target sequence belongs to another gene. Although true mediators of migration may be recovered by their direct match shRNAs throughout the screen, the hits recovered that belong to the wrong shRNA target sequence will only be discovered after additional validation using either: 1) individual shRNAs designed to target the supposed gene associated with migration or 2) use of multiple shRNAs targeting different areas of the supposed mRNA transcript, in combination with inhibitors and additional assays for cell migration, some of which have been used in this study for validation of the positive control.

FUTURE DIRECTIONS

In summary, the results of the current study have contributed to the development of an RNAi based screen for mediators of cell migration using the chicken embryo model. These

results have demonstrated that HEp3 cells are transducible by two different shRNA lentiviral vectors, the TRC, pLKO.1-shRNA and the H&E, pGIPZ-shRNA-miR-30 and achieve a high level of knockdown for cortactin and rhoA using the TRC shRNA constructs. RNAi mediated inhibition of rhoA and cortactin have served to successfully demonstrate the feasibility of screening for migration mediators through *in vivo* assays, wherein knockdown of these genes resulted in marked decreases in cell migration and metastasis. Optimization of screening parameters allowed for the transition of an idea to reality by allowing the smooth execution of the first iteration of the RNAi library, screening for 5000 genes. In this screen, three migration mediators were identified: MESDC1, KIF3B, and ARHGAP12. The next steps in this project are to 1) complete further iterations of the screen, covering another set of 5000 genes until all genes in the genome (32,000) are represented and hits are identified and 2) validate hits using migration assays and individual shRNAs targeting multiple sites on the mRNA transcripts of target genes. To complete the screen and identify all hits, it is projected to take 6 months, as preparation of cells, animal turnover, screening, PCR and sequencing all add up to about a month's worth of work and there are 6 more iterations of 5000 genes to test. Validation of hits is dependent on the amount identified through screening, but if there are even two hits, the validation process could be upwards of a year, as this was the length of time taken to validate both cortactin and rhoA. In total it is projected that the entire genome could be screened and validated in 1-2 years, and again this is dependent on the amount of hits and the number of personnel assisting with the project. In the bigger picture, validation of such hits as successful could then be carried over to mouse models of metastasis to test how cells behave upon knockdown of migration target genes in another animal model. This model would also be used to administer alternative methods of inhibition, such as pharmacological inhibitors and could also test combination therapy such as the gold standard, chemotherapeutics. Altogether, the study at hand is the tip of the iceberg and completion of the screen will allow for more exciting, novel targets of cell migration to be uncovered.

Chapter 4

4 Materials and Methods

Cells and Cell Culture Reagents

Cell incubation conditions: 37°C with a 5% CO_2 humidified atmosphere. *Cell culture media:* **Growth media:** DMEM (GIBCO)+ 10% iFBS (GIBCO), 10,000 IU/mL penicillin (Invitrogen), 10,000 IU/mL streptomycin (Invitrogen), **Low antibiotic growth media:** DMEM (GIBCO) + 10% iFBS (GIBCO), 10 IU/mL penicillin (Invitrogen), 10 IU/mL streptomycin (Invitrogen), **High serum harvest media:** DMEM (GIBCO)+ 40% iFBS (GIBCO), 10,000 IU/mL penicillin (Invitrogen), 10,000 IU/mL streptomycin (Invitrogen), **p.LKO1 Infection media:** DMEM (GIBCO) + 16ug Hexadimethrine bromide (Sigma-Aldrich), 10% iFBS (GIBCO), 10 IU/mL penicillin (Invitrogen), 10 IU/mL streptomycin (Invitrogen), **pGIPZ Infecton media:** DMEM (GIBCO), **Invasion chamber media:** Top chamber, DMEM (GIBCO), 10,000 IU/mL penicillin (Invitrogen), 10,000 IU/mL streptomycin (Invitrogen). *Cells:* Fibrosarcoma (HT-1080) (ATCC CCL-121™), and human epidermoid cells (HEp3 and HEp3-GFP) (a gift from collaborator Dr. A. Zijlstra (Vanderbilt University, Nashville, Tennessee)) and were maintained in growth media under cell incubation conditions.

Cell Counting and Flow cytometry analysis

HT-1080 cells were seeded at $5x10^4$ cells per well in a 24-well plate in growth media and incubated for 4 hours. Growth media was replaced with 0.225 mL of pGIPZ infection media prior to viral transduction. 6, 5-fold serially diluted amounts (25X-78125X) of pGIPZ-empty non-silencing control viral stock (Open Biosystems) were created in pGIPZ infection media and 0.025 mL of each dilution was added to duplicate wells of the plated HT-1080 cells in 0.225 mL media. Cells were incubated for 4 hours and 1 mL growth media was added back to each well. Cells were incubated for 48 hours post-infection, after which cells were counted for GFP positive cells. 6 fields of view per dilution for duplicate wells were captured using a fluorescent inverted microscope (Olympus), attached to a

monitor and camera (Hamamatsu), and Image-Pro Analysis Software (Media Cybernetics ®). Images were captured at 100X in both the FITC and DIC channels to capture GFP positive cells and total cells in brightfield respectively. Images were counted using a tally clicker (VWR). Percent GFP positive cells were reported as:

$$\text{Percent GFP positive cells} = \frac{\text{number of cells with GFP signal in FITC channel}}{\text{number of cells in the DIC channel}} * 100$$

Following image acquisition, cells from each well were trypsinized with 0.25% Trypsin-EDTA (GIBCO) and washed with 1X PBS (GIBCO). Cells were centrifuged at 1200 rpm for 5 minutes (Thermo Scientific) and re-suspended in 1% formaldehyde (Sigma-Aldrich) in 1X PBS for flow cytometry analysis of the percent GFP positive cells for 10,000 events (Beckman Coulter).

Functional MOI calculation for pGIPZ lentivirus particles

HEp3 cells were plated at $1x10^5$ cells in 12-well plates in growth media and incubated for 4 hours. Media was replaced with pGIPZ infection media (1mL) immediately prior to infection. HEp3 cells were infected with pGIPZ-empty (non-silencing control lentivirus particles, Open Biosytems) using three different *non-functional* MOIs (1, 5, and 10) in triplicate wells. Amount of stock virus used for infection of HEp3 cells with each *non-functional* MOI was calculated by:

$$\text{Amount of stock virus (ul)} = \frac{\textit{Non-functional}\text{ MOI (1, 5, or 10)} * \text{cells plated (100,000 cells)}}{\text{Virus Titer (TU/ul) as determined by supplier in HEK293T cells}}$$

Corresponding volumes of stock virus were added to appropriate wells and cells were incubated for 4 hours post-infection followed by the addition of 1 mL growth media to each well. Cells were incubated for 48 hours post-infection after which, cell counting for GFP positive cells was performed. 6 FOV per MOI for triplicate wells were captured using a fluorescent inverted microscope (Olympus), attached to a monitor and camera (Hamamatsu), and Image-Pro Analysis Software (Media Cybernetics ®). Images were captured at 100X in both the FITC and DIC channels to capture GFP positive cells and total cells in brightfield respectively. Images were counted using a tally clicker (VWR). Percent GFP positive cells were reported as:

Percent GFP positive cells= number of cells with GFP signal in FITC channel *100
number of cells in the DIC channel

***In vivo* Colony forming assay**

$1x10^5$ or $5x10^4$ HEp3-GFP-pGIPZ-empty cells suspended in 50ul of serum-free DMEM were injected i.v into animals that were day 9 of embryonic development. Representative images were taken at 25X magnification immediately following injection and at 8 days post-injection using the upright, epifluorescence microscope (Axio Examiner, Carl Zeiss, Thornwood, NY) attached to a camera (Hamamatsu) and computer monitor. Whole CAM surfaces were imaged using the Velocity™ (Improvision, Lexington, MA) software by creating a 'well overlay' the same dimensions of the CAM and calibrating the motorized stage to effectively scan the entire overlay, stitching each image together in a montage. Montage images of animals 8 days post-injection were used to count the total number of colonies per image using a tally clicker (VWR) for 4 animals in each group ($1x10^5$ or $5x10^4$ cells). To calculate the amount of 'extractable' colonies, the number of colonies that were overlapping was subtracted from the total colony count.

Preparation of hairpin-pLKO.1 lentiviral vectors

Individual hairpin-pLKO.1 lentiviral vectors were shipped as Ecoli- glycerol stocks in a 96-well plate format. Plates were stored at -80°C until use, and during use, they were maintained on dry ice. Clones of interest were selected by stabbing the frozen stock and placing it in 5mL of LB broth, supplemented with 100 ug/mL of carbenicillin (Sigma-Aldrich). Bacterial cultures were shaken at 37°C for 12 hours. Purification of DNA from the bacterial cultures was performed using the EX-10 Spin Column Plasmid DNA Minipreps Kit (Bio Basic Inc.), according to the manufacturer's protocol. DNA quantity was measured using the NanoDrop (Thermo Scientific) and DNA yields were between 100-200 ng/uL. DNA digests were performed using separate reaction tubes for 100ng of each hairpin-pLKO.1 vector and the unique restriction enzymes Kpn1 (New England Biolabs) and EcoR1 (New England Biolabs). Digests were allowed to proceed for 40 minutes at 37°C, after which they were run on a 0.7% agarose gel (Sigma), stained with Ethidium Bromide (run at 125 Volts for 1 hour alongside 1Kb DNA ladders (New England Biolabs)). Gels were visualized using UV light from a Gel Doc™XR (BioRad) and

Quantity One Analysis Software (BioRad). Colonies in the proper orientation (presence of 2 DNA bands: 7Kb and 1.4 Kb) were used for preparation of lentivirus particles.

Preparation of hairpin-pLKO.1 lentivirus particles

HEK293T cells were plated at $1x10^5$ cells/mL in 6 mL of low antibiotic growth media in 6 cm dishes and incubated for 24 hours prior to transfection. Co-transfection of the three plasmid system was carried out using hairpin-pLKO.1 vector (1ug), envelope plasmid (VSVG/pMD2.G,100ng) and packaging plasmid (pCMV-R8.74psPAX2, 900ng) as described previously (Moffat 2006). Transfections were carried out in Opti-MEM (GIBCO) using Fugene6® Transfection Reagent (Roche) according to the manufacturer's protocol. Cells were incubated for 18 hours and transfection reagent was replaced with 6mL high serum harvest media. 40 hours post-transfection, the viral supernatant (6 mL) was collected, passed through a 0.22 um filter, and stored at 4°C. HEK293 high serum harvest media (6 mL) was replenished, and viral harvesting was repeated a second time, pooled with previous harvest, aliquoted, and stored at -80°C until further use. HEK293T cells, pLKO.1-shRNA clones, pMD2.G and pCMV-R8.74psPAX2 plasmids were all gifts from Dr. Jason Moffat, in collaboration with the Ontario Institute for Cancer Research (OICR), Terrence Donnelly Center for Cellular and Biomolecular Research, University of Toronto, Toronto, Canada.

***Functional* MOI calculation and Infection of HEp3 cells with hairpin-pLKO.1 lentivirus**

HEp3-GFP cells were plated at $5x10^4$ cells per 0.5mL of p.KLO.1 infection media in 12-well plates. Representative lentiviral stocks, obtained from the production of virus from two hairpin-pLKO.1 clones, were used to calculate the *functional* MOI of hairpin-pLKO.1 virus particles for HEp3-GFP cells using a modified method (Morris 1993). Briefly, HEp3-GFP cells were infected with 1 mL of 8, 2-fold serial dilutions (1-256X) of stock virus from each clone and the percentage of infected cells was counted and compared to growth control after puromycin (Sigma-Aldrich) selection (2ug/mL) using a hemocytometer:

Total cells/mL=

cell count * 10,000 (cells/mL in an area of hemocytometer grid) * 40 (dilution factor prior to counting)

Percent Growth=

$$\frac{\text{Total cells/mL for each virus dilution (1X-256X) - Total cells/mL for background control}}{\text{Total cells/mL for growth control}} * 100$$

Background control: cells with no virus and puromycin selection
Growth control: cells with no virus and no puromycin selection

Results from the titering assay demonstrate that the percentage of efficiently transduced cells (percent growth) was 40% and 60 % for each clone at the first dilution of 1mL (neat). When cross-reference to Poission's distribution table (Table 2), this translates to MOI values of 0.5 and 1. Therefore, 1 mL of hairpin-pLKO.1 lentiviruses, produced in the exact manner as these representative clones, will equal an MOI in the range of 0.5-1 when transduced into $5x10^4$ HEp3-GFP cells. To infect lentiviral stocks containing hairpin-pLKO.1 constructs of interest, 1 mL (neat) of lentivirus stocks from clones: 77 and 78 (shLUC), 145 and 146 (shGFP), 134, 135, 136, 137 and 138 (shCTTN), and 45, 46, 47, 48, and 49 (shRhoA) were added to 5×10^4 HEp3-GFP cells in 0.5 mL pLKO.1 infection media in 12-well plates to achieve similar MOI ranging between 0.5 and 1. 24 hours later post-infection, hairpin-pLKO.1-HEp3 cells were selected for puromycin resistance (2ug/mL) for 7 days, without clonal propagation.

Quantitative real time PCR (RT-PCR)

Total RNA was isolated using TRIZOL (Invitrogen) 14 days following retroviral transduction and puromycin selection. Amounts of RNA were quantified using a NanoDrop and 1ug of RNA for each sample was DNase I (Invitrogen) treated prior to reverse transcription to cDNA using SuperScript III Reverse Transcriptase (Invitrogen), as per the manufacturer's protocol. RT-PCR was performed on cDNA samples, 'reverse transcription negative' controls, and 'water-primer set only' controls using Platinum SYBER Green qPCR SuperMix (Invitrogen) and primer sets described as per Figure 2.2.2. Reactions were carried out in a 96-well plate format and were spun for 2500 rpm for 30 seconds prior to placing the plate in the Thermo Cycler (BioRad). HEp3-GFP-shRNA samples amplified with either rhoA or cortactin specific primers were reported relative to GAPDH as fold expression normalized to HEp3-GFP-shLUC samples.

Western Blotting

For analysis of Cortactin and RhoA expression, 80% confluent cultures of HEp3-GFP knockdown cells (shRhoA (45), (46), (47), (48), (49) and shCTTN (134), (135), (136), (137), (138), shLUC (78), shGFP (145) and HEp3-GFP (Parental) cells in 10 cm plates were lysed in cold lysis buffer (0.5% NP-40, 100mM NaCl, 50mMM Tris-HCL, pH 7.5 containing a protease inhibitor cocktail (Roche)) and scraped off the plates using a sterile cell scraper. Samples were collected into microcentrifuge tubes and centrifuged at 13 000 rpm for 10 minutes at 4°C. Protein concentration of supernatants were analyzed using a Bradford assay using Quick Start Bradford 1X Dye Reagent (BioRad) using the microplate method, and 10X bovine serum albumin (New England Biolabs) as the standard, according to the manufacturer's protocol (http://www.bio-rad.com/LifeScience/pdf/Bulletin_9004.pdf). 15ug of total protein was denatured in DL-Dithiothreitol (DTT) (Sigma-Aldrich) at 95°C for 5 minutes and was loaded into SDS-plyacrylamide gels (8% when blotting for Cortactin and 15% when blotting for RhoA). SDS-electrophoresis was carried out using the vertical blotting apparatus (mini-PROTEAN Tetra cell, BioRad) and proteins were transferred using a semi-dry unit (NuPage® Novex® Gel System, Invitrogen™) to hydrophobic polyvinylidene difluoride (PVDF) membranes (Amersham Hybond™-P, GE Healthcare). Membranes were cut in half to blot for either RhoA and Tubulin or Cortactin and Tubulin and blocked over-night in 5% skim milk (BioShop) in TBST (50mM Tris, 150mM NaCl and 0.05% Tween-20). To probe for either RhoA, Cortactin or Tubulin, a 1:2000 dilution of rabbit anti-RhoA monoclonal antibody (that does not detect the related RhoB or RhoC proteins, clone 67B9, Cell Signalling Technology ®, Danvers, MA) was added to the strips of membrane containing 20-25 KDa proteins, a 1:4000 dilution of mouse anti-Cortactin (p80/85) monoclonal antibody (clone 4F11, Upstate, Lake Placid, NY) was added to the membrane strips with proteins at 75-80 KDa, and a 1:1000 dilution of mouse anti-β-Tubulin monoclonal antibody (cone 2-28-33, Invitrogen™, Camarillo, CA) was added to membrane strips containing the 50 KDa proteins. All of these primary antibodies were incubated overnight in 5% Skim milk in TBST. A streptavidin-horseradish peroxidase conjugated secondary antibody, either anti-rabbit or anti-mouse (both from Amersham, GE Healthcare, Piscataway, NJ), was incubated for 1 hour following multiple washes of primary antibodies. Chemilumescence

was detected using ECL-Plus Western Blotting Detection Reagent and Hyperfilm ECL (both from Amersham, GE Healthcare).

All bands were a quantified by densitometry using ImageJ gel analysis tool and expression was reported relative to Tubulin expression and normalized to shLUC expression.

Human tumour cell motility and Invasion

In vitro invasion and migration assay

HEp3-GFP invasion for individual shRNA clones was tested using a BD Bioscience Matrigel ™ boyden chamber system as previously described using Matrigel™ without growth factors (Sahai, and Marshall 2003). Growth media was placed in the bottom chambers (0.5 mL) and HEp3-GFP-shRNA cells were plated in the upper chambers of a 12-well format, in triplicate, with 5 $x10^4$ cells per chamber in 0.5 mL of invasion assay media. Invasive, migratory cells were recovered from the underside of the 8um pore PET membranes located under the Matrigel ™ (Figure 2.2.4) after 22 hours of incubation. Inner chambers were removed and fixed/stained/washed using the Diff-Quick reagents (modified Wright Giemsa stain, Sigma) according to manufacturer's protocol. Insert wells were allowed to dry and images of 5 non-overlapping fields of view were imaged using the inverted microscope (Olympus), attached to a monitor and camera (Hamamatsu), and Image-Pro Analysis Software (Media Cybernetics ®). Images were captured at 100X in the DIC channel to capture total cells in brightfield. Images were counted using a tally clicker (VWR) and were reported as the number of invasive or migratory cells normalized to shLUC.

Intravital real-time imaging of tumor cell motility in the chicken embryo

Intravital imaging in the chicken embryo CAM was performed by both the imaging of single cells in micrometastases following an experimental metastasis model described by (Zijlstra 2002) or by the imaging of cells at the invasive tumour border using a spontaneous metastasis model by bolus injection as described by (Zijlstra 2008). For the *experimental metastasis model*, the motility of HEp3-GFP-shRNA (shCTTN, shRhoA, shLUC) were compared following the i.v injection of $1x10^5$ cells on embryonic day 9 and

allowing the cells to form micrometastases in the CAM for 3-5 days, post- injection, prior to imaging. For the *spontaneous metastasis model*, the motility of HEp3-GFP-shRNAs were compared following the injection of a primary tumor bolus into the mesenchyme of the CAM on embryonic day 9 animals that were allowed to form larger tumours for 2-4 days prior to imaging.

To achieve imaging of the CAM on live chicken embryos, in real-time, an imaging unit was used to house the animals for both enhanced focus and for temperature and humidity control (Zijlstra 2008). Imaging of single cells in micrometeastases and cells at the tumour border was performed using an upright, epifluorescent microscope with a motorized stage (Axio Examiner, Carl Zeiss, Thornwood, NY) controlled by Velocity™ (Improvision, Lexington, MA). For micrometastases, the stage was calibrated to toggle over three independent micrometastases per animal for each of the HEp3-GFP- shRNA groups and images were acquired every 10 minutes for 10 hours (60 frames) at 50X. Focus was adjusted manually every 9 minutes for the first 12 frames and every 120 minutes for the remaining frames. For tumours, the stage was calibrated to toggle over three non-overlapping edges of the tumour per animal for each of the HEp3-GFP-shRNA groups and images were acquired every 15 minutes for 8 hours (32 frames) at 100X. Focus was adjusted manually every 12 minutes for the first 15 frames and every 30 minutes for the remaining frames. Image drift and rotation were corrected for all image sequences or 'movies' using the Stack_Reg plugin (Biomedical Imaging Group http://bigwww.epfl.ch/) running in the open-source software ImageJ (NIH). Cell tracking of individual cells was quantified using the Manual_Tracking plugin from ImageJ, which requires manually 'clicking' on individual cells as they advance at every 10 minute interval (micrometastases) or 15 minute intervals (cells at invasive tumour border). These tracks were used to calculate the velocity of each cell by taking the total distance travelled (change in X and Y coordinates between frames) and dividing it by the frame interval, which was input into the 'properties' box in the ImageJ taskbar. The pixel width 'X' and height 'Y' was calibrated to match the objective used and this allowed the pixels to be represented in um. For the 5X objective used in the micrometastases, the calibration unit used was 0.8 and for the 10X objective used in the tumour boli, the calibration unit used

was 1. Wind-rose plots were created using the Chemotaxis and Migration plugin for ImageJ (Ibidi®, www.ibidi.de/applications/ap_chemo.html).

Quantitative Spontaneous Metastasis Assay

The quantitative spontaneous metastasis assay was performed as previously described (Zijlstra 2002). HEp3-GFP knockdown cells were placed directly on the CAM of day 10 animals forming a primary tumor in 7 days. Tumours were then extracted, weighed and stored at -20 for record. Livers were also extracted and frozen at -20 until further processing. Human DNA was detected by *alu* PCR after homogenization and extraction of DNA from 50mg of liver sample from each experimental and control groups using the SYBER® Green Extract-N-Amp Tissue PCR Kit (Sigma-Aldrich) according to manufacturer's protocol. As previously detailed by (Zijlstra 2002), primers against human *alu* sequences were used to amplify HEp3-GFP cell DNA out of a chicken embryo background, and using primers specific to chicken GAPDH, and the signal (as reported by CT value) for human DNA was normalized to total sample. To calculate the actual number of cells that are in each sample, a standard curve was run alongside the unknown samples to interpolate the number of cells in unknown samples to known concentrations of cells. To prepare the standard curve, 4-fold serial dilutions of HEp3-GFP ($7\text{-}1x10^5$ cells) in equal volumes were added to individual microcentrifuge tubes containing 50mg of homogenized naïve liver. The standard curve samples were processed identically to the experimental samples from this point. Normalized *alu* CT values were compared to the standard curve to calculate the number of HEp3-GFP cells per 50mg liver tissue and the unit calculation of HEp3-GFP cells in the liver per ug of tumor was reported. Representative livers from animals harboring primary tumours from each of the knockdown cells were taken using the fluorescent steromicroscope (Lumar, Carl Zeiss, Thornwood, NY) in both brightfield and FITC channels using a canon digital camera attachment or the 1.5X Objective respectively. The fluorescent images were acquired using the Velocity™ software and were zoomed up 20X and the brightfield images were zoomed in 10X.

shRNA screen

Use of a pooled lentiviral library has been described previously (Gazin 2007). In this study, $3x10^5$ HEp3-GFP cells were infected at a *functional* MOI of ~0.4 (*non-functional* MOI of 5) in a 10 cm dish with pooled pGIPZ-shmiR constructs in virus particle format. Transduced cells were selected using 2ug/mL puromycin and allowed to expand to ~20 million cells in 5, 15cm dishes (about 10 days). $1x10^5$ cells were administered i.v to animals of embryonic development day 9 in 50ul aliquoits for 150 animals. Colonies were allowed to form over 5-7 days post-injections and during this time, screening for compact colonies using the Axio Examiner upright epifluorescent microscope, attached to a camera, computer monitor and controlled by Velocity™, was used in the FITC channel at 25X for cursory screening and at 100X for more detailed identification. Compact colonies were marked by placement of pieces of cut, sterilized filter paper (Whatman, GE Healthcare) and were either resected on the day of identification or in the following days up to 7 days post-injection. Compact colonies were recorded by capturing an image in the FITC channel at both 50X and 100X magnification (for future reference) and were named and scored on the basis of 'compactness' 1-5, 1 being the most compact and 5 being the least. Compact colonies and close scoring relatives were extracted using dissecting equipment (tweezers and scissors) and were transferred to 96-well dishes with growth media supplemented with 2 ug/mL puromycin. Colonies were further homogenized in a tissue culture hood within the 96-well plate using microdissection scissors and were incubated until confluent (about 7 days). Confluent colonies were transferred to a 12-well plate and then a 10cm dish so that sub-colonies could be picked as described in the technical manual (http://www.openbiosystems.com/collateral/rnai/pi/Decode_GIPZ_manual.pdf). Genomic DNA was extracted from 5 sub-colonies per compact colony using the Rapid Animal Genomic DNA Extraction Kit (Bio Basic) according to the manufacturer's guidelines. Extracted DNA quantity was measured using a NanoDrop and used in the PCR reaction for amplification of the short-hairpin-miR. PCR reactions were set up using 100ng of DNA, 0.1uM final primer concentration for each of the forward and reverse primers supplied by Open Biosystems (pGIPZF-5284- 5' CGG TGC CTG AGT TTG TTT GAA TG 3' and pGIPZR-5824- 5' GGC ATT AAA GCA GCG TAT CCA 3') and Platinum Taq Polymerase (Invitrogen) according to manufacturer's protocol. The PCR was carried out in

the thermo cycler according to the following program: (Hotstart at 94°C for 2 minutes) x 1 cycle, (Melt at 94°C, 15 seconds, Anneal at 55°C, 30 seconds, Extend at 68°C, 1 minute) x 30 cycles, hold at 4°C.

A sample of PCR amplicons were run out on a 1% agarose gel stained with ethidium bromide and visualized using UV gel docking station (BioRad). PCR amplicons of the correct size, 561 nt, were cleaned using the EZ-10 Spin Column DNA Gel Extraction Kit (BioBasic) and samples were sent for sequencing with the sequencing primer provided by Open Biosystems (5'GCATTAAAGCAGCGTATC-3') at the DNA sequencing facility at Robarts Research Institute (University of Western Ontario, London, Ont.).

Statistical Analysis

Statistical analysis was performed in GraphPad Prism® 5 (GraphPad Software, La Jolla, CA). For grouped analysis, 2-way matched or unmatched ANOVA was performed, with a Bonferroni post-test. For three or more groups, 1-way ANOVA was performed with a Tukey's post-test. For comparison of two groups, a student's, unpaired, two-tailed T-test was performed. For proliferation curves, the data was baseline-corrected and subjected to a linear regression test with and a comparison of the slopes to test if they are significantly different.

References

Alshenawy, H.A. 2010, "Immunohistochemical Expression of Epidermal Growth Factor Receptor, E-Cadherin and Matrixmetalloproteinase-9 in Ovarian Epithelial Cancer and Relation to Patient Deaths", *Annals of Diagnostic Pathology,* vol. 14, no. 6, pp. 387-395.

Aplin, A.E. *et al.* 1998, "Signal Transduction and Signal Modulation by Adhesion Receptors: The Role of Integrins, Cadherins, Immunoglobulin-Cell Adhesion Molecules and Selectins", *Pharmacological Reviews,* vol. 50, no. 2, pp. 197-263.

Artym, V.V. *et al.* 2006, "Dynamic Interactions of Cortactin and Membrane Type 1 Matrix Metalloprotease at Invadopodia: Defining the Stages of Invadopodia Formation and Function", *Cancer Research,* vol. 66, no. 6, pp. 3034-3043.

Asnaghi, L. *et. al.* 2010, "E-Cadherin Negatively Regulates Neoplastic Growth in Non-Small Cell Lung Cancer: Role of Rho GTPases", *Oncogene,* vol. 29, pp. 2760-2771.

Boden, D. *et al.* 2004, "Enhanced Gene Silencing of HIV-1 Specific siRNA Using microRNA Designed Hairpins", *Nucleic Acids Research,* vol. 32, no. 3, pp. 1154-1158.

Boettcher, M. and Hoheisel, J.D. 2010, "Pooled RNAi Screens-Technical and Biological Aspects", *Current Genomics,* vol. 11, no. 3, pp. 162-167.

Boire, A. *et al.* 2005, "PAR1 is a Matrix Metalloprotease-1 Receptor that Promotes Invasion and Tumorogenesis of Breast Cancer Cells", *Cell,* vol. 120, no. 3, pp. 303-313.

Breitsprecher, D. *et al.* 2011, "Molecular Mechanism of Ena/VASP-Mediated Actin-Filament Elongation", *The EMBO Journal,* vol. 30, no. 3, pp. 456-467.

Bric, A. *et al.* 2009, "Functional Identification of Tumor Suppressor Genes Through an *in vivo* RNA Interference Screen in a Mouse Lymphoma Model", *Cancer Cell,* vol. 16, no. 4, pp. 324-335.

Cai, J. *et al.* 2010, "Expression of Cortactin Correlates with a Poor Prognosis in Patients with Stages II-III Colorectal Adenocarcinoma", *Journal of Gastrointestinal Surgery,* vol. 14, no. 8, pp. 1248-1257.

Cary, L.A. *et al.* 1996, "Stimulation of Cell Migration by Overexpression of Focal Adhesion Kinase and Its Association with Src and Fyn", *Journal of Cell Science,* vol. 109, no. Pt.7, pp. 1787-1794.

Cavallaro, U. and Christofori, G. 2004, "Cell Adhesion and Signaling by Cadherins and Ig-CAMs in Cancer", *Nature Reviews Cancer,* vol. 4, no. 2, pp. 118-132.

Ceteci, F. *et al.* 2007, "Disruption of Tumor Cell Adhesion Promotes Angiogenic Switch and Progression to Micrometastasis in RAF-Driven Murine Lung Cancer", *Cancer Cell,* vol. 12, no. 2, pp. 145-159.

Chambers, A. *et al.* 1995, "Steps in Tumor Metastasis: New Concepts from Intravital Videomicroscopy", *Cancer and Metastasis Reviews,* vol. 14, no. 4, pp. 279-301.

Chan, C.H. *et al.* 2010, "Deciphering the Transcriptional Complex Critical for RhoA gene Expression and Cancer Metastasis", *Nature Cell Biology,* vol. 12, no. 5, pp. 457-467.

Chang, K., Elledge, S.J. and Hannon, G.J. 2006, "Lessons from Nature: microRNA-Based shRNA Libraries", *Nature Methods,* vol. 3, no. 9, pp. 707-714.

Chen, H. *et al.* 2011, "CD147 is Required for Matrix Metalloproteinases-2 Production and Germ Cell Migration During Spermatogenesis", *Molecular Human Reproduction,* vol. 17, no. 7, pp. 405-414.

Cleary, M.A. *et al.* 2006, "Production of Complex Nucleic Acid Libraries Using Highly Parallel *in situ* Oligonucleotide Synthesis", *Nature Methods,* vol. 3, no. 9, pp. 241-247.

Cooi, C. *et al.* 1988, "Early Events in Determining Host Cell Permissiveness to Mouse Hepatitis Virus Infection", *Journal of General Virology,* vol. 69, pp. 1125-1135.

Croucher, D.R. *et al.* 2010, "Cortactin Modulates RhoA Activation and Expression of Cip/Kip Cyclin-Dependent Kinase Inhibitors to Promote Cell Cycle Progression in 11q13-Amplified Head and Neck Squamous Cell Carcinoma Cells", *Molecular and Cellular Biology,* vol. 30, no. 21, pp. 5057-5070.

Cullen, B.R., 2004, "Transcription and Processing of Human microRNA Precursors", *Molecular Cell,* vol. 16, no. 6, pp. 861-865.

Dang, D., Bamburg, J.R. and Ramos, D.M. 2006, "avb3 Integrin and Cofilin Modulate K1735 Melanoma Cell Invasion", *Experimental Cell Research,* vol. 312, no. 4, pp. 468-477.

Deramaudt, T.B. *et al.* 2011, "FAK-phosphorylation at Tyr-925 Regulates Cross-Talk Between Focal Adhesion Turnover and Cell Protrusion", *Molecular Biology of the Cell,* vol. 22, no. 1, pp. 964-975.

Deryugina, E.I. and Quigley, J.P. 2008, "Chick Embryo Chorioallantoic Membrane Model Systems to Study and Visualize Human Tumor Cell Metastasis", *Histochemistry and Cell Biology,* vol. 130, no. 6, pp. 1119-1130.

DesMarais, V. *et al.* 2004, "Synergistic Interaction Between the Arp2/3 Complex and Cofilin Drives Stimulated Lamellipod Extension", *Journal of Cell Science,* vol. 117, no. 3499-3510.

Di Modugno, F. *et al.* 2006, "The Cytoskeleton Regulatory Protein hMena (ENAH) is Overexpressed in Human Benign Breast Lesions with High Risk of Transformation and Human Epidermal Growth Factor Receptor-2-Positive/Hormonal Receptor-Negative Tumors", *Clincal Cancer Research,* vol. 12, no. 5, pp. 1470-1478.

Dickins, R.A. *et al.* 2005, "Probing Tumor Phenotypes using Stable and Regulated Synthetic miroRNA Precursors", *Nature Genetics,* vol. 37, no. 11, pp. 1289-1295.

Diederichs, S. *et al.* 2008, "Coexpression of Argonaute-2 Enhances RNA Interference Toward Perfect Match Binding sites", *PNAS,* vol. 105, no. 27, pp. 9284-9289.

Dua, P. *et al.* 2011, "Modified siRNA Structure With a Single Nucleotide Bulge Overcomes Conventional siRNA-Mediated Off-Target Silencing", *Molecular Therapy,* vol. [E-pub Ahead of Print].

Elbashir, S.M. *et al.* 2001, "Duplexes of 21-nucleotide RNAs Mediate RNA Interference in Cultured Mammalian Cells", *Nature,* vol. 411, pp. 494-498.

Finlayson, A.E. and Freeman, K.W. 2009, "A Cell Motility Screen Reveals Role for MARCKS-Related Protein in Adherens Junction and Formation and Tumorigenesis", *PLoS One,* vol. 4, no. 11, pp. e7833.

Fire, A. *et. al.* 1998, "Potent and Specific Genetic Interference by Double-Stranded RNA in Caenorhabditis elegans", *Nature,* vol. 391, no. 6669, pp. 806-811.

Fonseca, A.V. and Corbeil, D. 2011, "The Hematopoietic Stem Cell Polarization and Migration", *Communicative and Integrative Biology,* vol. 4, no. 2, pp. 201-204.

Friedl, P. and Wolf, K. 2003, "Tumour-Cell Invasion and Migration: Diversity and Escape Mechanisms", *Nature Reviews Cancer,* vol. 3, no. 5, pp. 362-374.

Fritz, G., Just, I. and Kaina, B. 1999, "RhoGTPases are Overexpressed in Human Tumors", *International Journal of Cancer,* vol. 81, no. 5, pp. 682-687.

Gazin, C. *et al.* 2007, "An Elaborate Pathway Required for Ras-Mediated Epigenetic Silencing", *Nature,* vol. 449, no. 7165, pp. 1073-1077.

Gentile, A. *et al.* 2008, "Met-Driven Invasive Growth Involves Transcriptional Regulation of ARHGAP12", *Oncogene,* vol. 27, no. 42, pp. 5590-5598.

Gingras, A.R. *et al.* 2010, "Central Region of Talin has a Unique Fold that Binds Vinculin and Actin", *The Journal of Biological Chemistry,* vol. 285, no. 38, pp. 29577-29587.

Gou, L. *et al.* 2011, "Proteomic Identification of RhoA as a potential Biomarker for Proliferation and Metastasis in Hepatocellular Carcinoma", *Journal of Molecular Medicine,* vol. [Epub ahead of print].

Gupton, S.L. and Waterman-Storer, C.M. 2006, "Spatiotemporal Feedback between Actomyosin and Focal-Adhesion Systems Optimizes Rapid Cell Migration", *Cell,* vol. 125, no. 7, pp. 1361-1374.

Hanahan, D. and Weinberg, R.A. 2011, "Hallmarks of Cancer: The Next Generation", *Cell,* vol. 144, no. 5, pp. 646-674.

Hanahan, D. and Weinberg, R.A. 2000, "Hallmarks of Cancer", *Cell,* vol. 100, no. 1, pp. 50-70.

Hannon, G.J. 2002, "RNA Interference", *Nature,* vol. 418, pp. 244-251.

Hess, A.R. *et al.* 2005, "Focal Adhesion Kinase Promotes the Aggressive Melanoma Phenotype", *Cancer Research,* vol. 65, no. 21, pp. 9851-9860.

Horiuchi, A. *et al.* 2003, "Up-Regulation of Small GTPases, RhoA and RhoC, Is Associated with Tumor Progression in Ovarian Carcinoma", *Laboratory Investigations,* vol. 83, no. 6, pp. 861-870.

Ilic, D. *et al.* 1995, "Reduced Cell Motility and Enhanced Focal Adhesion Contact Formation in Cells from FAK-Deficient Mice", *Nature,* vol. 377, no. 12, pp. 539-543.

Johnson, J.L. *et al.* 2009, "Tetraspanin CD151 Regulates RhoA Activation and the Dynamic Stability of Carcinoma Cell-Cell Contacts", *Journal of Cell Science,* vol. 122, no. 13, pp. 2263-2273.

Johnson, J.P. 1991, "Cell Adhesion Molecules of the Immunoglobulin Superfamily and their role in Malignant Transformation and Progression to Metastatic Disease", *Cancer and Metastasis Reviews,* vol. 10, no. 1, pp. 11-22.

Jones, C. and Ehrlich, H.P. 2011, "Fibroblast Expression of a-Smooth Muscle Actin, a2b1 Integrin and avb3 Integrin: Influence of Surface Rigidity", *Experimental and Molecular Pathology,* vol. 91, no. 1, pp. 394-399.

Kallergi, G. *et al.* 2011, "Epithelial-Mesenchymal Transition Markers Expressed in Circulating Tumor Cells of Early and Metastatic Breast Cancer Patients", *Breast Cancer Research,* vol. 13, no. 3.

Kamai, T. *et al.* 2010, "Increased Rac1 Activity and Pak1 Overexpression are Associated with Lymphovascular Invasion and Lymph Node Metastasis of Upper Urinary Tract Cancer", *BMC Cancer,* vol. 10, no. 164, pp. 1-13.

Ke, A. *et al.* 2009, "Role of Overexpression of CD151 and/or c-Met in Predicting prognosis of Hepatocellular Carcinoma", *Hepatology,* vol. 49, no. 2, pp. 491-503.

Kessenbrock, K., Plaks, V. and Werb, Z. 2010, "Matrix Metalloproteinases: Regulators of the Tumor Microenvironment", *Cell,* vol. 141, no. 1, pp. 52-67.

Kim, K.B. *et al.* 2011, "Cell-Surface Receptor for Complement Component C1q (gC1qR) Is a Key Regulator for Lamellipodia Formation and Cancer Metastasis", *The Journal of Biological Chemistry,* vol. 286, no. 26, pp. 23093-23101.

Kitzing, T.M. *et al.* 2010, "Formin-like 2 Drives Amoeboid Invasive Cell Motility Downstream of RhoC", *Oncogene,* vol. 29, no. 16, pp. 2441-2448.

Lai, F.P.L. *et al.* 2009, "Cortactin Promotes Migration and Platelet-Derived Growth Factor-Induced Actin Reorganization by Signaling to Rho-GTPases", *Molecular Biology of the Cell,* vol. 20, pp. 3290-3223.

Lara, R. *et al.* 2011, "An siRNA Screen Identifies RSK1 as a Key Modulator of Lung Cancer Metastasis", *Oncogene,* vol. [E-pub ahead of print], pp. 1-9.

Lee, R.C., Feinbaum, R.L. and Ambros, V. 1993, "The C. elegans Heterochronic Gene *lin-4* Encodes Small RNAs with Antisense Complementarity to *lin-14*", *Cell,* vol. 75, no. 5, pp. 843-854.

Lee, S.B. and Esteban, M. 1994, "The Interferon-Induced Double Stranded RNA-Activated Protein Kinase Induces Apoptosis", *Virology,* vol. 199, no. 2, pp. 491-496.

Leroy-Dudal, J. *et al.* 2005, "Transmigration of Human Ovarian Adenocarcinoma Cells Through Endothelial Extracellular Matrix Involves apha-v Integrins and the Participation of MMP2", *International Journal of Cancer,* vol. 114, no. 1, pp. 531-543.

Lim, Y. *et al.* 2008, "PyK2 and FAK connections to p190Rho Guanine Nucleotide Exchange Factor Regulate RhoA Activity, Focal Adhesion Formation and Cell Motiity", *The Journal of Cell Biology,* vol. 180, no. 1, pp. 187-203.

Liu, J. *et al.* 2004, "Argonaute2 is the Catalytic Engine of Mammalian RNAi", *Science,* vol. 305, no. 5689, pp. 1437-1441.

Liu, Y.P. and Berkhout, B. 2011, "miRNA Cassettes in Viral Vectors: Problems and Solutions", *Biochimica et Biophysica Acta,* vol. [E-pub ahead of print].

Lochmatter, D. and Mullis, P.E. 2011, "RNA Interference in Mammalian Cell Systems", *Hormone Research in Paediatrics,* vol. 75, no. 1, pp. 63-69.

Loureiro, J.J. *et al.* 2002, "Critical Roles of Phosphorylation and Actin Binding Motifs, but Not the Central Proline-Rich Region, for Ena/Vasodilator-Stimulated Phosphoprotein (VASP) Function During Cell Migration", *Molecular Biology of the Cell,* vol. 13, no. 7, pp. 2533-2546.

Lynch, C.C. *et al.* 2010, "Cleavage of E-Cadherin by Matrix Metalloproteinase-7 Promotes Cellular Proliferation in Nontransformed Cell Lines Via Activation of RhoA", *Journal of Oncology,* vol. 2010, pp. 1-11.

Lyva, F.L. *et al.* 2011, "Evaluation of Transduction Efficiency in Macrophage Colony Stimulating Factor Differentiated Human Macrophages using HIV-1 Based Lentiviral Vectors", *BMC Biotechnology,* vol. 11, no. 13, pp. 1-10.

Mader, C. *et al.* 2011, "An EGFR-Src-Arg-Cortactin Pathway Mediates Functional Maturation of Invadopodia and Breast Cancer Cell Invasion", *Cancer Research,* vol. 71, no. 5, pp. 1730-1741.

Maekawa, M. *et al.* 1999, "Signaling from Rho to the Actin Cytoskeleton through Potein Kinases ROCK and LIM-Kinase ", *Science,* vol. 285, no. 5429, pp. 895-898.

Mason, S.D. and Joyce, J. 2011, "Proteolytic Networks in Cancer", *Trends in Cell Biology,* vol. 21, no. 4, pp. 228-237.

Miki, H., Suetsugu, S., and Takenawa, T. 1998, "WAVE, a Novel WASP-Family Protein Involved in Actin Reorganization Induced by Rac", *The EMBO Journal,* vol. 17, no. 23, pp. 6932-6941.

Moffat, J. *et al.* 2006, "A Lentiviral RNAi Library for Human and Mouse Genes Applied to an Arrayed Viral High-Content Screen", *Cell,* vol. 124, no. 6, pp. 1283-1298.

Morris, V.L. *et al.* 1993, "Early Interactions of Cancer Cells with the Microvasculature in Mouse Liver and Muscle During Hematogenous Metastasis: Videomicroscopic Analysis", *Clinical Experimental Metastasis,* vol. 11, no. 5, pp. 377-390.

Narumiya, S., Tanji, M., and Ishizaki, T. 2009, "Rho signalling, ROCK and mDia1, in Transformation, Metastasis and Invasion", *Cancer and Metastasis Reviews,* vol. 28, no. 1-2, pp. 65-76.

Olsen, M.F. and Sahai, E. 2009, "The Actin Cytoskeleton in Cancer Cell Motility", *Clinical Experimental Metastasis,* vol. 26, no. 4, pp. 273-287.

Palmer, T.D. *et al.* 2011, "Targeting Tumor Cell Motility to Prevent Metastasis", *Advanced Drug Delivery Reviews,* vol. in press.

Pan, S.H. *et al.* 2011, "The Ability of LCRMP-1 to Promote Cancer Invasion by Enhancing Filopodia Formation is Antagonized by CRMP-1", *Journal of Clinical Investigation,* vol. [E-pub Ahead of Print].

Perl, A.K. *et al.* 1998, "A Causal role for E-Cadherin in the Transition from Adenoma to Carcinoma", *Nature,* vol. 392, no. 6672, pp. 190-193.

Pollard, T.D. 2007, "Regulation of Actin Filament Assembly by Arp2/3 Complex and Formins", *Annual Review of Biophysics and Molecular Structure,* vol. 36, pp. 451-477.

Pula, G. and Krause, M. 2008, "Role of Ena/VASP Proteins in Homeostasis and Disease", *Protein-Protein Interactions as New Drug Targets,* vol. 186, no. 1, pp. 39-65.

Ribatti, D. 2010, "Chorioallantoic Membrane Vasulature." in *The Chick Embryo Chorioallantoic Membrane in the Study of Angiogenesis and Metastasis*, ed. D. Ribatti, 1st edn, Springer, , pp. 1-13.

Root, D.E. *et al.* 2006, "Genome-Scale Loss -of-Function Screening with a Lentiviral RNAi Library", *Nature Methods,* vol. 3, no. 9, pp. 715-719.

Rowe, R.G. and Weiss, S.J. 2008, "Breaching the Basement Membrane: Who, When, and How?", *Trends in Cell Biology,* vol. 18, no. 11, pp. 560-574.

Sahai, E. and Marshall, C.J. 2003, "Differing Modes of Tumor Cell Invasion have Distinct Requirements for Rho/ROCK Signalling and Extracellular Proteolysis", *Nature Cell Biology,* vol. 5, no. 8, pp. 711-719.

Salmon, P. and Trono, D. 2006, "Production and Titration of Lentiviral Vectors" in *Current Protocols in Neuroscience*, ed. Wenshuo Zhang, 3rd edn, John Wiley and Sons Inc, Malden, MA, pp. 4.21.1-4.21.24.

Sandy, P., Ventura, A. and Jacks, T. 2005, "Mammalian RNAi: A Practical Guide", *BioTechniques,* vol. 39, no. 2, pp. 215-224.

Sastry, L. *et al.* 2002, "Titering Lentiviral Vectors: Comparison of DNA, RNA and Marker Expression Methods", *Gene Therapy,* vol. 9, no. 17, pp. 1155-1162.

Schuuring, E. 1995, "The Involvement of the Chromosome 11q13 Region in Human Malignancies: Cyclin D1 and EMS1 are Two New Candidate Oncogenes-A Review", *Gene,* vol. 159, no. 1, pp. 83-96.

Scudiero, D.A. *et al* 1988, "Evaluation of a Soluble Tetrazolium/Formazan Assay for Cell Growth and Drug Sensitivity in Culture Using Human and Other Tumor Cell Lines", *Cancer Research,* vol. 48, no. 17, pp. 4827-4833.

Shieh, D.B. *et al.* 1999, "Cell Motility as a Prognostic Factor in Stage 1 Nonsmall Cell Lung Carcinoma", *Cancer,* vol. 85, no. 1, pp. 47-57.

Silva J. *et al.* 2005, "Second-Generation shRNA Libraries Covering the Mouse and Human Genomes", *Nature Genetics,* vol. 37, no. 11, pp. 1281-1288.

Simpson, K.J. *et al.* 2008, "Identification of Genes that Regulate Epithelial Cell Migration Using and siRNA Screening Approach", *Nature Cell Biology,* vol. 10, pp. 1027-1038.

Smolen, G.A. *et al.* 2010, "A Genome-Wide RNAi Screen Identifies Multiple RSK-Dependent Regulators of Cell Migration", *Genes and Development,* vol. 24, pp. 2654-2655.

Somlyo, A.P. and Somlyo, A.V. 2000, "Signal Transduction by G-Proteins, Rho-Kinase and Protein Phosphatase to Smooth Muscle and Non-Muscle Myosin II.", *The Journal of Physiology,* vol. 522, no. Pt 2, pp. 177-185.

Stoletov, K. *et al.* 2010, "Visualizing Extravasation Dynamics of Metastatic Tumor Cells", *Journal of Cell Science,* vol. 23, no. 13, pp. 2332-2341.

Talmadge, J.E. and Fidler, I.J. 2010, "AACR Centennial Series: The Biology of Cancer Metastasis: A Historical Perspective", *Cancer Research,* vol. 70, pp. 5649-5669.

Tomar, A. and Schlaepfer, D.D. 2009, "Focal Adhesion Kinase: Switching Between GAPs and GEFs in the Regulation of Cell Motility", *Current Opinion in Cell Biology,* vol. 21, no. 5, pp. 676-683.

Tomita, K. *et al.* 2000, "Cadherin Switching in Human Prostate Cancer Progression", *Cancer Research,* vol. 60, no. 13, pp. 3650-3654.

Toyoda, A. *et al.* 2009, "Aberrant Expression of Human Ortholog of Mammalian Enabled (hMena) in Human Colorectal Carcinoma: Implications for its Role in Tumor Progression", *International Journal of Oncology,* vol. 34, no. 1, pp. 53-60.

Valencia-Sanchez, M.A. *et al.* 2006, "Control of Translation and mRNA Degradation by miRNAs and siRNAs", *Genes and Development,* vol. 20, no. 5, pp. 515-524.

Van Belle, P.A. *et al.* 1999, "Progression-Related Expression of b3 Integrin in Melanomas and Nevi", *Human Pathology,* vol. 30, no. 5, pp. 562-567.

Van Roy, F. and Berx, G. 2008, "The Cell-Cell Adhesion Molecule E-Cadherin", *Cellular and Molecular Life Sciences,* vol. 65, no. 23, pp. 3756-3788.

Walch, A. *et al.* 2008, "Combined Analysis of Rac1, IQGAP1, Tiam1 and E-cadherin Expression in Gastric Cancer", *Modern Pathology,* vol. 21, no. 5, pp. 544-552.

Walzer, T. and Vivier, E. 2011, "G-Protein-Coupled Receptors in Control of Natural Killer Cell Migration", *Trends in Immunology,* vol. [E-pub ahead of print].

Wang, L.H. *et al.* 2010, "The Mitotic Kinase Aurora-A Induces Mammary Cell Migration and Breast Cancer Metastasis by Activating the Cofilin-F-actin Pathway", *Cancer Research,* vol. 70, no. 22, pp. 9118-9128.

Wang, Y. *et al.* 2011, "Regulation of VEGF Induced Endothelial Cell Migration by Mitochondrial Reactive Oxygen Species", *American Journal of Physiology. Cell Physiology,* vol. [E-pub ahead of print].

Wianny, F. and Zernicka-Goetz, M. 2000, "Specific Interference with Gene Function by Double-Stranded RNA in Early Mouse Development", *Nature Cell Biology,* vol. 2, no. 2, pp. 70-75.

Wiesner, C. *et al.* 2010, "KIF5B and KIF3A/KIF3B Kinesins Drive MT1-MMP Surface Exposure, CD44 Shedding, and Extracellular Matrix Degradation in Primary Macrophages", *Blood,* vol. 116, no. 9, pp. 1559-1569.

Wines, M.E. *et al.* 2001, "Identification of Mesoderm Development (mesd) candidate genes by Comparative Mapping and Genome Sequence Analysis.", *Genomics,* vol. 72, no. 1, pp. 88-98.

Wolf, K. *et al.* 2007, "Multi-Step Pericellular Proteolysis Controls the Transition from Individual to Collective Cancer Cell Invasion", *Nature Cell Biology,* vol. 9, no. 8, pp. 893-904.

Wyckoff, J.B. *et al.* 2006, "Rock-and Myosin-Dependent Matrix Deformation Enables Protease-Independent Tumor Cell Invasion In Vivo.", *Current Biology,* vol. 16, no. 15, pp. 1515-1523.

Wyckoff, J.B. *et al.* 2000, "A Critical Step in Metastasis: *In Vivo* Analysis of Intravasation at the Primary Tumor", *Cancer Research,* vol. 60, no. 9, pp. 2504-2511.

Yamaguchi, H. *et al.* 2005, "Molecular Mechanisms of Invadopodium Formation: The Role of the N-WASP-Arp2/3 Complex Pathway and Cofilin.", *The Journal of Cell Biology,* vol. 168, no. 3, pp. 441-452.

Yansong, L. *et al* 2001, "Cortactin Potentiates Bone Metastasis of Breast Cancer Cells", *Cancer Research,* vol. 61, no. 18, pp. 6906-6911.

Zang, Y. and Hancock, W.O. 2004, "The Two Motor Domains of KIF3A/B Coordinate for Processive Motility and Move at Different Speeds", *Biophysical Journal,* vol. 87, no. 3, pp. 1795-1804.

Zebda, N. *et al.* 2000, "Phosphorylation of ADF/Cofilin Abolishes EGF-indcuced Actin Nucleation at the Leading Edge and Subsequent Lamellipod Extension", *Journal of Cell Biology,* vol. 151, no. 5, pp. 1119-1127.

Zhang, H.Y. *et al.* 2011, "S100A4 Mediated Cell Invasion and Metastasis of Esophageal Squamous Cell Carcinoma Via the Regulation of MMP-2 and E-cadherin Activity", *Molecular Biology Reports,* vol. [E-pub ahead of print].

Zhang, Z. *et al.* 2002, "Cloning and Characterization of ARHGAP12, a Novel Human RhoGAP Gene", *The International Journal of Biochemistry & Cell Biology,* vol. 34, no. 4, pp. 325-331.

Zheng, H.C. *et al.* 2008, "Arp2/3 Overexpression Contributed to Pathogenesis, Growth and Invasion of Gastric Carcinoma", *Anticancer Research,* vol. 28, no. 4B, pp. 2225-2232.

Zijlstra, A. *et al.* 2008, "The Inhibition of Tumor Cell Intravasation and Subsequent Metastasis through the Regulation of I*n Vivo* Tumor Cell Motility by the Tetraspanin CD151", *Cancer Cell,* vol. 13, no. 3, pp. 221-234.

Zijlstra, A. *et al.* 2002, "A Quantitative Analysis of Rate-Limiting Steps in the Metastatic Cascade Using Human-Specific Real-Time Polymerase Chain Reaction", *Cancer Research,* vol. 62, no. 23, pp. 7083-7092.

Zuo, J.H. *et al.* 2011, "Activationof EGFR Promotes Squamous Carcinoma SCC10A Cell Migration and Invasion via Inducing EMT-like Phenotype Change and MMP-9-Mediated Degradation of E-Cadherin", *Journal of Cellular Biochemistry,* vol. [E-pub ahead of print].

Appendices

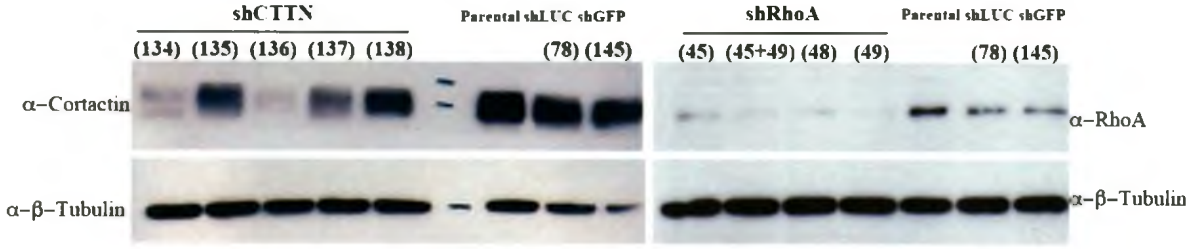

Appendix A: Detection of Cortactin or RhoA protein in HEp3-GFP cell lysates

Western blots probed with either anti-cortactin (left panel) or anti-RhoA (right panel) for HEp3-GFP control (Parental, shLUC and shGFP) and the various constructs of HEp3-GFP knockdown cells (shCTTN, shRhoA) (Top blots), relative to the loading control, anti-Tubulin (Bottom blots). The Cortactin blot results promoted the selection of shCTTN constructs 134 and 136 for further RT-PCR analysis.

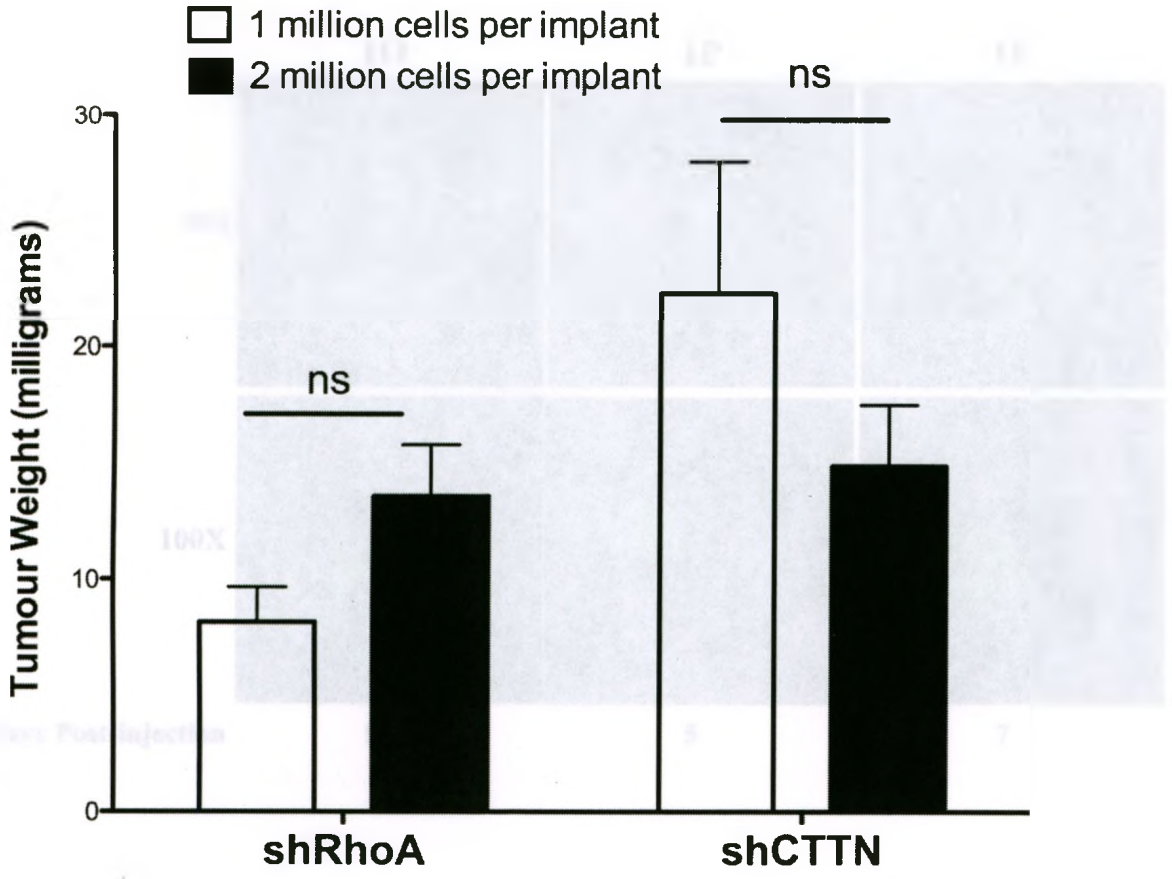

Appendix B: Comparison of tumour weights for shRhoA or shCTTN cells upon administration of different tumour cell amounts onto the CAM

Administration of 1 million shRhoA or shCTTN cells (white bars) or 2 million shRhoA or shCTTN cells (black bars) onto the ectoderm of the CAM did not result in a significant increase in tumour weight (mg) when harvested 7 days post-administration (as determined by a 2-way, unmatched ANOVA, and Tukey's post test).

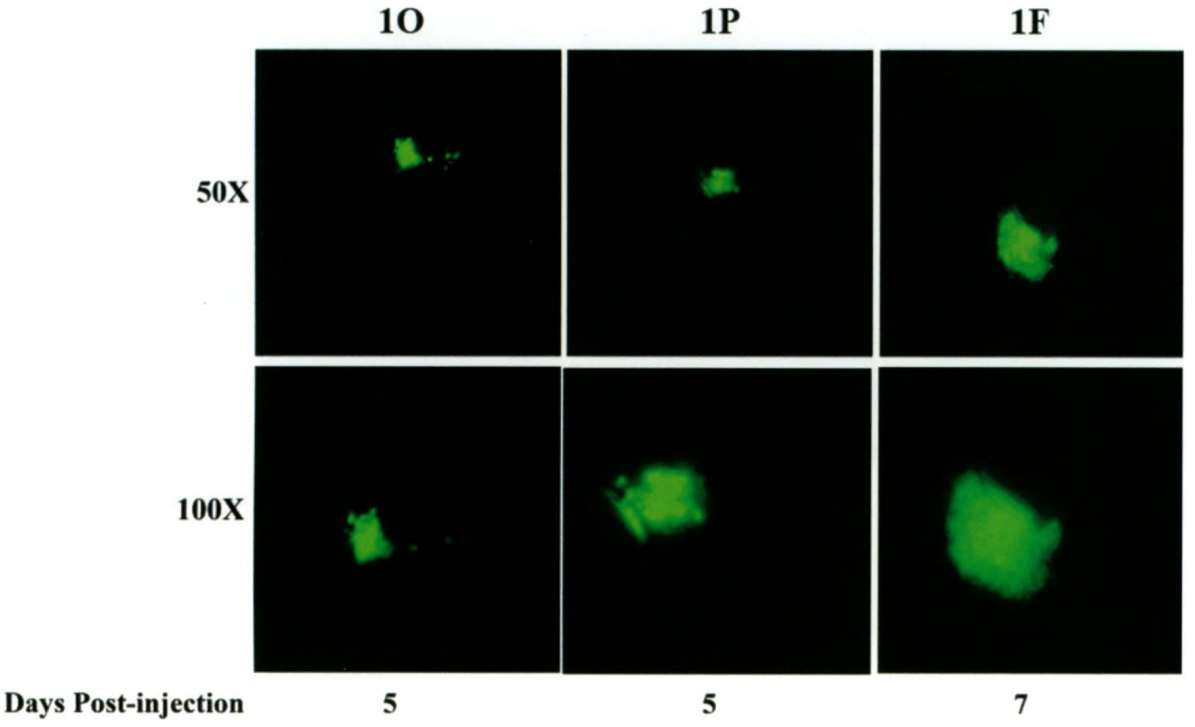

Appendix C: Compact colonies extracted from the CAM and scored as 1 (highly compact)
Images of the compact colonies within the CAM that were extracted for identification of the shRNA construct responsible for the loss of cell migration. Colonies O, P and F are ranked as highly compact and are a '1' on a scale of 1-5. Only colony F survived tissue culture post-extraction and was subsequently sequenced. Images were taken on tumour colonies between days 5 and 7 post-injection using either the 5 or 10X objective and the Axio Examiner upright epifluorescent microscope in the FITC channel on live chicken embryos.

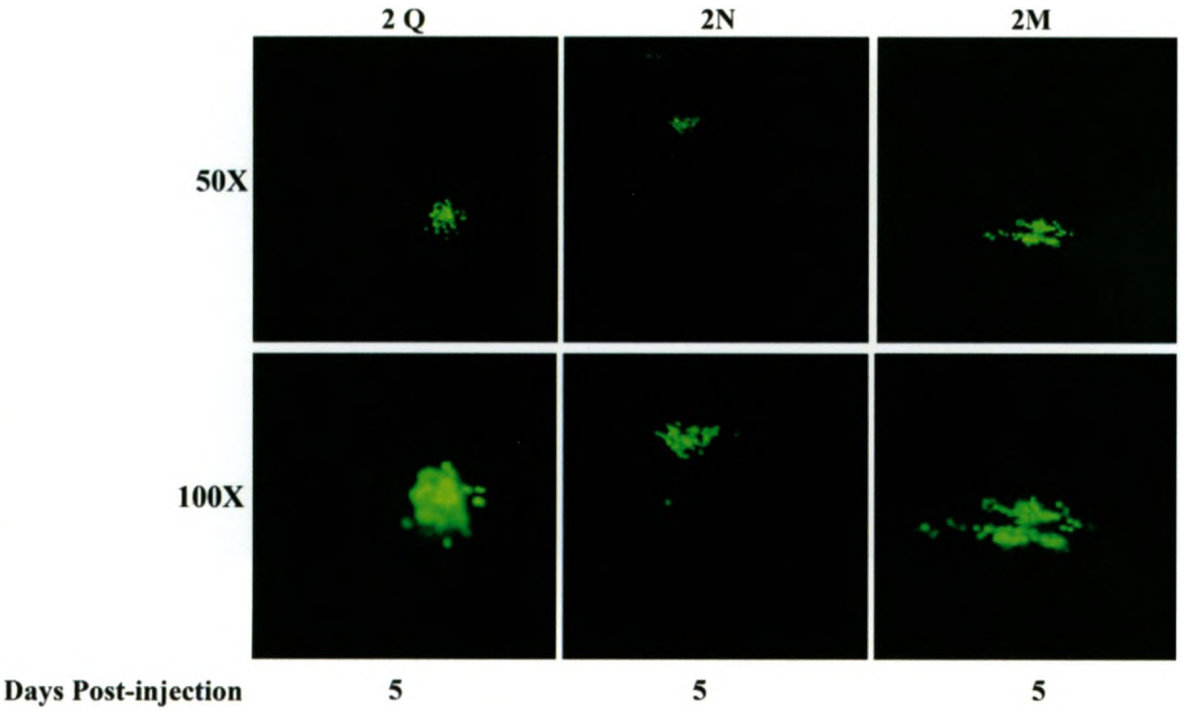

Appendix D: Compact colonies extracted from the CAM and scored as 2 (compact)
Images of the compact colonies within the CAM that were extracted for identification of the shRNA construct responsible for the loss of cell migration. Colonies Q, N and M are ranked as compact and are a '2' on a scale of 1-5. None of these colonies survived in tissue culture post-extraction. Images were taken on tumour colonies 5 days post-injection using either the 5 or 10X objective and the Axio Examiner upright epifluorescent microscope in the FITC channel on live chicken embryos.

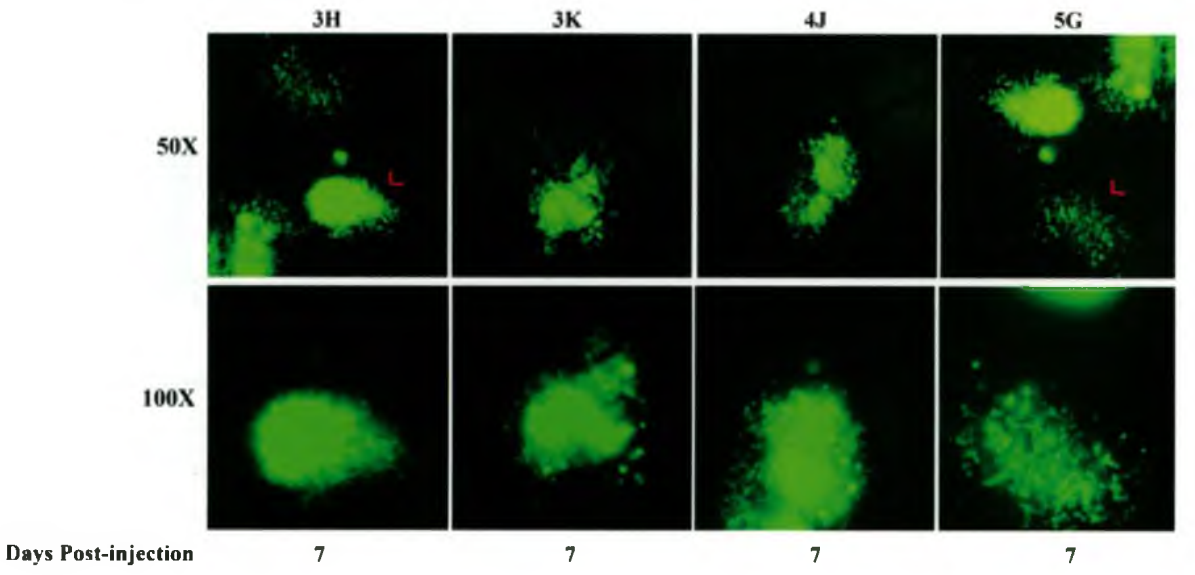

Appendix E: Colonies extracted from the CAM and scored as 3 (medium compact), 4 (somewhat compact) and 5 (diffuse)

Images of the compact colonies within the CAM that were extracted for identification of the shRNA construct responsible for the loss of cell migration. Colonies H and K are ranked as medium compact and are a '3' on a scale of 1-5. J and G are ranked as somewhat compact and diffuse, respectively, and are a '4' or '5' on a scale of 1-5, respectively. None of these colonies survived in tissue culture post-extraction. Images were taken on tumour colonies 7 days post-injection using either the 5 or 10X objective and the Axio Examiner upright epifluorescent microscope in the FITC channel on live chicken embryos.

Appendix F: Ethics Approval number for working with the chicken embryo model

AUS # 2007-087-10

Entitled: "Migration-mediated intravasation and tumour cell metastasis in cancer"

Western

October 10, 2007

This is the Original Approval for this protocol
A Full Protocol submission will be required in 2011

Dear Dr. Lewis:

Your Animal Use Protocol form entitled:
Migration-mediated Intravasation and Tumor Cell Metastasis in the Dissemination of Cancer
Funding Agency NCIC - Grant #018178

has been approved by the University Council on Animal Care. This approval is valid from **October 10, 2007** to **October 31, 2010.** The protocol number for this project is **2007-087-10.**

1. This number must be indicated when ordering animals for this project.
2. Animals for other projects may not be ordered under this number.
3. If no number appears please contact this office when grant approval is received.
   If the application for funding is not successful and you wish to proceed with the project, request that an internal scientific peer review be performed by the Animal Use Subcommittee office.
4. Purchases of animals other than through this system must be cleared through the ACVS office. Health certificates will be required.

ANIMALS APPROVED FOR 1 YR.

Species	Strain	Other Detail	Pain Level	Animal # Total for 1 Year
Bird-Domestic	Chick	embryos	B	250

REQUIREMENTS/COMMENTS
Please ensure that individual(s) performing procedures on live animals, as described in this protocol, are familiar with the contents of this document.

1. Please let Trish Kirkpatrick know the number of eggs/embryos used in this project on a monthly basis for CCAC documentation.

c.c. Approved Protocol V. A. Lewis, T. Kirkpatrick
Approval Letter T. Kirkpatrick

Oct 17/07

The University of Western Ontario
Animal Use Subcommittee/University Council on Animal Care
Health Sciences Centre • London, Ontario • CANADA - N6A 5C1
Phone: 519-661-2111 ext. 86770 • Fax: 519-661-2028 • www.uwo.ca/animal